Development, Implementation, and Improvements on an Effective Electrochemical Wastewater Treatment and Recycling Unit as a Sustainable Sanitation Solution for the Developing World

Thesis by

Clément A. Cid

In Partial Fulfillment of the Requirements for

the degree of

Doctor of Philosophy

CALIFORNIA INSTITUTE OF TECHNOLOGY

Pasadena, California

2018

(Defended January 26, 2018)

Clément A Cid
ORCID: 0000-0002-7293-035X

Dedication

Dedicated with love to my wife Emily and my son Sébastien

ACKNOWLEDGMENTS

When I joined the Hoffmann group at Caltech in 2011 to perform research for my Master thesis, I did not imagine that I would spend the next 6 years of my life on this beautiful campus: first as a student researcher and then as a PhD student. I also did not imagine that only a few weeks after my return to the United States in late 2011, I would meet the woman who would eventually become my wife and the mother of my son. During my graduate studies at Caltech, I had the opportunity to learn trust, to change research path when necessary, and to explore new opportunities such as starting a business or being actively involved in writing an international standard on toilets.[1]

All of this could not have happened without the guidance and support of my advisor, Professor Michael R. Hoffmann. Mike gave me the autonomy to explore new research directions, to work across multiple disciplines, to collaborate with other researchers, and to develop my knowledge in science, engineering, and business… and international travels! Mike was also very supportive of my personal endeavors with advice on health, marriage, and a lot of other things.

I also want to thank the other members of my Thesis Committee: Prof. William (Bill) Goddard, Prof. Mitchio Okumura, and Dr. Mamadou Diallo. All three were present when I needed advice on the direction of my thesis work. I would also like to thank Dr. Will West for all his help and guidance during the period I worked on

[1]ISO/PC 305 "Sustainable non-sewered sanitation systems"

lithium batteries. I enjoyed having the opportunity to perform some work at JPL with you and your team.

During my PhD work, I had many opportunities to meet and collaborate with fantastic people. Among them, my first gratitude goes to Dr. Doulaye Kone and Dr. Carl Hansman from the Bill & Melinda Gates Foundation. Doulaye and Carl were the people without whom I might not have centered my PhD on “reinventing the toilet”. I am grateful of the warm welcome they gave me at the Fecal Sludge Management conference in Durban in 2012. There I was able to meet with people that are literally “dealing with shit”. Those encounters made me realize the importance my work could have on solving the sanitation crisis. It is also at the same conference that I met Prof. Ioannis (Yannis) Ieropoulos and his microbial fuel cells. His support and advice were crucial in the development of Chapter 3 of this thesis.

My work in the development of the Caltech Solar Toilet led me to collaborate with many people from diverse cultures. Among them I particularly thank Mr. Ramya Bhatt from the Ahmedabad Municipal Corporation, Bincy Baby, Midhu S. V., and Harsh Kumar from Eram Scientific, Prof. Malavika Subramanyam and Prof. Babji Srinivasan from IIT Gandhinagar with his students Gaurav Kumar and Sarojini Tiwari for their help, support, and motivation in testing our AMD pre-alpha prototype in Ahmedabad. I also thank Prof. C. T. Aravindakumar with his students Arun Babu and Shalu Achu at Mahatmah Gandhi University in Kottayam for hosting, using, and testing our KYM pre-prototype. All of this endeavor could not have been achieved without the early support of Dr. Tae-Kyu Lee from Nanopac Inc. in building the electrodes and electrochemical reactor systems. I am also grateful to Ma Li and Zhou Xiaogang from

Yixing Eco-Sanitary Manufacture Co. for helping us translate our academic achievements into what I hope will become a great commercial enterprise.

It was also a great honor to work with other past and current members of the Hoffmann research group. My work on toilets would not have been possible without the continuous support of the following post-docs, graduate students, and staff researchers: Dr. Yan Qu, Dr. Justin Jasper, Cody Finke, Dr. Yang Yang, Eitam Shafran, Heather Crummer, Dr. Eric Huang, Dr. Kangwoo Cho, Dr. Asghar Aryanfar, and many others. A particular thank you to Anastiasia Hanan for all her support during the business plan competitions, and SBIR grant writing and support, as well as her research and design work for our Reinvented Toilets and the Seva project. I would also like to thank Dr. Su Young Ryu for her continuous help as co-safety officer and Dr. A. J. Colussi for his help during the early part of my work at Caltech. It was also a great pleasure for me to mentor the following SURF and visiting students: Mark Lorden, Jean-Alexandre Turban, Tony Wong, Zeineb Jelif, Elizabeth Terlinden, Prateek Kachoria, and Hugo Léandri. Many thanks to Dr. Nathan Dalleska for all his technical support at the Environmental Analysis Center of the Linde+Robinson Laboratories at Caltech.

I am also grateful to Dr. John Duffy from the Bill & Melinda Gates Foundation for supporting my work on “reinventing the toilet”. I am also grateful to June Sugiyama from the Vodafone Americas Foundation and to the Roy and Patricia Disney Foundation for their interest and support in the development of the smart maintenance technology Seva.

Finally, I would like to thank my wife Emily for being here when I needed her most. Thank you to my father-in-law and mother-in-law for their help and support – you are my US family. À *ma famille restée France : mes parents, mon frère, ma sœur, ainsi que mes grands-parents. Sans votre support au fil des ans, je ne serai pas arrivé où je suis. Merci !*

ABSTRACT

In this thesis, I present my work on the development of a self-contained toilet wastewater treatment and recycling system, the "Caltech Solar Toilet". The Caltech Solar Toilet technology is based on electrolysis of toilet wastewater with TiO_2-coated semiconductor anodes and stainless steel cathodes. This is a potentially viable onsite sanitation solution in parts of the world that lack the needed infrastructure for centralized wastewater treatment.

Prototypes of Caltech Solar Toilets were designed to fit in shipping containers in order to provide toilets and onsite wastewater treatment with clean water recycling. Units were designed to handle the waste of 25 users per day (or 130 L of toilet wastewater). The various prototypes were able to provide for the disinfection of pathogens, reduction of chemical oxygen demand (COD), [NH_3], and color at an average energy consumption of 35 Wh L^{-1}. The treated wastewater was recycled for use as toilet flushing water.

The addition of a microbial fuel cell system for urine pre-treatment was investigated to lower the overall energy consumption of the Solar Toilets. The microbial fuel cell system used consisted of two stacks of 32 cells connected in parallel. An average power density of 23 mW m^{-2} was produced at an effective current density of 65 mA m^{-2} for more than 120 days. [NH_3], total inorganic carbon, COD, and total organic carbon levels were monitored frequently to understand the chemical energy conversion to electricity as well as to determine the best electrical

configuration of the stacks. Archaeal and bacterial population on selected anode felts and in the anolyte of both stacks were investigated as well.

In addition to treating toilet wastewater, pilot-scale and bench-scale experiments demonstrated that electrolysis can remove phosphate by cathodic precipitation as hydroxyapatite at no additional energy cost. Phosphate removal could be predicted based on initial phosphate and calcium concentrations, and up to 80% total phosphate removal was achieved. While calcium was critical for phosphate removal, magnesium and bicarbonate had only minor impacts on phosphate removal rates at concentrations typical of toilet wastewater.

PUBLISHED CONTENT AND CONTRIBUTIONS

The material presented in **Chapter 2** is in preparation for publication by the listed authors. C. A. C. is the principal and coordinating author of the manuscript. C. A. C. and Y. Q. designed and constructed the prototypes. C. A. C. directed the field testing and sampling methods, and analyzed and interpreted the data. M. R. H. and Y. Q. provided guidance as well as intellectual and writing contributions.

Cid, C. A., Yan Q., & Hoffmann, M. R., in preparation. Design and preliminary implementation of onsite electrochemical wastewater treatment and recycling toilets for the developing world.

The material presented in **Chapter 3** is in preparation for publication by the listed authors. C. A. C. is the principal and coordinating author of the manuscript. C. A. C. designed the study, performed the sampling, and analyzed and interpreted the data. C. A. C. performed the DNA extraction and purification. H. Y. graciously scheduled the DNA sequencing and C. A. C. analyzed the data. I. I. provided the MFC system prototypes and remote and in-person support on their operation. M. R. H. provided intellectual and writing contributions.

Cid, C. A., Ieropoulos, I., & Hoffmann, M. R., in preparation. Urine microbial fuel cells in a semi-controlled environment for onsite urine pre-treatment and electricity production.

The material presented in **Chapter 4** is published in Cid *et al* (2018). C. A. C. is the principal and coordinating author of the manuscript. C. A. C. and J. T. J. planned the study, performed the laboratory experiments, and analyzed and interpreted the data.

C. A. C. performed the SEM/EDS imaging, XRD measurements, and thermogravimetric analysis. J. T. J. performed the simulations for total phosphate removal.

Cid, C. A., Jasper, J. T., & Hoffmann, M. R. (2018). Phosphate Recovery from Human Waste via the Formation of Hydroxyapatite during Electrochemical Wastewater Treatment. *ACS Sustainable Chemistry & Engineering*. doi:10.1021/acssuschemeng.7b03155

The patent for the Caltech Solar Toilet described in **Chapter 2** has been filed under the United States Patent and Trademark Office application number US20140209479. The patent application describes the invention of the "Self-contained, PV-powered domestic toilet and wastewater treatment system". C. A. C. was one of the inventors. C. A. C. participated in the preparation of the materials for the patent.

Hoffmann, M.R., Aryanfar, A., Cho, K., Cid, C.A., Kwon, D., Qu, Y. (2013) US Patent Application 20140209479 (A1) Washington, DC: U.S. Patent and Trademark Office. Available from the US PTO Patent Application Full Text and Image Database.

The smart maintenance solution described in **Chapter 5** has been filed under the United States Patent and Trademark Office application number US20170008775. The patent application described the invention of the "Maintenance self-diagnosis and guide for a self-contained wastewater treatment system". C. A. C. was one of the inventors. C. A. C. participated in the preparation of the materials for the patent.

Finke, C.E., Cid, C.A., Hoffmann, M.R., Hanan, A.K., Pinkston III, D.H., Vanier, M.C. (2016) US Patent Application 20170008775 (A1) Washington, DC: U.S. Patent and Trademark Office. Available from the US PTO Patent Application Full Text and Image Database.

TABLE OF CONTENTS

LIST OF ILLUSTRATIONS

Supplementary figures

LIST OF TABLES

Supplementary tables

Chapter 1

INTRODUCTION

1.1. A global sanitation crisis

In 2000, the United Nations defined a set of eight international development goals known as Millennium Development Goals to be achieved by 2015 (United Nations, 2016). These goals were aimed at eradicating extreme poverty and hunger, giving access to primary education, promoting gender equality, reducing child mortality, improving maternal health, combatting diseases, ensuring environmental sustainability, and developing a global partnership for development. Target 7C under Goal 7 to "ensure environmental sustainability" was to "halve, by 2015, the proportion of the population without sustainable access to safe drinking water and basic sanitation". The World Health Organization (WHO)/ United Nations Children's Fund (UNICEF) Joint Monitoring Programme for Water Supply, Sanitation, and Hygiene (JMP) has been the team responsible for reporting progress in country (Figure 1.1), regional, and global estimates of access to drinking water, sanitation, and hygiene since 1990 (WHO/UNICEF JMP, 2017a).

Between 1990 and 2015, progress was made to reach Target 7C. For example, global access to improved drinking water[2] supply increased from 76% to 91% of the world population (Figure 1.2 a) and access to improved sanitation[3] increased from 54% to 68% of the world population (Figure 1.2 b). Despite the progress made in all aspects of access to water, sanitation, and hygiene during the 1990-2015 period

[2] Improved drinking water sources are defined by the JMP as having a household connection to a potable water network, a public standpipe, a borehole, a protected dug well, a protected spring, or a rain water collection system.

[3] Improved sanitation is defined by the JMP as having a private toilet connected to a public sewer or a septic system, a pour-flush latrine, a simple pit latrine, or a ventilated improved pit latrine.

(World Health Organization, 2015), only access to improved drinking water has met the Millennium Development Goals target of at least 88% coverage. Access to improved sanitation remained 9% below its Millennium Development Goals target of 77%. But having access to improved drinking water alone does not guarantee that this water is not contaminated by fecal residues. Most low- and middle-income countries present non-negligible microbial contamination of their improved drinking water sources (Figure 1.3). This fecal contamination of improved drinking water sources ranges from approximately 10% in Europe to more than 25% in South East Asia, Eastern Mediterranean region, and Africa. Therefore, access to safe and clean water alone cannot happen without having access to proper sanitation.

In its 2017 report, the JMP introduced the sanitation ladder with five levels. These levels are built on previous indicators with the addition of criteria relative to the quality of the sanitation services. These levels are from least sanitary to most sanitary: open defecation (no service); unimproved sanitation services with bucket latrines or pit latrines without a slab or platform; limited sanitation services, which are improved facilities shared between two or more households; basic sanitation services which are improved facilities belonging to a single household; and safely managed sanitation services for which excreta are safely disposed of *in situ* (*e.g.,* ventilated improved pit latrine) or treated off-site (*e.g.,* wastewater treated in a municipal plant). Based on these updated levels, only 39% of the global population has access to safely managed sanitation (Figure 1.4). Thus, 61% of the world population, or 4.5 billion people, lack access to safely managed sanitation.

Access to safe sanitation is crucial to people's health and wellbeing: the lack of safe sanitation is directly correlated to high number of waterborne diseases such as Hepatitis A, diarrheal diseases, Cholera, Poliomyelitis, etc. through the contamination of water bodies by human excreta (Ashbolt, 2004; Montgomery & Elimelech, 2007). For instance, more than half-million children under 5 years old die annually from diarrheal diseases only (Julian, 2016), while the WHO estimates that 88% of diarrheal diseases are directly linked to unsafe water supplies and inadequate sanitation and hygiene (World Health Organization, 2014).

Sanitation projects that are designed for implementation in the developing world have traditionally used a segmented approach to improve sanitation (World Health Organization and UNICEF, 2014), breaking sanitation down to a value chain (Figure 1.5, top) composed of toilets or latrines (user interface), collection of excreta, transportation of excreta, treatment of excreta, and the extraction and use of potentially valuable by-products (Dijk, 2012). Each step of the value chain is a potential vector for mishandling of the waste and contamination of the environment. For instance, the Shit Flow Diagram (SFD) for the city of Dhaka, Bangladesh (Figure 1.5) shows that 99% of the population has access to improved sanitation; however, only 20% of the population has flush toilets connected to sewers and 79% has access to onsite toilets, but only 2% of the fecal waste is being effectively treated (Blackett, Hawkins, & Heymans, 2014). The remaining 98% is discharged to the environment with no adequate treatment. This extreme example illustrates the complexity of dealing with each step of the sanitation value chain separately when each step often

requires coordination among public and private actors in order to be achieved correctly.

The development of a system that safely treats the human waste close to the toilet(s) would also prevent contamination of the local environment and significantly reduce the risk of foodborne disease transmission by acting as an effective primary barrier against direct and indirect transmission or transport of disease agents (bacteria, viruses, protozoa and helminthes) to other humans (Figure 1.6). As a consequence, such a system would act as a strong and effective primary barrier to lower the risk associated when relying on secondary barriers related to hygienic practices on food handling and preparation as methods to prevent foodborne and waterborne diseases (Trench, Narrod, Roy, & Tiongco, 2012).

1.2. Current processes for safe sanitation

Safe sanitation technologies employ one or multiple processes to treat human waste. These processes are physical, chemical, biological, or a combination thereof. Physical treatment of human waste is often done thermally in simple drying processes, pressure during centrifugation, or by a combination of heat and pressure with pasteurization. These processes are very effective for treating biosolids such as the sludge material from pit latrines (Strauss, Larmie, & Heinss, 1997) or aerobic sludge from wastewater treatment plants (Metcalf & Eddy, 2014; Whitmore & Robertson, 1995). Physical processes can guarantee pathogen-free residuals but are often energy-intensive for small-scale systems. For instance, portable incinerating toilets can be used in remote environments and guarantee pathogen-free residuals but the incineration process destroys N-based nutrients in the waste (U.S. Environmental Protection Agency, 1999).

Chemical processes used in human waste disinfection are often oxidative processes carried out in a wide variety of scales for wastewater treatment. These processes range from chlorination of wastewater with addition of sodium hypochlorite (U.S. Environmental Protection Agency, 2003) or chlorine gas, to advanced oxidation processes using UV/ozone photochemical processes for hydroxyl radical generation (White, 2010). Although seldom used, direct or indirect electrochemical oxidation of pollutants in wastewater are “potential next-generation technologies for the treatment of contaminated water” (Radjenovic & Sedlak, 2015). Biosolid waste can also be treated chemically with reactions such as alkaline

hydrolysis that can be carried out on the biosolids when soda ash is added to sludge from a pit latrine (Neyens, Baeyens, & Creemers, 2003).

Biological processes are commonly employed in the treatment of wastewaters with aerobic and anaerobic microorganisms used in wastewater treatment plants (Metcalf & Eddy, 2014). Controlled microorganisms populations are also directly used for onsite treatment processes ranging from small scale wastewater treatment plants to composting (Langergraber et al., 2004) or even vermicomposting toilets (Adhikary, 2012). Anaerobic digestion of toilet waste to biogas is often suggested as a way to combine treatment and energy recovery but issues related to cost, maintenance, smell, and sometimes cultural adoption make those systems limited to rural areas (Schouten & Mathenge, 2010). Electrochemical biotechnologies such as microbial fuel cells are sometimes used to oxidize nutrients in wastewaters while producing electricity (Logan & Rabaey, 2012).

Despite all these technological developments, as stated in section 1.1, 4.5 billion people still lack access to safe sanitation. This global crisis is unacceptable to the Bill & Melinda Gates Foundation. This untenable situation became the driving force behind the research and development presented in this thesis.

1.3. The Gates Foundation's "Reinvent The Toilet Challenge"

In February 2011, The Bill & Melinda Gates Foundation announced a major challenge to university researchers to "Reinvent the Toilet" (Bill & Melinda Gates Foundation, 2013). The primary goal of the Bill & Melinda Gates Foundation was to engage universities in the development of new and innovative processes to treat human bodily wastes at the site of origin without discharge to the ambient environment or discharge to conventional sewer systems, septic tanks, cesspools, or open drainage systems. The overarching goal of the Bill & Melinda Gates Foundation Global Development Program within the context of their Water, Hygiene and Sanitation initiative was to develop practical low-cost solutions that could be implemented in regions of the world that lack access to safe and affordable sanitation. The primary challenge was to develop a comprehensive approach to designing, developing, testing, and prototyping systems that could collect and process human waste on-site at the source of origin and at the same time produce useful byproducts, including fertilizer, mineral salts, energy, purified, and disinfected water with no solid of liquid discharge to the environment. A cost constraint was set at a maximum of $0.05 per person per day including capital costs and operating expenses. In this thesis, I present my work on the development of a "Reinvented Toilet": a self-contained toilet wastewater treatment and recycling system, called the "Caltech Solar Toilet".

1.4. The Caltech Solar Toilet

The Caltech Solar Toilet was invented as a response to the challenge set by the Bill & Melinda Gates Foundation described in section 1.3. The Caltech Solar Toilet has at its core unit an electrochemical reactor using semiconductor anodes for chloride oxidation to reactive chlorine that can provide complete disinfection of indicator microorganisms (Huang et al., 2016), oxidize organic nitrogen (Cho & Hoffmann, 2014; Kim, Choi, Choi, Hoffmann, & Park, 2013), and eventually mineralize the organic material (Jasper, Shafaat, & Hoffmann, 2016) present in the wastewater. The system has been designed to be autonomous and infrastructure-free: it does not need a connection to a water source, a sewer system, or an electrical grid (Hoffmann et al., 2013).

Three generations of Solar Toilet prototypes have been developed and tested across the world since 2012 (Table 1.1, Figure 1.1), they are based on the following treatment stream: one or multiple toilets, urinals, and washbasins are connected to a collection tank (wastewater tank) with the potential for biological pre-treatment, then wastewater is pumped into the electrochemical reactor in which it undergoes electrolysis for a fixed amount of time. The treated water passes through a filter before being pumped into a storage tank where it can be reused as toilet flushing water. The whole process is automatized and can be connected to grid electricity or run on solar panels with backup battery storage for use throughout 24 hours of continuous operation. The simplified flow diagram of the first-generation prototypes is schematized in Figure 1.7 along with the implication of Chapters 2, 3, and 4 of this thesis.

1.5. Thesis overview

Chapter 2 of this thesis provides more details on the Solar Toilet prototypes and their testing under field conditions in India and China. The general concept, specific design elements, and treatment approach proven to be viable for the treatment of raw domestic wastewater, human urine, and human feces. After several hours of photovoltaic-powered (PV-powered) electrochemical treatment, the turbid, black-water influent can be clarified with the elimination of the suspended particles along with the reduction or total elimination of the chemical oxygen demand (COD), total enteric coliform disinfection via *in situ* reactive chlorine species generation, and the elimination of measurable protein after 3 to 4 hours of electrochemical treatment.

In **Chapter 3** of this thesis, the energy efficiency of the Solar Toilets is improved by the addition of a microbial fuel cell system for urine pre-treatment. The microbial fuel cell system used consists of two stacks of 32 fuel cells connected in parallel. The pre-treatment of human urine by anodic microorganisms occurred with concomitant electrical energy recovery. This usage of microbial fuel cells can lower the energy cost for treating human waste while recovering the necessary electrical energy to divert the urine flow, making this approach an overall energy gain for the entire onsite self-contained human waste treatment system.

Chapter 4 of this thesis provides information on nutrient recovery from the Caltech Solar Toilets. It describes the co-production of crystallized Mg-containing hydroxyapatite during the treatment of wastewater. The purpose of this study was to evaluate the potential for phosphate removal from human wastewater during electrochemical treatment using the same combined anode-cathode system

described in Chapter 2. Phosphate-containing precipitates were identified and phosphate removal efficiencies were measured in authentic and synthetic toilet wastewater. Experiments in synthetic wastewater allowed quantification of the effects of ion composition, buffering capacity, current density, and electrode surface area to volume ratio on phosphate removal kinetics and equilibria.

Chapter 5 of this thesis provides more practical applications of my work in developing the Caltech Solar Toilets. A key finding from the field studies of Chapter 2 was the need for a maintenance plan. I and several of my coworkers are developing a smart maintenance technology for onsite wastewater systems. Another key finding from Chapter 3 was that the use of a MFC system for pre-treating urine could be even more effective and easier to install in a Solar Toilet if all the flush water could enter the MFC. This approach is under investigation. The development of a standard on "Reinvented Toilets" is also addressed in Chapter 5.

Table 1.1: Description of the Caltech Solar Toilet prototypes of different generations (Gen.) with manufacturing and field partners in the USA, India, China, and South Africa.

Map ref.	Gen.	Configuration	Testing		Manufacturing and field partners
			Location	Period	
PAS	1	PV-powered self-contained bathroom with wastewater treatment and recycling unit in a shipping container. Design for 40-60 users/day.	Pasadena, CA, USA	06/2013 to 06/2017	-
KYM			Kottayam, Kerala, India	04/2014 to 01/2016	Mahtamah Gandhi University of Science and Technology
YXG			Yixing, Jiangsu, China	12/2014 to 05/2015	Yixing Eco-Sanitary Manufacture Co.
AMD	1	Grid-powered wastewater treatment and recycling unit connected to an "eToilet" public toilet (Eram Scientific, Trivandrum, Kerala, India). Design for 40 users/day.	Ahmedabad, Gujarat, India	04/2014 to 01/2016	Eram Scientific and Indian Institute of Technology (IIT) Gandhinagar
COI	2	Grid-powered wastewater treatment and recycling unit connected apartment buildings. Designed for 5 families.	Coimbatore, Tamil Nadhu, India.	10/2015 to 08/2017	The Kohler Company (design and construction) and RTI International (field testing).
YXG	2	PV-powered self-contained bathroom with wastewater treatment and recycling unit in a shipping container with advanced anaerobic/aerobic pre-treatment. Designed from 40-60 users/day to 200 users/day.	Yixing, Jiangsu, China	05/2015 to present	Yixing Eco-Sanitary Manufacture Co.
COI	3	Grid-powered wastewater treatment and recycling unit with advanced anaerobic/aerobic pre-treatment connected apartment buildings. Designed for 5 families.	Coimbatore, Tamil Nadu, India.	10/2017 to present	The Kohler Company (design and construction) and RTI International (field testing).
DUR	3	PV-powered self-contained bathroom with wastewater treatment and recycling unit in a shipping container with advanced anaerobic/aerobic pre-treatment. Designed from 40-60 users/day to 200 users/day.	Durban, South Africa	01/2018 to present	Yixing Eco-Sanitary Manufacture Co. (design and construction) and Water Research Council for South Africa (field evaluation).

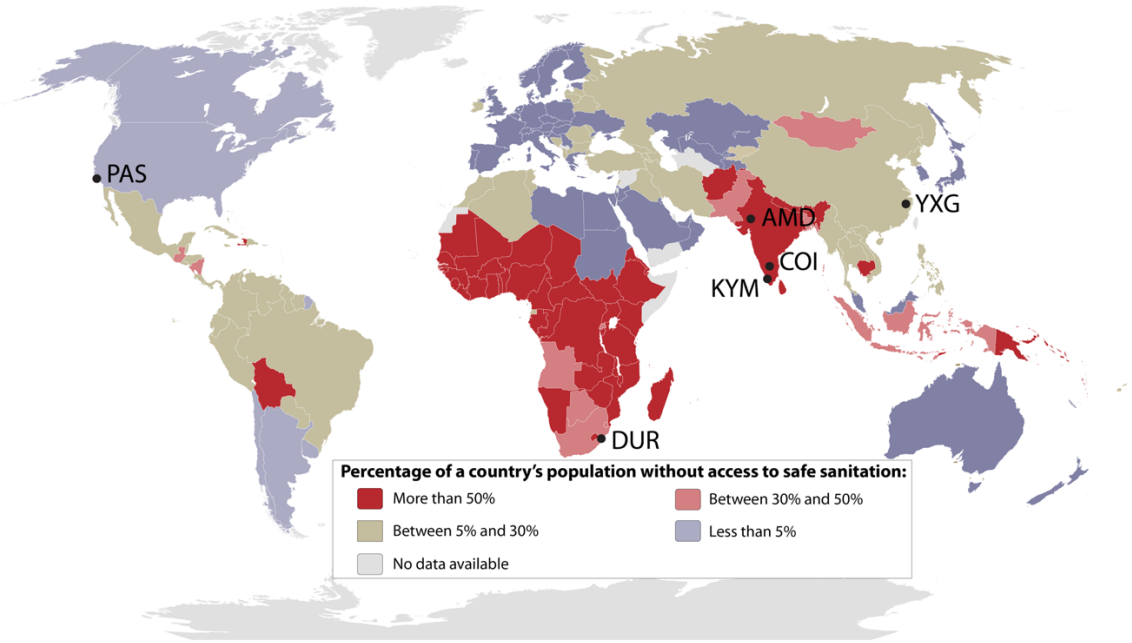

Figure 1.1: Percentage of a country's population without access to safe sanitation in 2015 according to the World Health Organization (World Health Organization 2015). Location of the prototype testing sites across the world: AMD, Ahmedabad, Gujarat, India; COI, Coimbatore, Tamil Nadu, India; DUR, Durban, Kuazulu-Natal, South Africa; KYM, Kottayam, Kerala, India; PAS, Pasadena, California, USA; YXG, Yixing, Jiangsu, China.

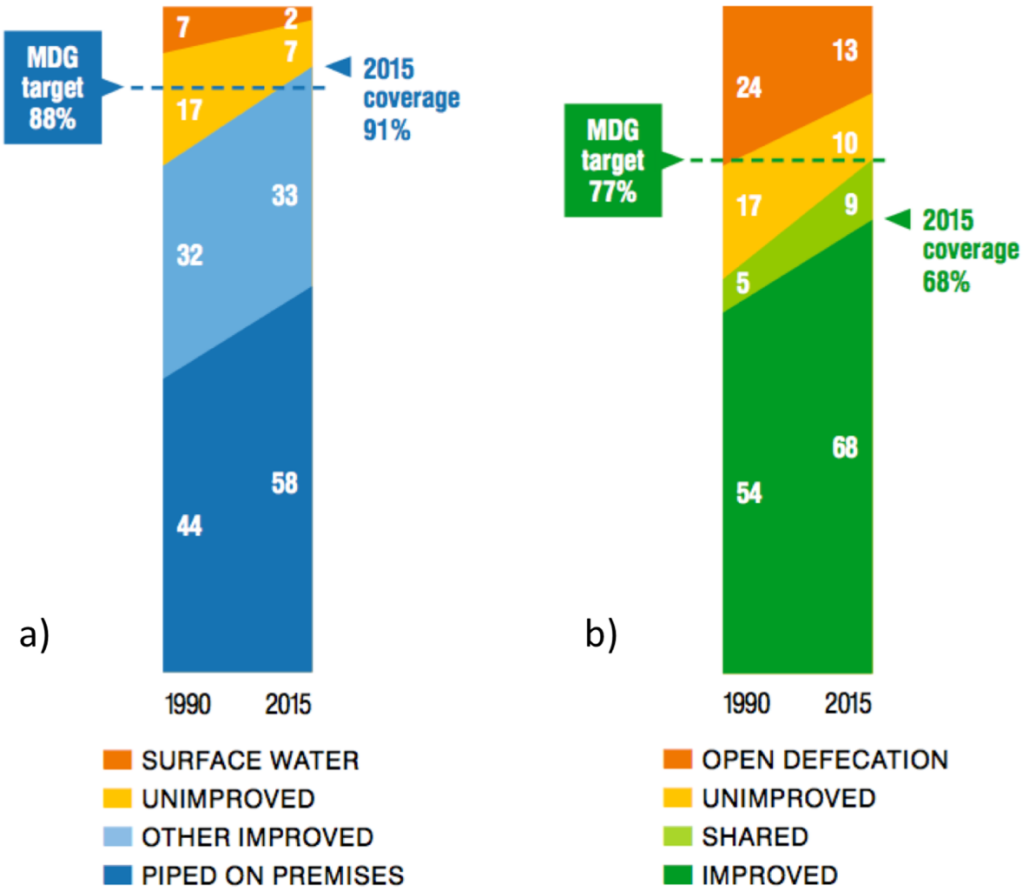

Figure 1.2: Trends in global drinking water (a) and sanitation (b) coverage and Millenium Development Goal target coverage (%), 1990-2015. Reproduced from *Progress on sanitation and drinking water: 2015 update and MDG assessment* with the permission of the World Health Organization and UNICEF (World Health Organization, 2015).

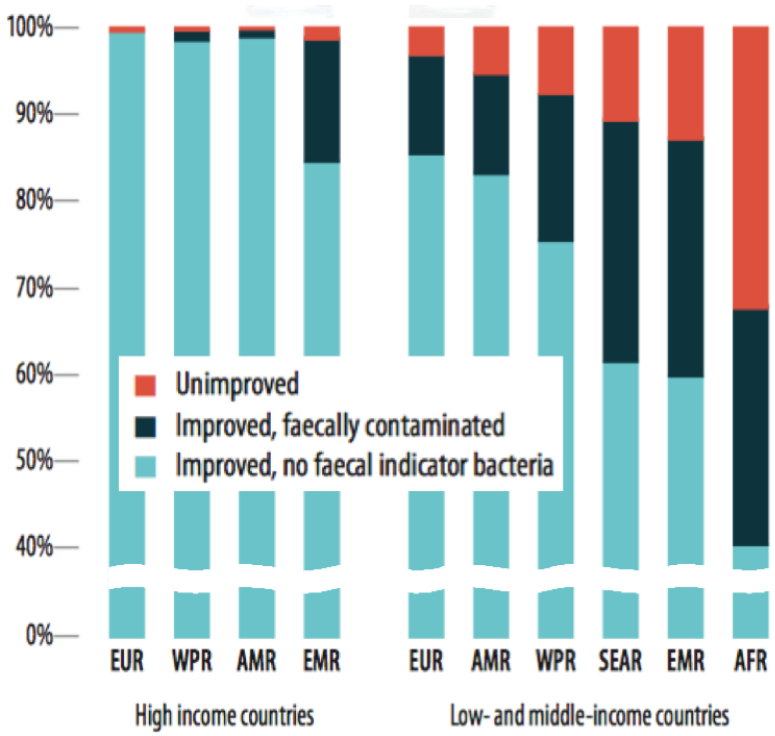

Figure 1.3: "Proportion of population accessing difference types of drinking water, by region and by microbial contamination level, 2012. AFR: Africa; AMR: Americas; EMR: Eastern Mediterranean; EUR: Europe; SEAR: South East Asia; WPR: Western Pacific. Microbially contaminated water has detectable E. coli or thermotolerant coliforms in a 100 mL sample, while samples showing no detectable faecal indicator bacteria (<1 per 100 mL) are compliant with WHO guideline values and most national standards." Reproduced from *Preventing diarrhoea through better water, sanitation and hygiene: exposures and impacts in low-and middle-income countries* with the permission of the World Health Organization (World Health Organization, 2014).

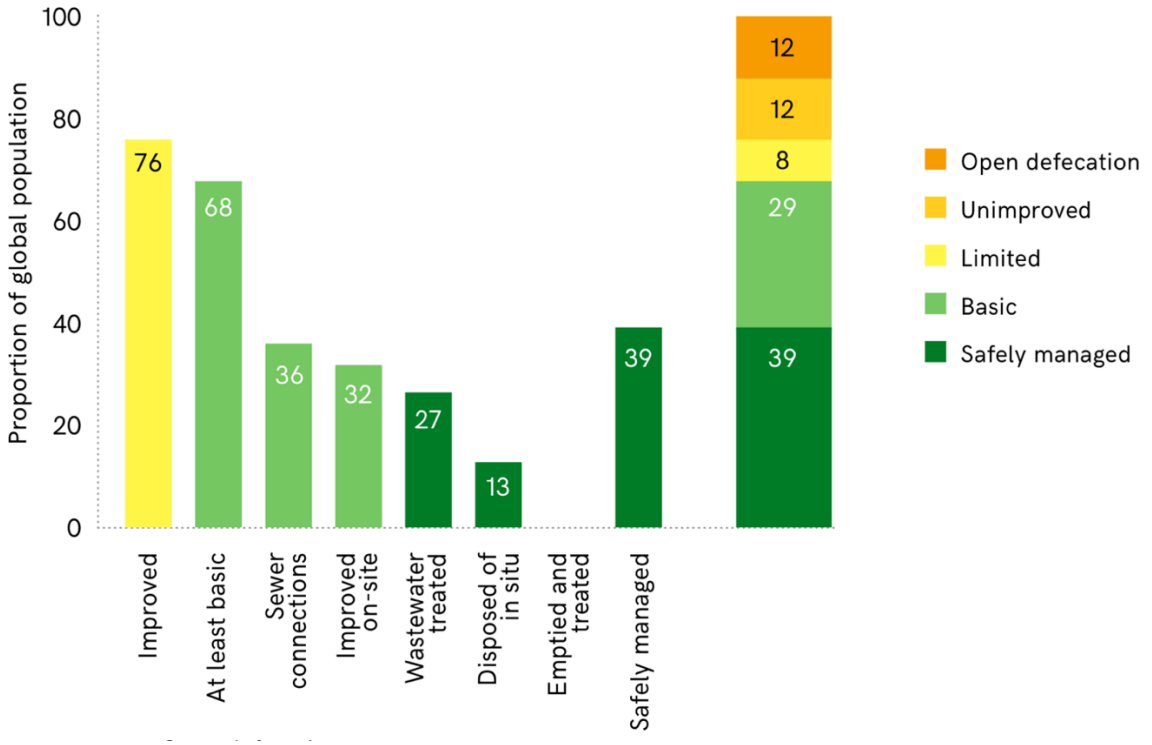

Figure 1.4: Proportion of the global population using sanitation facilities meeting specific criteria for safely managed services. Reproduced from *Progress on drinking water, sanitation and hygiene: 2017 update and SDG baselines* with the permission of the World Health Organization (WHO/UNICEF JMP, 2017b).

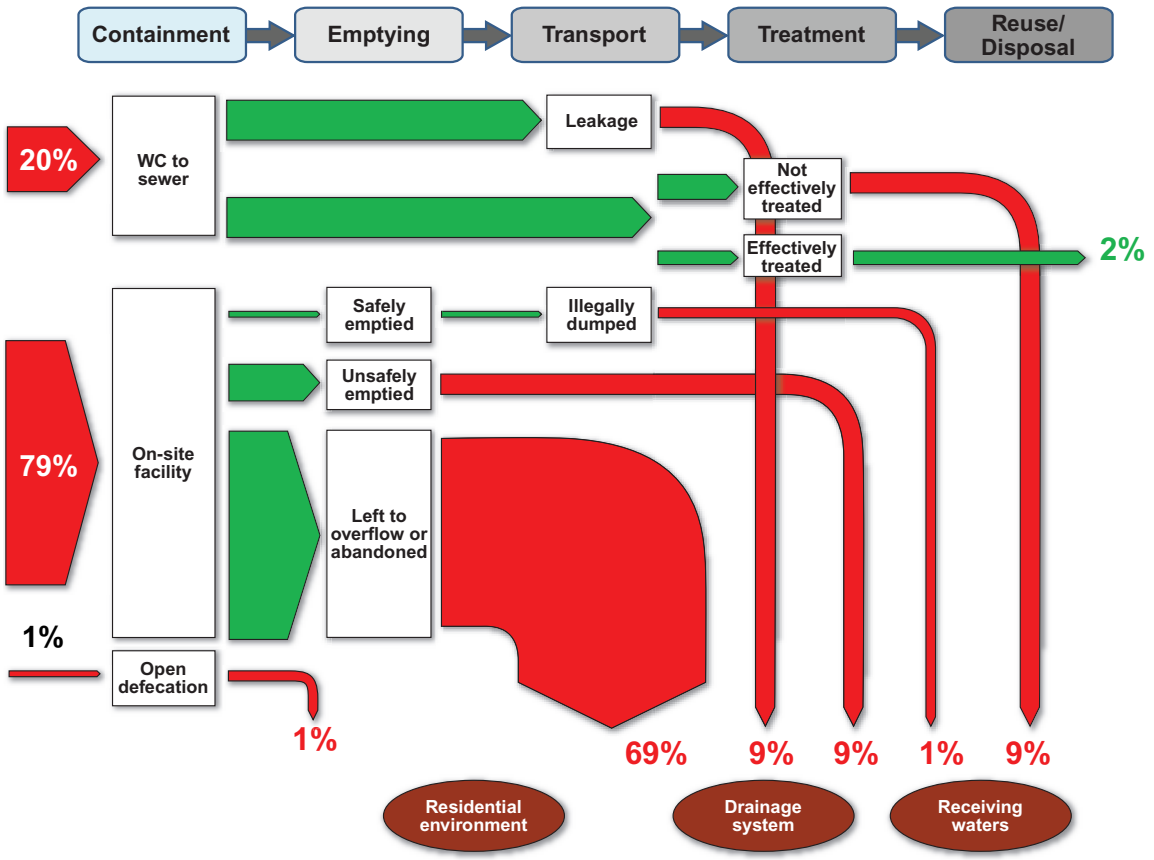

Figure 1.5: Sanitation value chain (top) and Shit Flow Diagram (SFD) for the city of Dhaka, Bangladesh. Reproduced with the permission of The World Bank Group (Blackett et al., 2014).

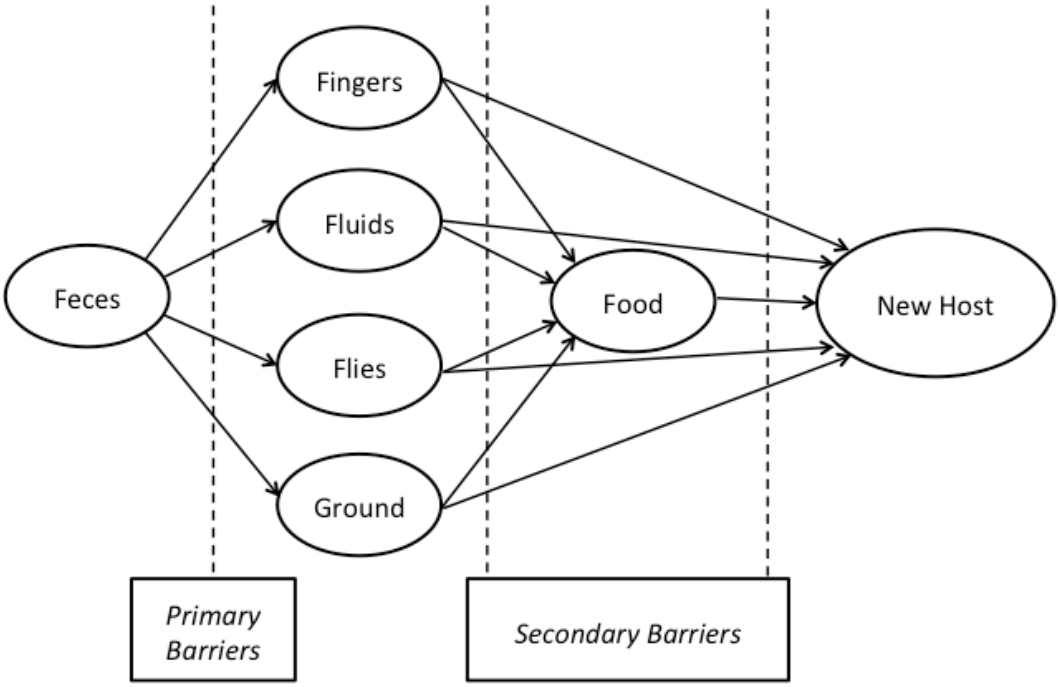

Figure 1.6: Waterborne and foodborne diseases transmission and control. (Water Supply and Sanitation Collaborative Council & World Health Organization, 2005)

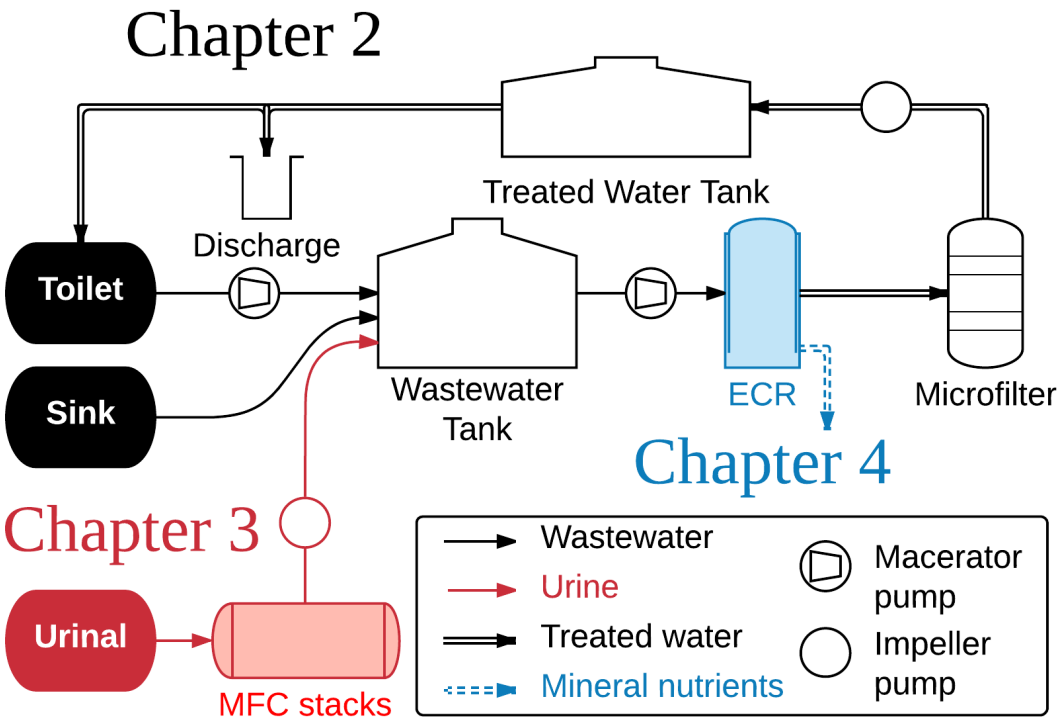

Figure 1.7: System flow diagram of the 2014 Caltech Solar Toilet prototypes with capacity and residence time of the relevant components. Relevant components to chapters 2, 3, and 4 of this thesis are highlighted with a different color. Chapter 2 (black): design and preliminary implementation of onsite electrochemical wastewater treatment and recycling toilets for the developing world. Chapter 3 (red): urine microbial fuel cells in a semi-controlled environment for onsite urine pre-treatment and electricity production. Chapter 4 (blue): phosphate recovery from human waste via the formation of hydroxyapatite during electrochemical wastewater treatment.

1.6. References

Adhikary, S. (2012). Vermicompost, the story of organic gold: A review. *Agricultural Sciences, 3*(7), 905.

Ashbolt, N. J. (2004). Microbial contamination of drinking water and disease outcomes in developing regions. *Toxicology, 198*(1), 229-238. doi:10.1016/j.tox.2004.01.030

Bill & Melinda Gates Foundation. (2013). Water, Sanitation & Hygiene: Reinvent The Toilet Challenge.

Blackett, I., Hawkins, P., & Heymans, C. (2014). The Missing Link in Sanitation Service Delivery – A Review of Fecal Sludge Management in 12 Cities.

Cho, K., & Hoffmann, M. R. (2014). Urea Degradation by Electrochemically Generated Reactive Chlorine Species: Products and Reaction Pathways. *Environmental science & technology, 48*(19), 11504-11511. doi:10.1021/es5025405

Dijk, M. P. v. (2012). Sanitation in Developing Countries: Innovative Solutions in a Value Chain Framework. In H. Sun (Ed.), *Management of Technological Innovation in Developing and Developed Countries*.

Hoffmann, M. R., Aryanfar, A., Cho, K., Cid, C. A., Kwon, D., & Qu, Y. (2013). Self-contained, pv-powered domestic toilet and wastewater treatment system: Google Patents.

Huang, X., Qu, Y., Cid, C. A., Finke, C., Hoffmann, M. R., Lim, K., & Jiang, S. C. (2016). Electrochemical disinfection of toilet wastewater using wastewater electrolysis cell. *Water Research, 92*, 164-172. doi:10.1016/j.watres.2016.01.040

Jasper, J. T., Shafaat, O. S., & Hoffmann, M. R. (2016). Electrochemical Transformation of Trace Organic Contaminants in Latrine Wastewater. *Environ Sci Technol, 50*(18), 10198-10208. doi:10.1021/acs.est.6b02912

Julian, T. R. (2016). Environmental transmission of diarrheal pathogens in low and middle income countries. *Environ Sci Process Impacts, 18*(8), 944-955. doi:10.1039/c6em00222f

Kim, J., Choi, W. J. K., Choi, J., Hoffmann, M. R., & Park, H. (2013). Electrolysis of urea and urine for solar hydrogen. *Catalysis Today, 199*(0), 2-7. doi:10.1016/j.cattod.2012.02.009

Langergraber, G., Rieger, L., Winkler, S., Alex, J., Wiese, J., Owerdieck, C., . . . Maurer, M. (2004). A guideline for simulation studies of wastewater treatment plants. *Water Science and Technology, 50*(7), 131-138.

Logan, B. E., & Rabaey, K. (2012). Conversion of Wastes into Bioelectricity and Chemicals by Using Microbial Electrochemical Technologies. *Science, 337*(6095), 686-690. doi:10.1126/science.1217412

Metcalf, & Eddy. (2014). *Wastewater Engineering: Treatment and Resource Recovery*: McGraw-Hill international ed.

Montgomery, M. A., & Elimelech, M. (2007). Water and sanitation in developing countries: including health in the equation: ACS Publications.

Neyens, E., Baeyens, J., & Creemers, C. (2003). Alkaline thermal sludge hydrolysis. *Journal of Hazardous Materials, 97*(1), 295-314. doi:10.1016/S0304-3894(02)00286-8

Radjenovic, J., & Sedlak, D. L. (2015). Challenges and Opportunities for Electrochemical Processes as Next-Generation Technologies for the Treatment of Contaminated Water. *Environmental science & technology, 49*(19), 11292-11302. doi:10.1021/acs.est.5b02414

Schouten, M., & Mathenge, R. (2010). Communal sanitation alternatives for slums: A case study of Kibera, Kenya. *Physics and Chemistry of the Earth, Parts A/B/C, 35*(13), 815-822.

Strauss, M., Larmie, S. A., & Heinss, U. (1997). Treatment of sludges from on-site sanitation — low-cost options. *Water Science and Technology, 35*(6), 129-136. doi:10.1016/S0273-1223(97)00103-0

Trench, P. C., Narrod, C., Roy, D., & Tiongco, M. (2012). Responding to health risks along the value chain. *Edited by Shenggen Fan and Rajul Pandya-Lorch*, 93.

U.S. Environmental Protection Agency. (1999). *Water Efficiency Technology Fact Sheet. Incinerating Toilets*. Retrieved from

U.S. Environmental Protection Agency. (2003). *Wastewater Technology Fact Sheet. Disinfection for Small Systems*. Retrieved from

United Nations. (2016). United Nations Millennium Development Goals. Retrieved from https://www.un.org/millenniumgoals/

Water Supply and Sanitation Collaborative Council, & World Health Organization. (2005). Sanitation and hygiene promotion: programming guidance.

White, G. C. (2010). *White's handbook of chlorination and alternative disinfectants*. Hoboken, NJ: John Wiley & Sons.

Whitmore, T. N., & Robertson, L. J. (1995). The effect of sewage sludge treatment processes on oocysts of Cryptosporidium parvum. *Journal of Applied Bacteriology, 78*(1), 34-38. doi:10.1111/j.1365-2672.1995.tb01670.x

WHO/UNICEF JMP. (2017a). About the JMP. Retrieved from https://washdata.org/how-we-work/about-jmp

WHO/UNICEF JMP. (2017b). *Progress on drinking water, sanitation and hygiene: 2017 update and SDG baselines*.

World Health Organization. (2014). *Preventing diarrhoea through better water, sanitation and hygiene: exposures and impacts in low-and middle-income countries*: World Health Organization.

World Health Organization. (2015). *Progress on sanitation and drinking water: 2015 update and MDG assessment*.

World Health Organization and UNICEF. (2014). *Progress on Drinking Water and Sanitation - 2014 update*.

Chapter 2

DESIGN AND PRELIMINARY IMPLEMENTATION OF ONSITE ELECTROCHEMICAL WASTEWATER TREATMENT AND RECYCLING TOILETS FOR THE DEVELOPING WORLD

Clément A. Cid[1]

in collaboration with

Yan Qu[1] and Michael R. Hoffmann[1]

[1]Linde-Robinson Laboratories, California Institute of Technology, Pasadena, CA

Prepared for submission to

Environmental Science: Water Research and Technology

C. A. C. is the principal and coordinating author of the manuscript. C. A. C. and Y. Q. designed and constructed the prototypes. C. A. C. directed the field testing and sampling methods, and analyzed and interpreted the data. M. R. H. and Y. Q. provided guidance as well as intellectual and writing contributions.

2.1. Abstract

Self-contained toilet wastewater treatment system prototypes based on electrochemical oxidation of feces and urine using bi-layered semiconductor anodes ($[Bi_2O_3]_z[TiO_2]_{1-z}/Ir_xTa_yO_2/Ti$) have been designed, constructed, and implemented in regions where access to proper and sufficient sanitation is limited. Prototypes were designed to fit in shipping containers in order to provide toilets and onsite wastewater treatment with clean water recycling. Units were designed to handle the waste of 25 users per day (or 130 L of toilet wastewater). The first prototype was tested on the Caltech campus (Pasadena, California) followed by improved second-generation prototypes that were subsequently installed in India (Ahmedabad, Gujarat and Kottayam, Kerala) and China (Yixing, Jiangsu) for open use in various public settings. The prototypes were able to provide for the disinfection of pathogens (<10 MPN *Total coliforms* and <1 MPN *Fecal coliform* indicator organisms per 100 mL), reduction of chemical oxygen demand (<100 mg O_2 L^{-1}), ammonia (<10 mg N L^{-1}), and color at an average energy consumption of 35 Wh L^{-1}. The treated wastewater was recycled for use as toilet flushing water.

Keywords

onsite sanitation; electrochemical wastewater treatment; chlorine disinfection

2.2. Introduction

In February 2011, The Bill & Melinda Gates Foundation (BMGF) announced a major challenge to university researchers to "Reinvent the Toilet." The primary goal of the BMGF was to engage universities in the development of new and innovative methods to treat human bodily wastes at the site of origin without discharge to the ambient environment or discharge to conventional sewer systems, septic tanks, cesspools, or open drainage systems. The overarching goal of the BMGF Global Development Program within the context of their Water, Hygiene and Sanitation initiative was to develop practical low-cost solutions that could be implemented in regions of the world that lack access to safe and affordable sanitation. The primary challenge was to develop a comprehensive approach to design, development, testing, and prototyping of systems that could collect and process human waste on-site at the source of origin and at the same time produce useful byproducts including fertilizer, mineral salts, energy, purified, and disinfected water with no solid or liquid discharge to the environment. The overarching objective is to provide suitable sanitary systems for the 2.6 billion people who currently lack access to safe and affordable sanitation (Figure 2.1). A cost constraint was set at a maximum of $0.05 per person per day include capital costs and operating expenses.

The development of integrated networks and facilities for the transport and subsequent treatment of domestic wastewater has been a key factor in the growth and development of modern urban environments. Sanitation has accompanied human development from early civilizations with rudimentary systems (De Feo et al., 2014) to mid-19th century first large-scale sewer networks in American and

European cities (Burian & Edwards, 2002; Gandy, 1999; Kaika & Swyngedouw, 2000). Although a well-constructed modern urban sewer network can be hygienic and efficient due to economies of scale (Metcalf & Eddy, 2014), they also have major drawbacks, which include nuisance odors from improper operation and maintenance (Boon, 1995), local groundwater contamination due to leakage from improper connections and corrosion of pipes and concrete sewers (American Society of Civil Engineers, 2013; Eiswirth & Hötzl, 1997), or prohibitively expensive capital investments (Corcoran et al., 2010).

For these reasons, developing countries have often turned to non-sewered sanitation (NSS) systems for the disposal of human bodily waste. Furthermore, in areas with limited access to water, technologies have traditionally been restricted to dry or manual pour-flush types of toilets such as composting toilets or pit latrines (Starkl, Stenström, Roma, Phansalkar, & Srinivasan, 2013). Although these waterless technologies appear attractive because of their limited need for water, they do not provide the olfactory or sanitary comfort of flush toilets (Lin et al., 2013). In addition, they are not always reliable for disinfection, pathogen removal (Montgomery & Elimelech, 2007), or for preventing subsequent pollution by latrine waste soils and groundwater (Dzwairo, Hoko, Love, & Guzha, 2006). In areas that have access to water, decentralized toilets using flush technologies are most often connected to septic tanks. Septic tank treatment systems require large land surface areas to build effective leaching fields that are necessary for the safe elimination of pathogens (Title V septic system in the United States) and can often lead to fecal contamination of local

water sources if improperly installed and maintained (Beal, Gardner, & Menzies, 2005; Yates, 1985, 1987).

Therefore, a technology capable of treating and recycling toilet wastewater at low cost would have significant advantages over traditional NSS solutions (*vide supra*). In this regard, Radjenovic and Sedlak have identified electrolysis processes such as potentiostatic electrochemical oxidation as "potential next-generation technologies for the treatment of contaminated water" (Radjenovic & Sedlak, 2015). Electrochemical oxidation of wastewater has been investigated for more than 30 years with a focus on organic pollutant degradation (Comninellis, 1994; Pletcher & Walsh, 1990), most systems rely on the anodic formation of free hydroxyl radical $OH^{\cdot}$ from water oxidation or the direct oxidation of the compounds of interest. Both processes consume a lot of energy to achieve appropriate contaminant removal (Comninellis & Chen, 2009).

Weres and collaborators (Kesselman, Weres, Lewis, & Hoffmann, 1997; H. Park, Vecitis, Choi, Weres, & Hoffmann, 2008; Hyunwoong Park, Vecitis, & Hoffmann, 2008) investigated the use of multilayer semiconductor anodes to generate surface-bound hydroxyl radicals $OH^{\cdot}$ for organics degradation (Hana Park, Choo, Park, Choi, & Hoffmann, 2013; Weres, 2009; Weres & O'Donnell, 2003). These multilayer semiconductor anodes have a low overpotential for the oxidation of chloride to chlorine (Cho & Hoffmann, 2014). This capability makes the multi-layer semiconductor anodes particularly suitable for the direct formation of Reactive Chlorine Species (RCS) from the oxidation of the chloride naturally present in the human wastewater (Cho & Hoffmann, 2015; Cho et al., 2014; Huang et al., 2016; Yang,

Shin, Jasper, & Hoffmann, 2016). Although the previously published laboratory results have shown the feasibility of anodic oxidation for toilet wastewater treatment (Cho et al., 2014; Huang et al., 2016; Jasper, Shafaat, & Hoffmann, 2016; Yang et al., 2016), there is no literature available about the automated, autonomous on-site electrochemical treatment of toilet wastewater under actual field operating and testing conditions. Herein, we present the results of field studies employing electrochemical wastewater treatment for the removal of chemical oxygen demand and for recycling of disinfected and clarified water for use as toilet flushing water.

2.3. Guidelines, materials and methods

2.3.1. Health considerations for an onsite wastewater recycling systems

The primary sources of biological and chemical contamination entering onsite wastewater treatment systems are from human excreta. The amount and the composition of human excreta varies greatly from one individual to another (Wignarajah, Litwiller, Fisher, & Hogan, 2006; Wydeven & Morton A. Golub, 1990) with an average of 1 L to 1.5 L of urine and 300 g to 450 g of feces per adult per day. Feces are often the major carrier of pathogens in human excreta (Sadowsky & Whitman, 2010) with an average number of 10^{11} CFU (colony-forming units) of bacteria per gram of feces for a healthy adult individual. Given that pathogen die-off times in untreated human excreta are between one and three months for bacteria and viruses, and several months for helminth eggs (Atlas, 1984), a reliable and rapid removal of pathogens down to acceptable levels is crucial for the success of an onsite human wastewater treatment technology. For example, the World Health Organization considers that a safe pathogen level appropriate for water reuse in agriculture is less than 1 CFU per 100 mL for typical indicator organisms *E. coli*. (World Health Organization, 2006).

When onsite wastewater treatment systems are installed close to their users in order to minimize installation costs, such systems can become potential threats to the health of humans living nearby when the wastes are not properly contained (Hynds, Thomas, & Pintar, 2014) or sufficiently treated. Natural barriers such as the leaching fields for septic tanks or clay or concrete walls for dry latrine pits are not always effective barriers (Dzwairo et al., 2006; Graham & Polizzotto, 2013). Risks of

contamination are further increased when the users come into contact with effluent streams (*e.g.*, treated water and/or biosolids) produced by onsite sanitation systems. Thus, the treated and recycled waters that are processed onsite must be free of pathogens and have an acceptable physicochemical composition that meets conventional water quality standards for reuse.

However, technical standards that have been adopted in many countries help to regulate the composition of recycled water for domestic reuse but they are often limited to large scale indirect and direct potable reuse of conventional wastewater treatment plant effluents (ISO 16075-1, 2012) or the treatment and reuse of non-fecal contaminated water (greywater) primarily from sinks, washers, and showers (NSF/ANSI Standard 350). Therefore, a toilet wastewater recycling system has to produce an effluent that does not damage the system itself, is safe for users, and contains enough residual disinfecting capacity to prevent subsequent chemical and microbial contamination due to exposure to the treated and recycled water.

In addition to the meeting the basic sanitary and water quality requirements, a self-contained toilet and wastewater treatment system for use in developing countries needs to be affordable, durable, and functional in an off-grid environment with limited access to electricity, fresh water, and sewers.

2.3.2. Choice of prototype testing locations

Four pre-alpha prototypes of a similar design (Figure 2.2) were tested in the USA, India, and China (Figure 2.1). The first pre-alpha prototype was tested on the campus of the California Institute of Technology (Caltech) in Pasadena, California (PAS prototype, Figure 2.2 a) for preliminary data gathering and early design adjustments;

two additional pre-alpha prototypes (AMD and KYM) were designed and built on the Caltech campus and then shipped to India for field trials in two different locations. The prototype designated as AMD (Figure 2.2 c) was installed in a public park in the city of Ahmedabad in Gujarat State of northwest India. Ahmedabad has a semi-arid climate and is the sixth largest city of India with more than 6.3 million inhabitants. The prototype designated as KYM (Figure 2.2 b) was installed in the campus of Mahatma Gandhi University near the School of Environmental Sciences in Amalagiri district of Kottayam City in the State of Kerala, which is located in southwestern India. Kottayam has a tropical climate with a population of 200,000 inhabitants. A fourth pre-alpha prototype was constructed and tested in the Municipal Yixing Elementary School of Yixing, China (YXG prototype, Figure 2.2 d) in collaboration with Yixing Eco-Sanitary Manufacture Co.

2.3.3. Monitoring and evaluation methods

Chemical oxygen demand (COD), total nitrogen (TN), total suspended solids (TSS), and indicator organisms *E. coli*, *Total coliform*, and *Fecal coliform* bacteria were measured to assess the wastewater treatment efficacy. Because an effective removal of pathogens can often be observed when COD and TN decrease during the course of the treatment (Metcalf & Eddy, 2014; Sharma, Tyagi, Saini, & Kazmi, 2016), the measurement of indicator microorganisms was limited to few non-consecutive days of operation.

The voltage at the electrodes and the current delivered by the power supply to the electrode arrays were continuously measured using a personalized data logger (Programmed Scientific Instruments, Arcadia CA) at regular intervals (*e.g.*, every 10

seconds). The activation and deactivation of pumps as well as the status of water level sensors were monitored and recorded using the same data logger. At each recording time, the data logger stored a new line of values of the different components of the system in a daily Comma Separated Values (CSV) file. The data was tagged with the local time and date and stored in a solid-state device in the computer controlling the system. The CSV files were regularly retrieved by an operator.

2.3.4. Analytical methods

COD was measured using a reflux digestion system with water condensers followed by titration according to Standard Method 5220 (Water Environmental Federation & American Public Health Association, 2005) or via colorimetric method similar to Hach Method 8000 (Hach Company, Loveland CO). TN was determined using persulfate digestion (Hach Method 10071). Total Kjeldahl Nitrogen (TKN) was determined by distillation (Indian Standard 5194-1969). Cl^-, $NH_4^+ + NH_3$, Ca^{2+}, and Mg^{2+} concentrations were determined by ion chromatography (Dionex ICS 2000; AS19G anions, CS12A cations).

Disinfection was assessed by estimating the quantity of indicator organisms *E. coli*, *Total coliforms*, and *Fecal coliforms* with the following respective EPA methods: 1103.1 (U.S. Environmental Protection Agency, 2010a), 9132 (U.S. Environmental Protection Agency, 1986), and 1680 (U.S. Environmental Protection Agency, 2010b) with appropriate dilutions. Free chlorine (FC) was measured by reaction with N,N-diethyl-p-phenylenediamine (DPD) indicator in accordance with Standard Method 4500-Cl G (Water Environmental Federation & American Public Health Association, 2005) and Hach Method 8021. Total chlorine (TC) was measured by the

Amperometric Titration Method in accordance with Standard Method 408 C (Water Environmental Federation & American Public Health Association, 2005).

Cathodic and anodic potentials relative to Normal Hydrogen Electrode (vs. NHE) were measured using a 3.5 M Silver/Silver Chloride (Ag/AgCl, E_0 = 0.205 V vs. NHE) reference electrode (RE-5B, Bioanalytical Systems Inc., USA) connected to a three-electrode potentiostat (Biologic, France) measuring the potential between the reference electrode and the anode used for chlorine production (see below).

2.4. Design of the self-contained toilet and treatment systems

2.4.1. Sizing considerations

A flow diagram of the overall treatment process is presented Figure 2.3 and Figure S2.1 and a picture of a typical treatment system as installed in the field-tested prototypes (PAS, AMD, KYM) is reproduced Figure 2.4. The mix of urine, feces, and flush water (toilet wastewater) was macerated and pumped (Jabsco Macerator Pump 18590-2094, Xylem USA or Saniflo Sanigrind Grinder Pump for Bottom Outlet Toilets, SFA France) into a 1-m^3 polypropylene sedimentation tank for a residence time of $\tau_{bio} \geq 7$ days. During this residence time, the toilet wastewater underwent decantation and some level of anaerobic digestion, similarly to a septic tank (Whelan & Titamnis, 1982). The prototypes were designed for treating the waste from approximately 25 daily uses: this is the equivalent to having a single toilet for a family of five people, the average household size in India in 2011 (Ministry of Home Affairs, 2011). Each of the family members flushing five times per day on average (Mayer & DeOreo, 1999) with a flush volume of 1.28 US gallons or 5 L (US EPA WaterSense) and considering that one person produces approximately 1.5 L of urine in one day (Putnam, 1971), the total daily volume of toilet wastewater to treat was estimated to be V_d = 132 L day^{-1} so the sedimentation tank should be sized to hold at least $\tau_{bio} * V_d \approx 1$ m^3.

After decanting in the sedimentation tank, the toilet wastewater was macerated and pumped (Jabsco Macerator Pump 18590, Xylem USA) to an electrochemical reactor (ECR) system (see below for description) for batch processing at constant voltage with active recirculation (10 L min^{-1}) during a period τ_{elec}, the electrochemical

residence time. The working volume needed for the ECR V_{ECR} was determined by (eqn. 1) with α the fraction of the daily time during which the ECR is running.

$$V_{ECR} = \frac{V_d}{24\ \alpha\ \tau_{elec}} (= 22\ \text{L}) \quad (1)$$

After electrolysis in the ECR for a period τ_{elec}, the water was filtered through a 200 μm-mesh microfiltration unit (Grainger USA). The treated effluent was then pumped with a drain pump (Jabsco PAR Max 3, Xylem USA) to a storage tank to use for flushing the toilet. The treated water tank (TWT) was capable of storing flushing water for one day of operation. Excess treated water in the cycle due to urination and personal hygiene (*e.g.*, anal cleansing) was discharged from the system with an overflow mechanism from TWT. Four complete toilet and associated wastewater treatment and recycling systems were operated in the US, China, and India (Table 2.1).

2.4.2. Electrochemical reactor system

The ECR tank body is made of a poly(methyl methacrylate) (PMMA) welded together (Nanopac. Yongin-Gun, South Korea) in a rectangular cuboid shape with the following dimensions: 63.5 cm * 35.6 cm * 16.5 cm (height * width * depth; Figure S2.2). Two 6-mm thick PMMA plates of respective dimensions 25 cm * 14 cm and 56 cm * 14 cm with 1.5 cm diameter holes spaced every 2.5 cm were used to hold the electrode array in place at a distance of 7 cm above the bottom of the ECR. 0.75-inch and 1-inch diameter National Pipe Tapered (NPT) thread holes were drilled on the side and the bottom of the ECR tank to connect sampling ports and plumbing. Circulation of fluid inside the ECR tank was assured by a brushless centrifugal pump (Fortric ZKWP04 24V, Fortric China). The ECR tank was connected to the other

components of the system using braid-reinforced polyurethane hose or polyvinyl chloride (PVC) pipes of sufficient diameter.

At the core of the ECR, electrode plates were assembled as an array in alternate configurations of doubly-coated anodes sandwiched between two stainless cathodes (*e.g.*, CA_nCA_{n+1}…C, etc.) where each electrode plate was separated by a 3-mm spacing; nylon screws, nuts, and washers were used for structural integrity. The arrays composed of eight stainless-steel (316 Grade) cathodes "C" and seven doubly-layered semiconductor anodes "A" ($[Bi_2O_3]_z[TiO_2]_{1-z}/Ir_xTa_yO_2/Ti$) (Nanopac, South Korea) that were coated on both sides. The manufacturing process and the effect of the outer layer composition ($[Bi_2O_3]_z[TiO_2]_{1-z}$) have previously been described in the literature (Cho & Hoffmann, 2015; Yang et al., 2016). The total exposed surface area of the anodes was 1.8 m^2. The ECR electrode array was powered at an electrical potential between 3.3 V and 3.5 V using a potentiostatic power supply (Program Scientific Instruments, USA).

2.4.3. Automation for the wastewater treatment and recycling

The daily number of users and the frequency of usage of the toilets were not controlled in any of the systems. For this reason, it was necessary to ensure that a sufficient amount of treated water was available for flushing at all time to support the continuous operation of the treatment system without direct supervision. This was achieved with a computer-controlled automation algorithm (Figure 2.3) programmed on a dedicated software package (Program Scientific Instruments, Arcadia CA) running on a Panel PC PPC-L62T (Advantech, China) with Windows 7 operating system (Microsoft, USA). Capacitive level sensors CD50 DC (Carlo Gavazzi,

Italy) were used as triggers for the automation mechanism. Pumps with a programmed maximum running time were used as actions (*e.g.*, macerator pump turns on) or as triggers when they changed state (*e.g.*, circulation pump stops running). ECR power status (or change of status) was used as a trigger, an action, and a feedback for the automation algorithm.

The algorithm is composed of two main parts (Figure 2.3): the start of a treatment cycle (lines 1-3) and the treatment cycle loop (lines 4.1 – 4.5). A treatment cycle starts when the level of water in the treated water tank falls below the sensor TWT_S1 (line 1), placed approximately at 20% of the tank's height. The macerator pump MP switches on for a fixed duration to fill up the ECR tank, the ECR power supply starts, and the circulation pump CP starts. At the end of the treatment cycle (τ_{elec}), the ECR tank is emptied by the drain pump DP into the treated water tank TWT. After that, if the water level in TWT is still below TWT_S1, a new treatment cycle begins. The treatment cycles will continue until the level of the treated water tank is above the TWT_S2 sensor, positioned close to 90% of the tank's height.

2.4.4. Energy distribution across to the system

The energy consumption of the entire system and ECR was monitored using non-invasive current sensors installed on the wires connecting the control system to its power source. The power source was a combination of grid electricity at 220 – 240 V AC when available, and 24 V DC power source from a 330 W solar panel (Xunlight, USA) stored in two 12 V Blue Top lead-acid backup batteries (Optima, USA) via a Conext MPPT 60 PV (Schneider Electric, Germany) charge controller (Figure S2.3). A

backup battery recharge was also implemented using a TRUECharge 2 40 A (Xantrex, USA) battery charger connected to grid electricity.

2.4.5. Integration

All components of the entire system were housed in customized steel shipping containers with an integrated public bathroom when necessary (Figure S2.4). AMD and PAS prototypes were modified 10-ft and 30-ft long containers cut from standard length 20-ft and 40-ft international shipping containers, respectively. KYM and YXG prototypes were repurposed 20-ft standard shipping containers. All containers were insulated and retrofitted with in-wall electrical wiring and on-wall plumbing in copper, cross-linked polyethylene (PEX), or PVC pipes. Doors and windows were added to improve access to the treatment system, increase air circulation, and provide a physical work environment for sampling and on-site measurements (Figure 2.4).

2.5. Results and discussion

2.5.1. Free chlorine production

Chlorination is a cost-effective way to remove pathogens in water, if allowed sufficient contact time for a given free or total chlorine concentration (Baumann & Ludwig, 1962; White, 1999). In our prototype systems, chlorine is continuously generated via the electrochemical oxidation of chloride, (i.e., the Chlorine Evolution Reaction, CER), at a fixed potential 3.5 V ± 0.25 V across the electrodes. The CER is an apparent first-order reaction with respect to the concentration of chloride in solution. In a large-electrode array (ECR) as shown in (Figure S2.5), the CER rate is shown to vary from 11 to 17 ppm Cl_2 min^{-1}; after an extended period of operation the CER stabilized at a near constant level (Figure S2.6).

Due to a consistent input of urine into the system , the $[Cl^-]$ was found to variable at any point in time, in part, because the treated water that was recycled also allowed for a build-up of total chloride in the anaerobic holding tank. Variations in $[Cl^-]$ were observed depending on the type and frequency of usage as well as the location of the unit (Table 2.2). In theory, when the system is running at full capacity after an initial set up period, the steady-state $[Cl^-]_{ss}$ should be approximately equal to the concentration of chloride in urine, which ranges between 53 mM to 240 mM (Putnam, 1971). However, lower concentrations (typically 10 – 20 mM) were actually observed (Table 2.2); the lower concentrations are most likely due to the use of excesss non-recycled water for additional flushing or for personal hygiene in the public bathrooms.

For an electrical potential of 3.5 V between the anodes and cathodes, the measured anodic potential is 1.4 ± 0.2 V vs. NHE. This potential is sufficient for the production of surface-bound hydroxyl radicals on titanium dioxide at pH between 6 and 9 (Martinez-Huitle & Ferro, 2006; Panizza & Cerisola, 2009) but is not sufficient to generate free hydroxyl radicals ($E_0(HO^{\cdot}) = 2.31$ V vs. NHE) in solution (Augusto & Miyamoto, 2011).

The detailed electrochemical surface reactions (Figure 2.6), previously identified and classified by Comninellis (Comninellis, 1994) consists of a two-step electron transfer for the oxidation of water on the surface of the metal-oxide electrode. In the case of TiO_2, a one-electron surface oxidation of water locally reduces titanium from Ti(IV) to Ti(III) with chemisorption of $^{\cdot}OH$ (1); then the surface metal hydroxy adduct undergoes deprotonation with the concomitant release of an electron (2) and the corresponding oxidation of Ti(III) back to Ti(IV) coupled with the formation of O_2 or the direct surface oxidation of organic matter (3). Comninellis has also shown that the metal-hydroxyl bond (>Ti(III)OH·) can directly oxidize electron-donating organic matter, leading to subsequent mineralization (4), or simply oxidize Ti(III) back to Ti(IV) with deprotonation and liberation of O_2 (5). In the presence of chloride and a sufficient concentration, the surface-bound hydroxyl radical of >Ti(III)OH· can directly oxidize Cl^- to form Cl_2 and subsequently HOCl due to hydrolysis of molecular chlorine (6) (Cho & Hoffmann, 2014). FC is defined as the sum of concentrations of hypochlorous acid, [HOCl], and hypochlorite ion, [ClO^-], which are in an acid-base equilibrium ($HOCl \rightleftharpoons H^+ + {}^-OCl$, $pK_a = 7.53$).

The measured CER rate in 20 mM NaCl solutions varied from 11 ± 0.5 ppm Cl_2 min^{-1} before the electrodes had any contact with wastewater and decreased to 7 ± 0.7 ppm Cl_2 min^{-1} after approximately 50 hours of electrolysis of toilet wastewater (Figure S2.6). The observed decrease in the rate of the CER was most likely due to the formation of a layer of organic compounds on the surface of the anodes. The net effect was a reduction in the CER rate by almost 40%; however, after stabilization of the CER, the removal of organic matter was stable (*vide infra*).

2.5.2. Removal of undesired organic and inorganic contaminants

The electrochemically produced FC (Figure 2.5 (1)) can oxidize ammonia to form chloramines (2) while also oxidizing organic matter (3) present in the wastewater (Deborde & von Gunten, 2008). The ammonia was present in the collected toilet wastewater was formed primarily from hydrolysis of urea (4). Although bicarbonate formed from the hydrolysis of urea combined with that generated via the oxidation of organic matter could interfere with the CER by adsorption on active anodic surfaces, thereby limiting the sites available for the oxidation of Cl^- to FC. The increase in TC concentration was correlated with the removal of TN because formation of chloramines (Figure 2.7). The TC concentration reached a steady state due to the reduction of chloramines to N_2 in the solution as well as the reduction of ClO^- back to Cl^- at the cathode surfaces. For instance, the ammonia monitored in the YXG prototype over the first 30 days of operation (Figure 2.8) showed 70% of NH_3 removal efficiency once the system stabilized.

The oxidation and mineralization of the organic matter (Figure 2.5 (3)) was observed through the decrease of COD during electrolysis (Figure 2.7). For instance,

the COD monitored in the AMD prototype over 1000 hours of operation showed between 70% and 80% removal efficiency when the chloride concentration was above 500 ppm and the applied potential was 3.5 V (Figure 2.9 and Table 2.4). Furthermore, COD removal kinetics from prototype MGU (designated as KYM above) (Figure S2.7) were consistent with the first-order kinetic model expressed by Martinez-Huitle and Ferro (Martinez-Huitle & Ferro, 2006) for transport-limited electrolytic oxidation with fitting coefficients reproduced Table S2.1.

2.5.3. Disinfection

A summary of disinfection analysis performed at the MGU (KYM) unit installed in Kottayam, India is reproduced Table 2.3: disinfection occurred after 2 to 3 hours of treatment (equivalent to 10 – 20 Wh L^{-1} electrolysis energy), as indicated by the levels of the major indicator organisms being below the detection limit (*Fecal coliforms* and *E. coli*) or below drinking water safety standards (*Total coliforms*). These results are in accordance with the amount of chlorine and chloramines produced as well as the residence time in the ECR: 25 ppm TC assumed to be mostly chloramines because breakpoint chlorination was not reached; the equivalent contact time Ct value for 4 hours operation was greater than 6,000 mg min L^{-1}, which is more than 5 times higher than the recommended Ct value for 3-log inactivation of *Giardia* cycst at 20°C, and almost 10 times of recommended Ct value for 4-logs virus inactivation at 20°C (U.S. Environmental Protection Agency, 1999). Similar results were observed in AMD and PAS units.

2.5.4. Energy consumption

The amount of electrical power drawn by the electrode arrays and by the overall system was measured on a regular basis (Figure S2.8). On average, 35 Wh were needed to treat 1 L of toilet wastewater, among which more than 95% of the electricity was used by the electrochemical treatment itself and the remaining 5% was used to compensate the power supply losses and to power the pumps. A large share of the energy used during electrolysis is for COD removal, especially when more than 200 mg O_2 L^{-1} removal is needed (Figure 2.10), and the electrolysis energy consumption is between 30 and 40 Wh L^{-1}. Despite drastic changes in the input COD level and over the course of close to 700 h of toilet wastewater electrolysis, the COD removal energy requirements remained relatively stable at approximately 10 Wh L^{-1} for 100 mg O_2 L^{-1} and up to 40 Wh L^{-1} for 200 mg O_2 L^{-1} initial COD.

2.5.5. Applicability of the technology in the context of a developing country

The AMD prototype unit was connected to a public toilet produced by ERAM Scientific; the “eToilet” had remote monitoring capacity. All of the eToilet uses were recorded over the course of the testing period as well as the number of treatment cycles logged by the AMD unit (Figure 2.11). The treatment capacity of the unit was adequate for the number of users since there was no limitation in the number of eToilet uses from lack of treated water. Issues related to the engineering connections between the eToilet-AMD unit prevented use for more than 6 months. Mechanical and electrical issues detected by the maintenance engineer in residency on the AMD testing site were solved with remote or on-site assistance of the authors. The parts that were replaced during the testing period included pumps that failed for

mechanical reasons and failures in the electrical energy storage subsystem (TRUECharge 2 40 A grid to 24 V converter and 12 V Blue Top lead-acid backup batteries, Figure S2.3). The mechanical failures of the pumps were due to fatigue and solids (sand) abrading the impeller and/or the diaphragms. The electrical failures of the energy storage subsystem were probably due to over-drainage events of the batteries when the system was used in the park but disconnected from the grid for very long periods (12 hours or more) and several grid electricity failures. These issues highlight the necessary trade-off between increasing the overall capital expenditure of a system with components prone to less failure such as higher-grade pumps or sufficient solar panels to provide a backup source of power, and managing the operational expenditures due to frequent replacement of parts and grid electricity costs. These issues also highlight the necessity for frequent monitoring of the toilet wastewater treatment system in order to minimize the potential negative health impact on the users. A solution could be in the form of an automatic detection and maintenance system that could investigate the status of the treatment system via a suite of sensors and potentially self-repair or provide a step-by-step guide for repairs that necessitate the presence of a technician or a lesser qualified person.

2.5.6. Possible prototype improvements for commercialization

The efficacy of the electrochemical treatment technology to clarify and disinfect toilet wastewater by generating chlorine without addition of water or chemicals makes this technology attractive as a non-sewered sanitation system, especially since it does not depend on the type of toilet used (*e.g.*, “western-style” flush toilet, squat pan) and does not require specific training or any change of behavior of the user.

Nevertheless, several improvements to the pre-alpha prototypes can be made to increase the robustness and energy efficiency of this electrochemical technology to meet the goals of the RTTC. A replacement of the sedimentation tank at the input of the process (Figure S2.1) by more advanced biological pre-treatment technologies such as small-size coupled aerobic/anaerobic systems (Metcalf & Eddy, 2014) or microbial fuel cells (Li, Yu, & He, 2014) could effectively decrease the amount of undesired organic and inorganic contaminants entering the electrochemical reactor. This approach would drastically reduce the operational expenses of the system by lowering the amount of electricity needed to complete the electrochemical treatment. Also, the biosolid residuals from the pre-treatment step as well as the filtered materials (Figure S2.1) should be properly decontaminated before being extracted from the system via a targeted decontamination process such as ohmic heating (Yin, Hoffmann, & Jiang, 2018).

2.6. Summary

In response to the Bill and Melinda Gates Foundation challenge to "Reinvent the Toilet", our research group at Caltech developed several self-contained, decentralized waste treatment systems that were designed to treat human domestic toilet waste at its source with discharge to the environment. After toilet flushing the discharged waste is stored in a wastewater tank. After some decantation, the effluent water from the wastewater tank is pumped into an electrochemical reactor array upon demand for the electrochemical oxidation of the residual organic and inorganic constituents. Disinfection is achieved via *in situ* chlorine generation resulting from anodic oxidation of chloride. Electrons released during anodic oxidation flow to the electronically coupled cathodes to produce molecular hydrogen via water reduction. The sequential biological and electrochemical treatment reduces the COD and microbial levels to below WHO agricultural reuse standards, while denitrification takes place due to breakpoint chlorination. In the field-level prototype systems, the treated black water is recycled into flush water reservoirs without significant discharge to the surrounding environment.

2.7. Acknowledgments

The authors acknowledge Mr. Garvit Singh (Indian Institute of Technology, Ahmedabad, Gujarat), Mr. Arun Babu, and Mr. Shalu Achu (Mahatma Gandhi University, Kottayam, Kerala) for their help with the technical analyses in the respective field testing sites, as well as Ms. Heather Crammer (California Institute of Technology, Pasadena, California) for her help with the bacterial analyses and Mr. Asghar Aryanfar for the CAD rendering reproduced Figure S2.2 and Figure S2.4. This research was supported by the Bill and Melinda Gates Foundation under RTTC Grants OPP 1069500 and OPP 1111246.

Table 2.1: Information about the different toilet wastewater treatment and recycling units installed in the world.

Configuration	Ref	Location	Testing period	Average daily usage during testing
Self-contained bathroom + wastewater treatment and recycling unit in a shipping container	PAS	Pasadena, USA	06/2013 to 06/2016	<5
	KYM	Kottayam, India	04/2014 to 01/2016	6
	YXG	Yixing, China	12/2014 to 05/2015	35
Wastewater treatment and recycling unit connected to an "eToilet" public toilet (Eram Scientific, Trivandrum, Kerala, India)	AMD	Ahmedabad, India	04/2014 to 01/2016	7

Table 2.2: Typical toilet wastewater composition in the different prototypes.

Parameter	Unit	Prototype reference			
		PAS[1]	AMD[2]	KYM[3]	YXG[3]
COD	mg O_2 L^{-1}	150-250	100	335	550
Cl^-	mmol L^{-1}	11-20	11	15	24
NH_3 + NH_4^+	mg NH_3 L^{-1}	80	30-40	235	480
PO_4^{3-} + HPO_4^{2-}	mmol L^{-1}	0.64		-	-
Alkalinity as $CaCO_3$	mmol L^{-1}	17	-	10.7	27
pH	-	8.3	7.4	7.5	8.5

[1] after 16 months of collection and 6 months of recycling water,
[2] no recycled water used
[3] after 2 months of running

Table 2.3: Indicator organisms *Total coliform*, *Fecal coliform*, and *E. coli* detection test results during electrochemical treatment cycles. Analysis performed by the Topical Institute of Ecological Sciences of Mahatmah Gandhi University (Kottayam, Kerala, India) and Albio Technologies (Kochi, Kerala, India).

Reaction time	***Total coliforms***	***Fecal coliforms***	***E. coli***
(energy consumed)	MPN/100ml	MPN/100ml	CFU/ml
11/17/14			
0 h (0 Wh L^{-1})	>1100	>1100	200
2 h (11 Wh L^{-1})	<1	<1	<1
4 h (22 Wh L^{-1})	<1	<1	<1
3/28/15			
0 h (0 Wh L^{-1})	>2400	75	Present
1 h (4.1 Wh L^{-1})	1100	0	Absent
2 h (8.2 Wh L^{-1})	23	0	Absent
3 h (12 Wh L^{-1})	15	0	Absent
7/25/15			
0 h (0 Wh L^{-1})	>2400	120	Present
1 h (6.7 Wh L^{-1})	1100	75	Present
2 h (13 Wh L^{-1})	93	4	Present
3 h (20 Wh L^{-1})	43	3	Present
4 h (27 Wh L^{-1})	9	0	Absent
9/18/15			
0 h (0 Wh L^{-1})	75	0	Absent
2 h (12 Wh L^{-1})	23	0	Absent
4 h (24 Wh L^{-1})	9	0	Absent

Table 2.4: Typical wastewater quality parameters measured before and after a 3-hour electrolysis cycle over the course of the field testing of the AMD prototype. Values are average of three replicates.

Date*	COD (mg O_2/L)		TKN or NH_3 (mg N/L)		TSS (mg/L)		Chloride (mg Cl^-/L)		Total/Free Chlorine (mg Cl_2/L)	
	Before	After	Before	After	Before	After	Before	After	Before	After
18/09/2014	32	-	n.d.	-	-	-	-	-	-	-
14/10/2014	100	-	31	-	100	-	-	-	-	-
03/11/2014	90	n.d.	-	-	100	50	182	35.1	-	-
29/11/2014[a]	43	11	15	2	-	-	100	30	-	-
23/02/2015	100	48	-	-	-	-	-	-	-	-
27/08/2015	-	-	-	-	-	-	-	-	0[b]	39[b]
09/09/2015	-	-	-	-	-	-	-	-	5[b]	21[b]
01/12/2015	240	40	43	5	-	-	-	-	9[b]	25[b]
16/01/2016	223	26	-	-	-	-	235	203	<1[c]	-
02/02/2016	371	95	-	-	-	-	886	382	<1[c]	2.73[c]
31/03/2016	320	50	1.05[d]	2.04[d]	245	87	-	-	-	-
11/04/2016	234	56	25[d]	40[d]	180	35	425	390	<1[c]	<1[c]

*Date format: dd/mm/yyyy)

[a] Analyses performed by third-party (Ahmedabad Municipal Corporation Central Lab). Total Nitrogen was measured.

[b] Total Chlorine

[c] Free Chlorine

[d] Potential Interference for Ammonia measurement

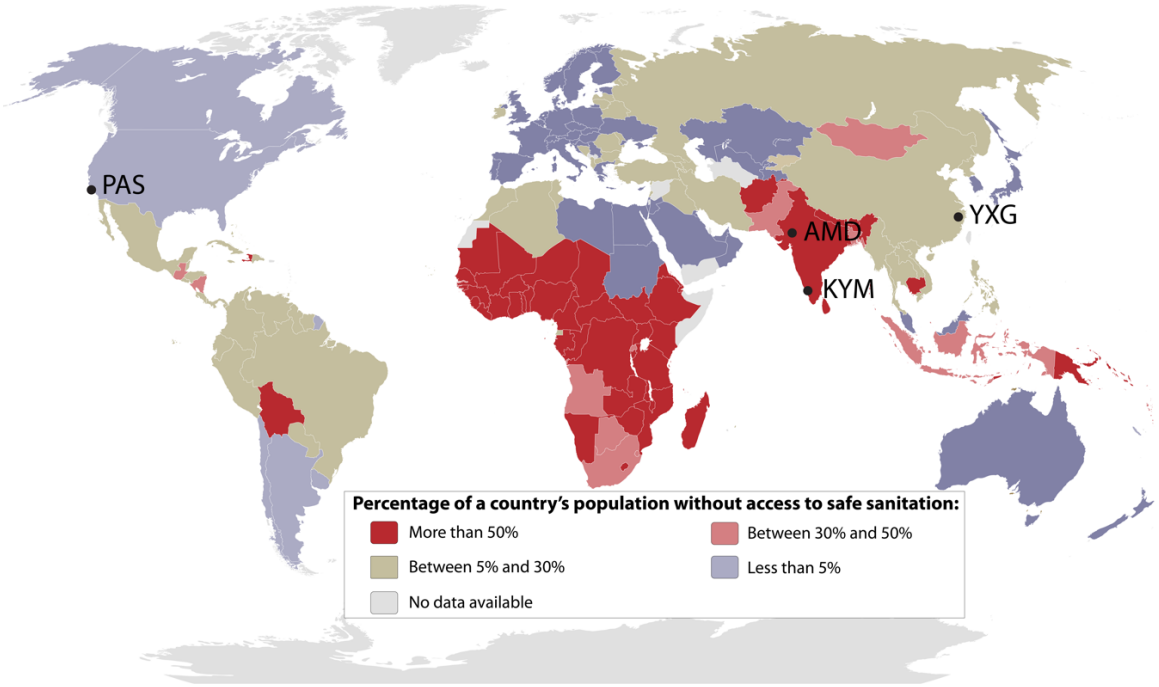

Figure 2.1: Percentage of a country's population without access to safe sanitation in 2015 according to the World Health Organization (World Health Organization, 2015). Location of the four prototype testing sites across the world: PAS, Pasadena, California, USA; AMD, Ahmedabad, Gujarat, India; KYM, Kottayam, Kerala, India; YXG, Yixing, Jiangsu, China.

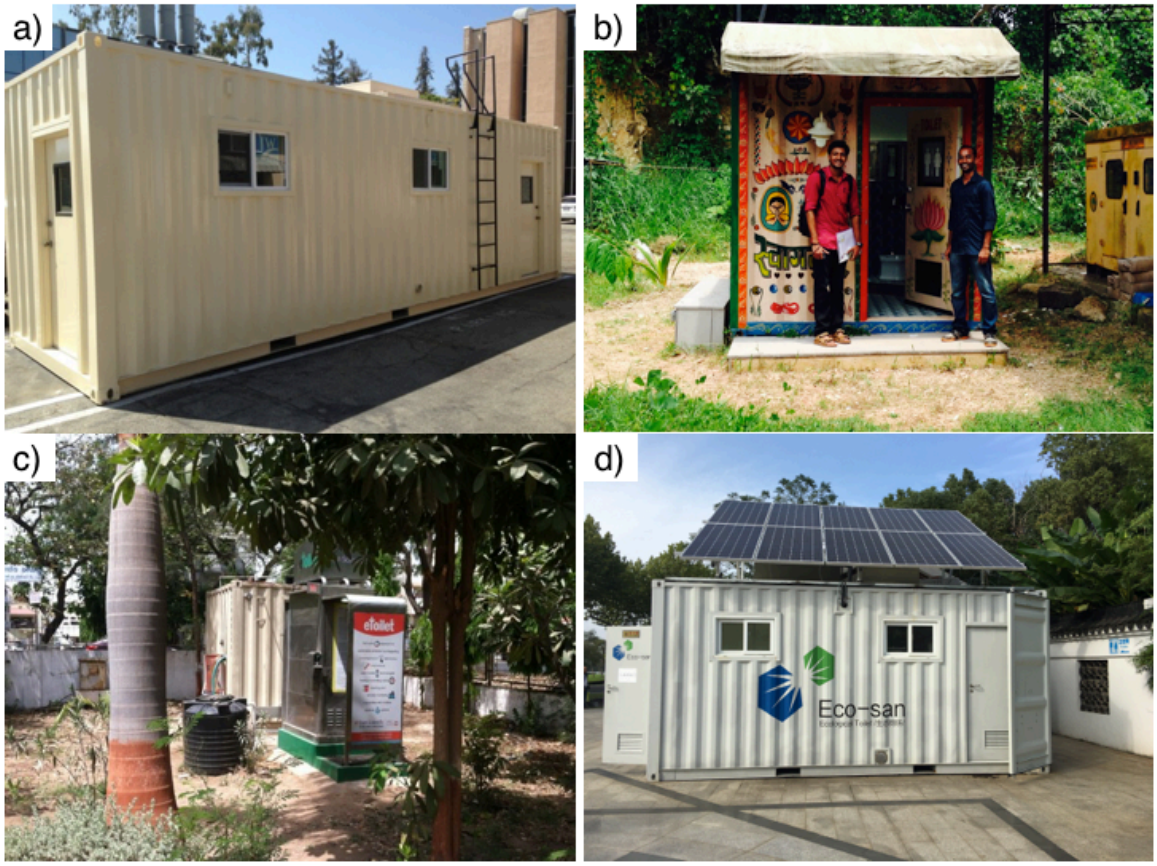

Figure 2.2: Caltech Solar Toilet system prototypes: a) Prototype PAS (Pasadena, CA); b) Prototype KYM (Kottayam, Kerala, India); c) Prototype AMD (Ahmedabad, Gujurat, India); d) Prototype YXG (Yixing, Jiangsu, China).

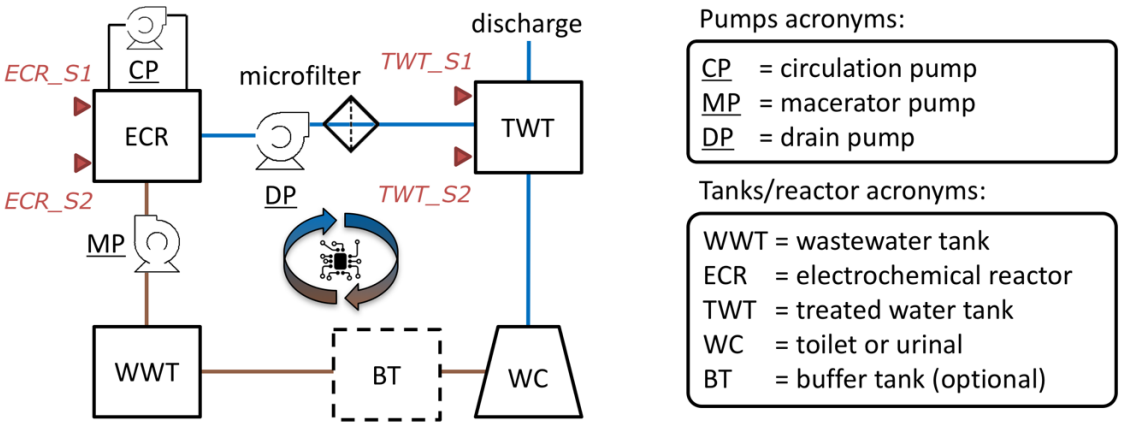

1. When the water level in the Treated Water Tank goes below TWT_S1, start the cycle:
   TWT_S1 (on ⟶ off) & *ECR_S2* off ➔ MP starts
2. When the reactor is drained, start a new batch:
   ECR_S2 (on ⟶ off) & *TWT_S1* off ➔ MP starts
3. Same as 1. with TWT_S2 (redundancy):
   TWT_S2 (on ⟶ off) & *ECR_S2* off ➔ MP starts
4. Treatment cycle:
   - 4.1 MP (off ⟶ on) ➔ ECR starts — *Electrolysis starts when filling the reactor*
   - 4.2 ECR (off ⟶ on) ➔ CP starts — *When electrolysis starts, the circulation pump starts*
   - 4.3 ECR (on ⟶ off) ➔ CP stops — *When electrolysis is over, the circulation pump stops*
   - 4.4 ECR (on ⟶ off) ➔ DP starts — *When electrolysis is over, the reactor is drained*
   - 4.5 ECR_S2 (on ⟶ off) ➔ DP stops — *At the end of the drainage, the drain pump stops*

Figure 2.3: System flow diagram (top left, see Figure S2.1 for volumes and residence times) with automation algorithm description for the onsite toilet wastewater treatment and recycling systems. Pumps are underlined. Capacitive level sensors are represented by red triangles. Brown lines illustrate the flow of untreated wastewater while blue lines illustrate the flow of treated and recycled wastewater.

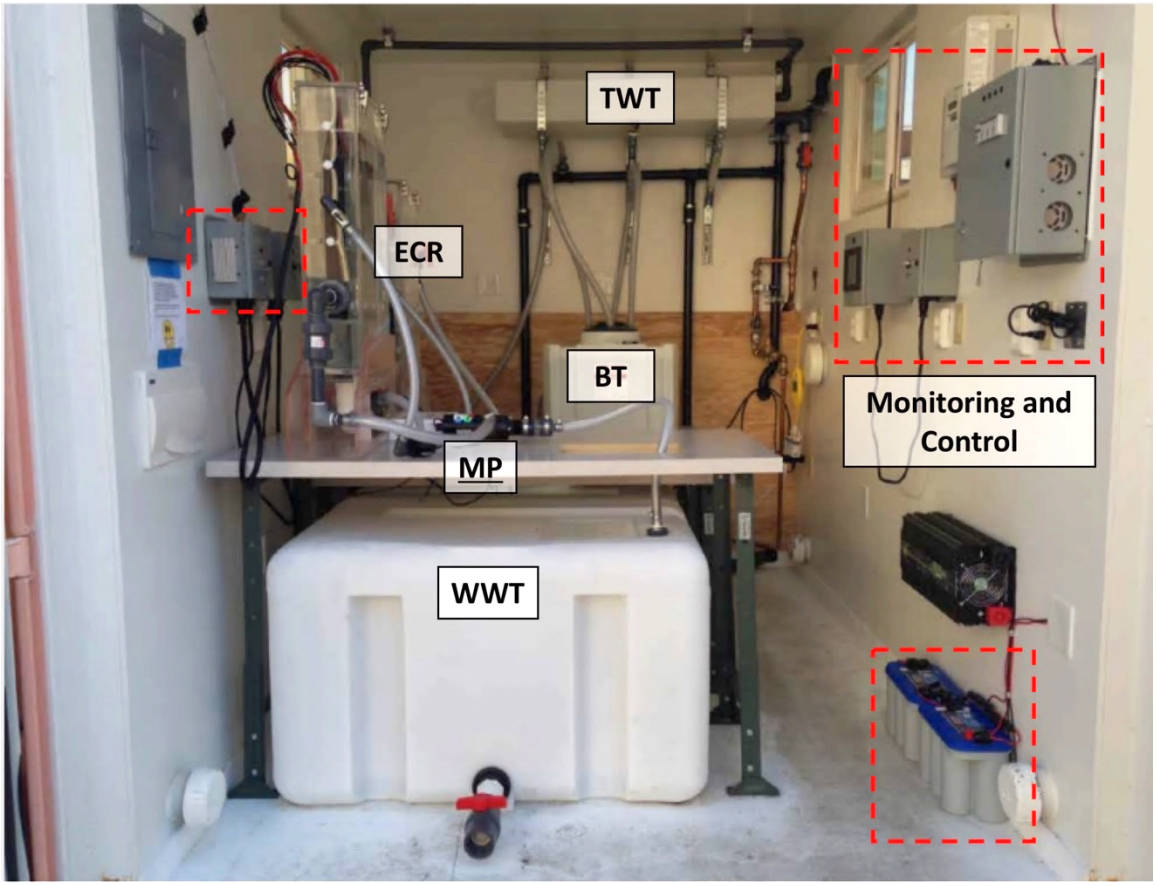

Figure 2.4: Photograph of the layout of one of the self-contained electrochemical treatment prototypes installed in the field. The combined power, monitoring, and control system are highlighted in red dashes. Refer to Figure 2.3 for meaning of acronyms.

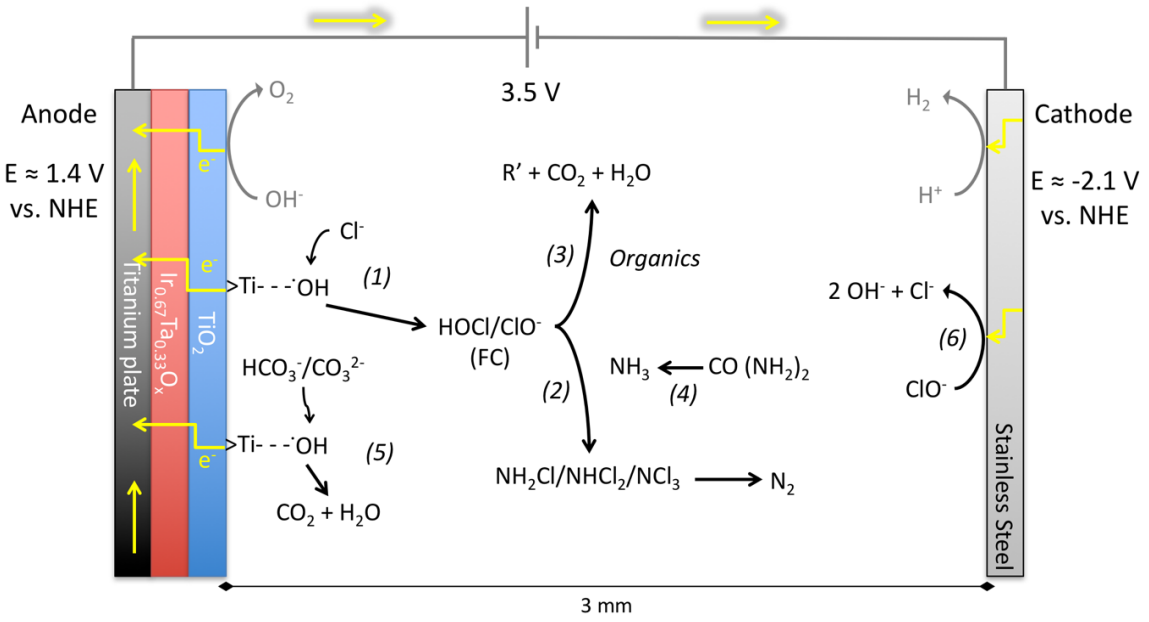

Figure 2.5: Electrons flow and main chemical reactions in the ECR illustrating the production and the fate of FC during electrochemical treatment (1) –(3). The yellow arrows represent the flow of electrons in the electrodes and across the wires.

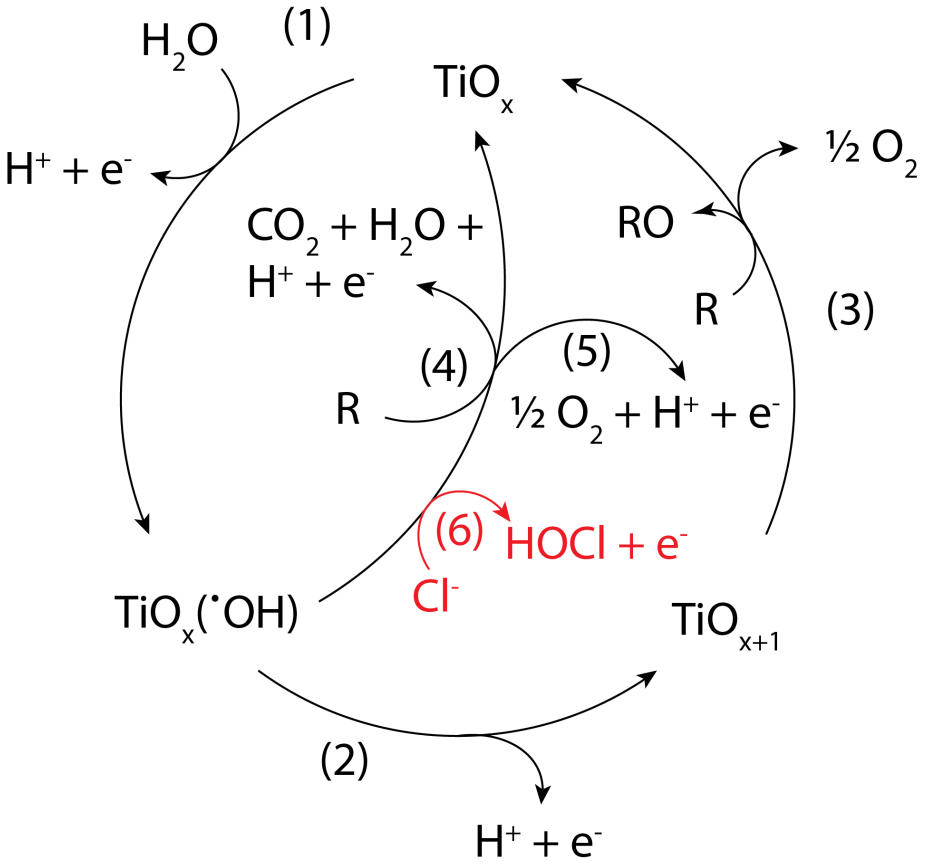

Figure 2.6: Scheme of the electrochemical oxidation of organic compounds and chloride ions on a metal oxide electrode. Adapted from Comninellis with the permission of Elsevier (Comninellis, 1994; Panizza & Cerisola, 2009).

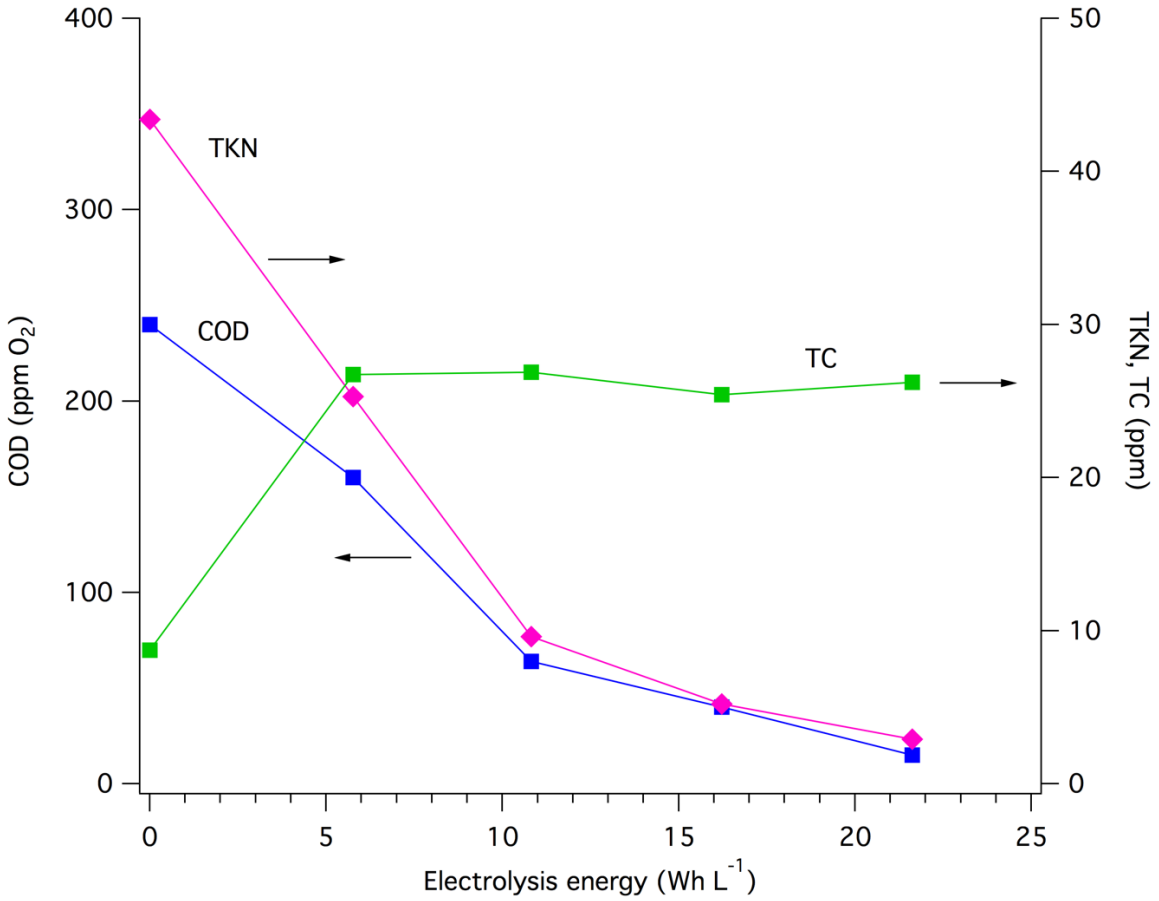

Figure 2.7: Typical evolution of the COD, TKN, and TC during the treatment of toilet wastewater in AMD prototype.

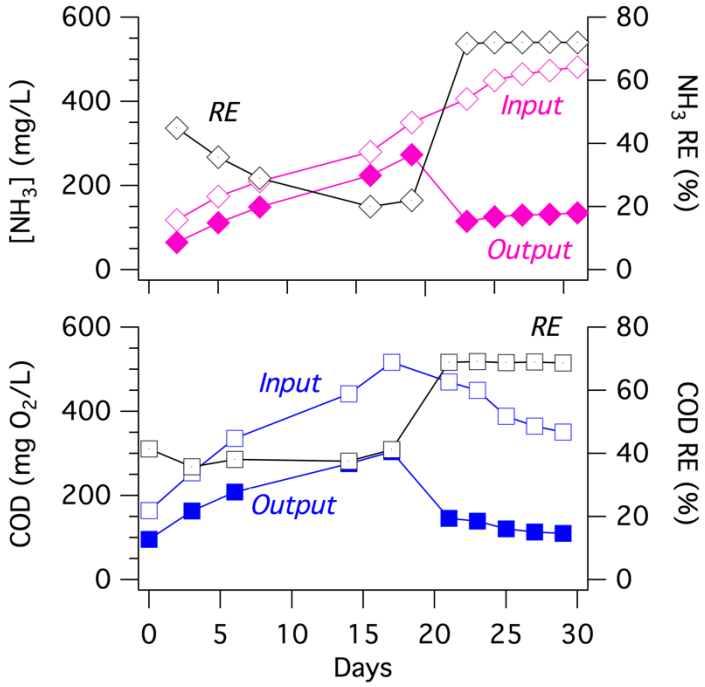

Figure 2.8: NH_3 (top) and COD (bottom) averaged concentrations before (input) and after (output) a typical electrochemical treatment cycle of 4 hours with respective Removal Efficiencies (RE) for 30 continuous days of operation of YXG prototype. Day 0 corresponds to the beginning of usage of the prototype.

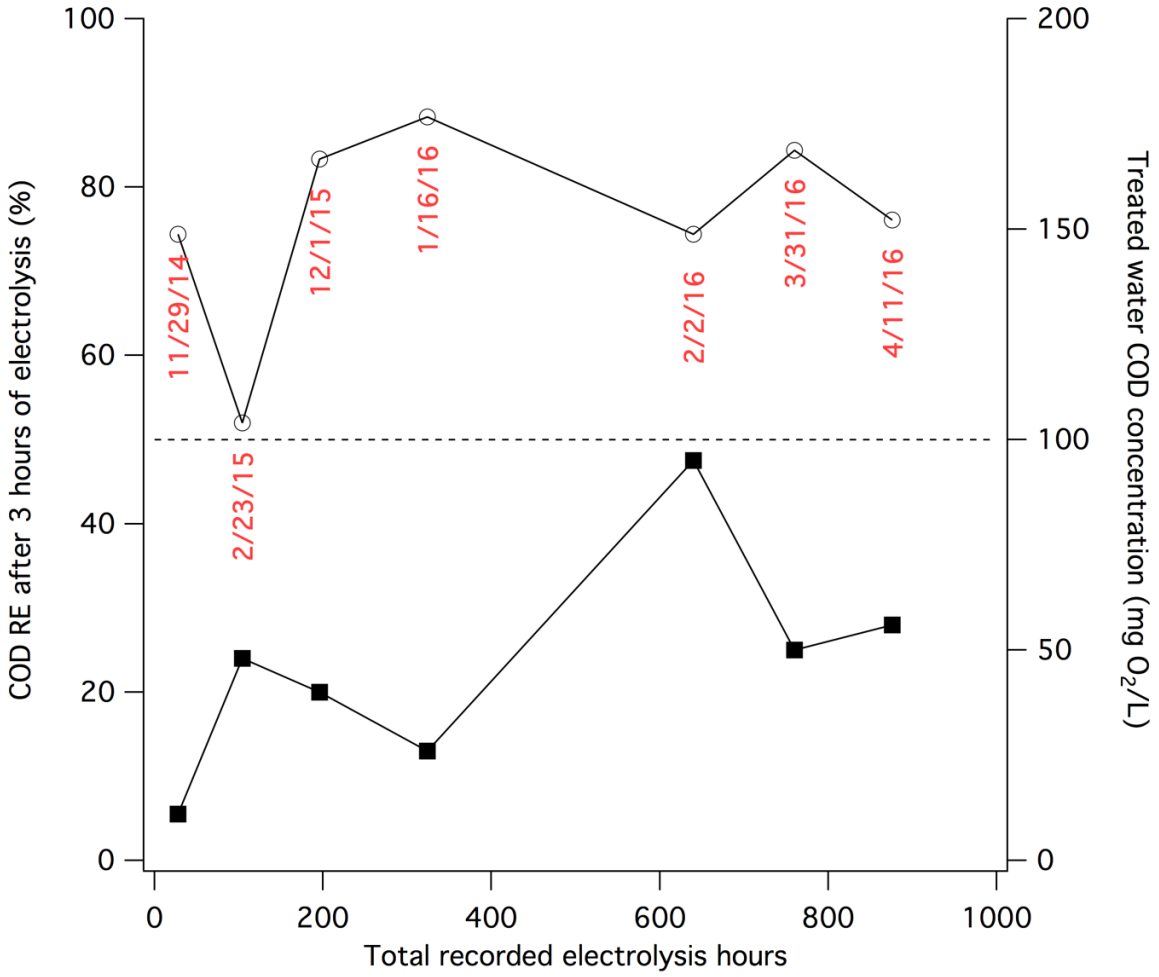

Figure 2.9: COD removal efficiency (RE) and output COD value of treated toilet wastewater of AMD prototype. Effective sampling dates are written vertically.

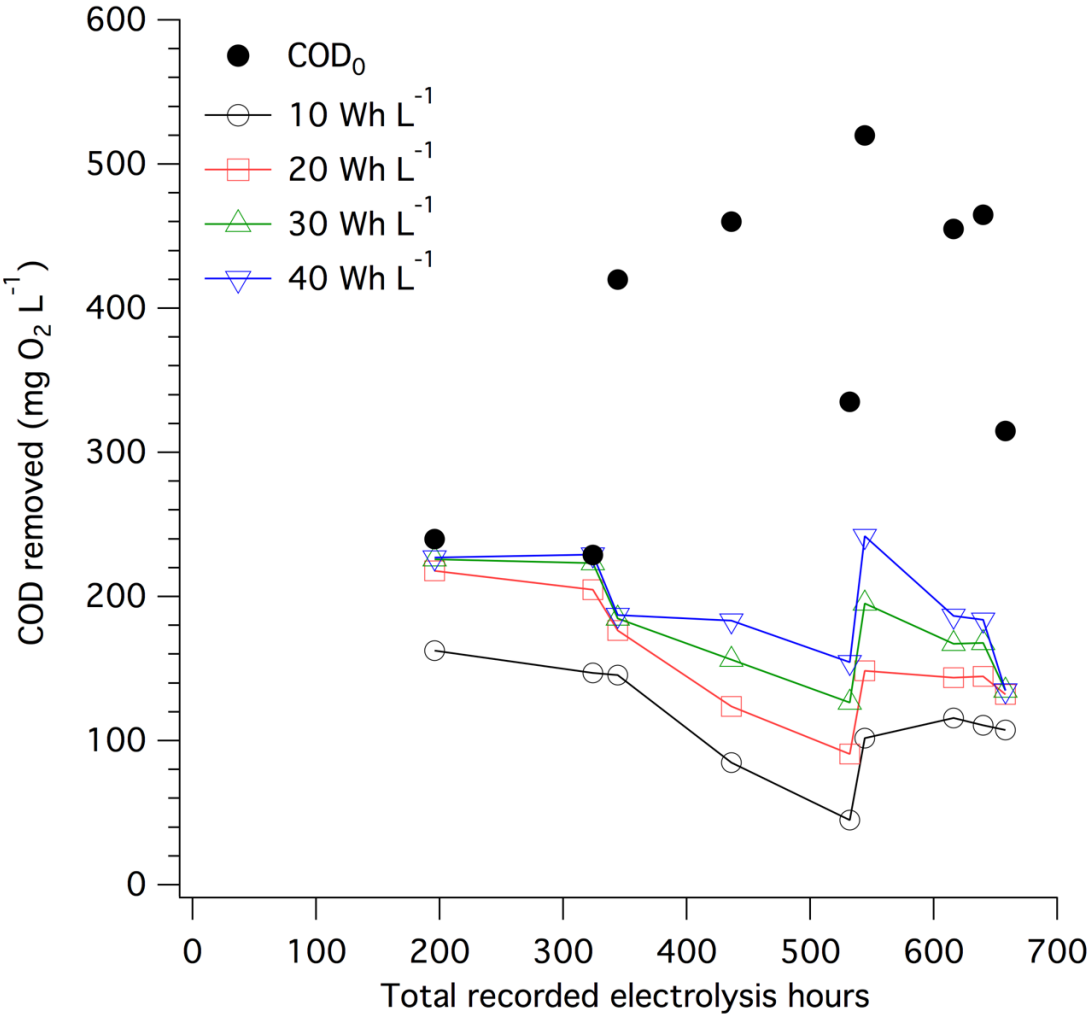

Figure 2.10: COD removal at different levels of electrical energy consumption for toilet wastewater of original COD_0 value. Extrapolation is based on a first-order kinetic model for electrochemical COD removal, see Figure S2.7 (Martinez-Huitle & Ferro, 2006).

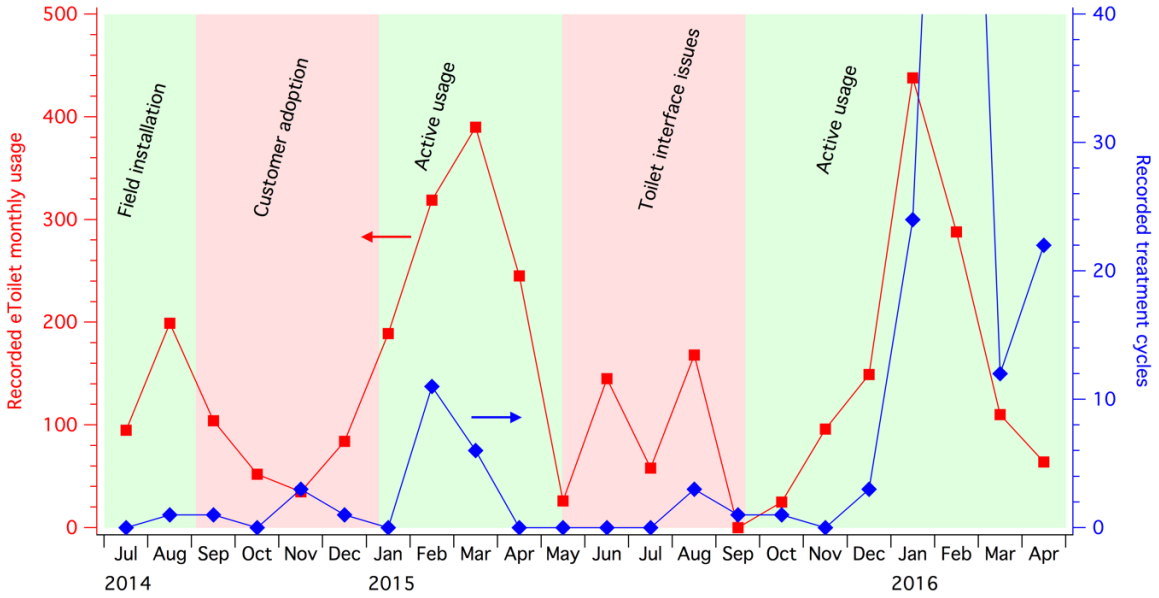

Figure 2.11: Recorded monthly usage of eToilet (left) and electrolysis treatment cycles during operation in Ahmedabad, Gujarat, India (AMD).

2.8. Supplementary figures and table

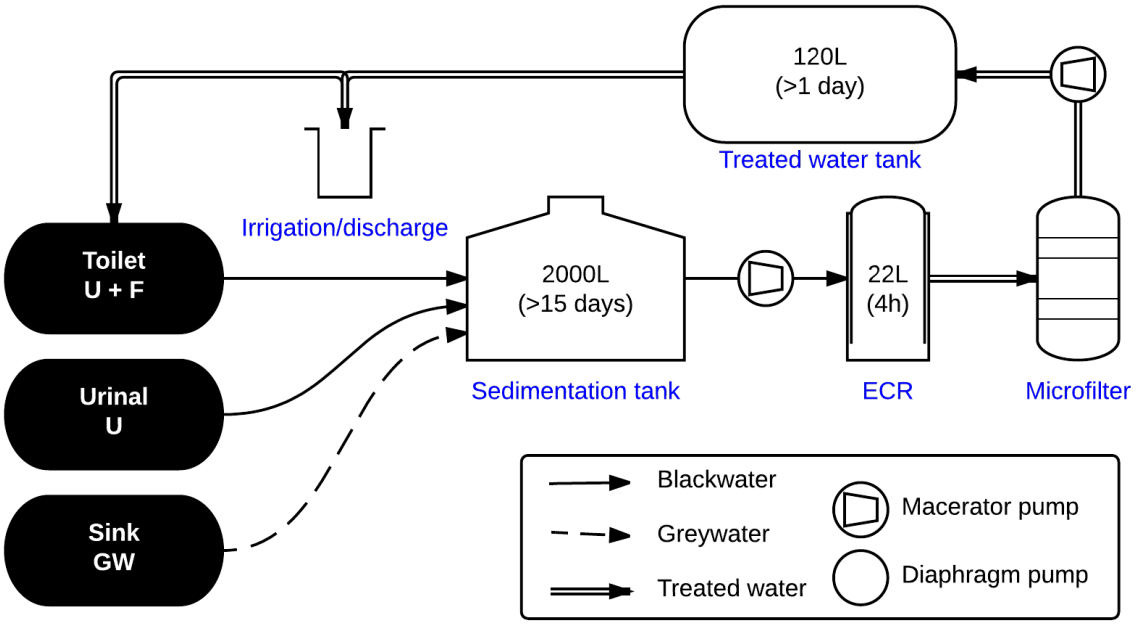

Figure S2.1: System flow diagram of the self-contained toilet electrochemical treatment system with capacity and residence time of the relevant components.

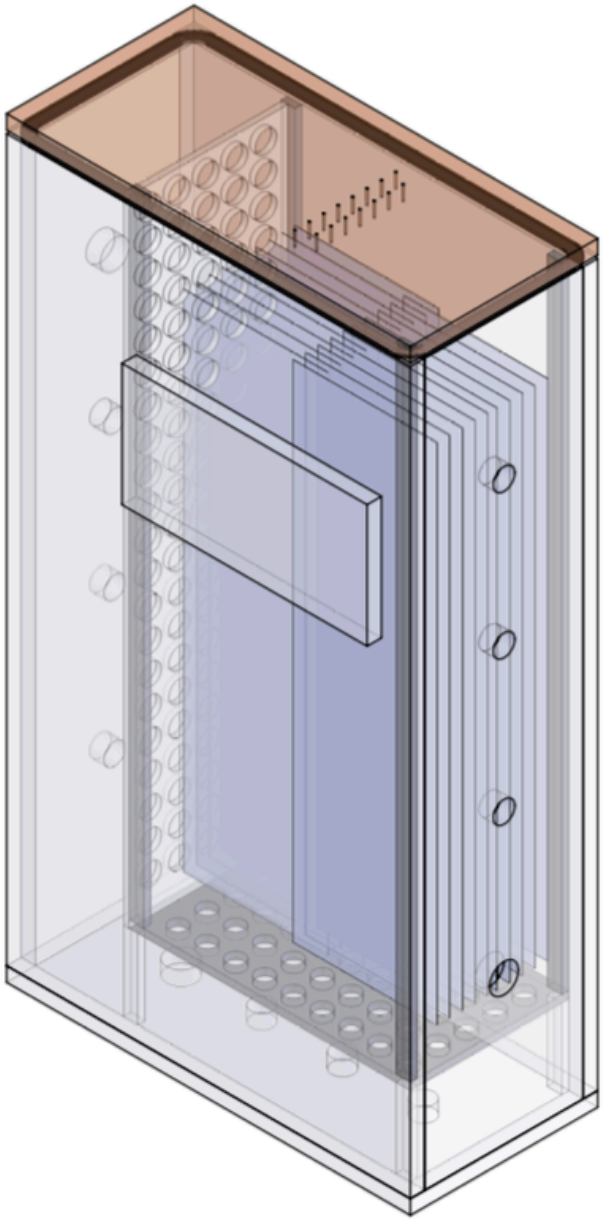

Figure S2.2: CAD rendering of the electrochemical reactor (ECR) boddy with an artist view of the electrode array in its core.

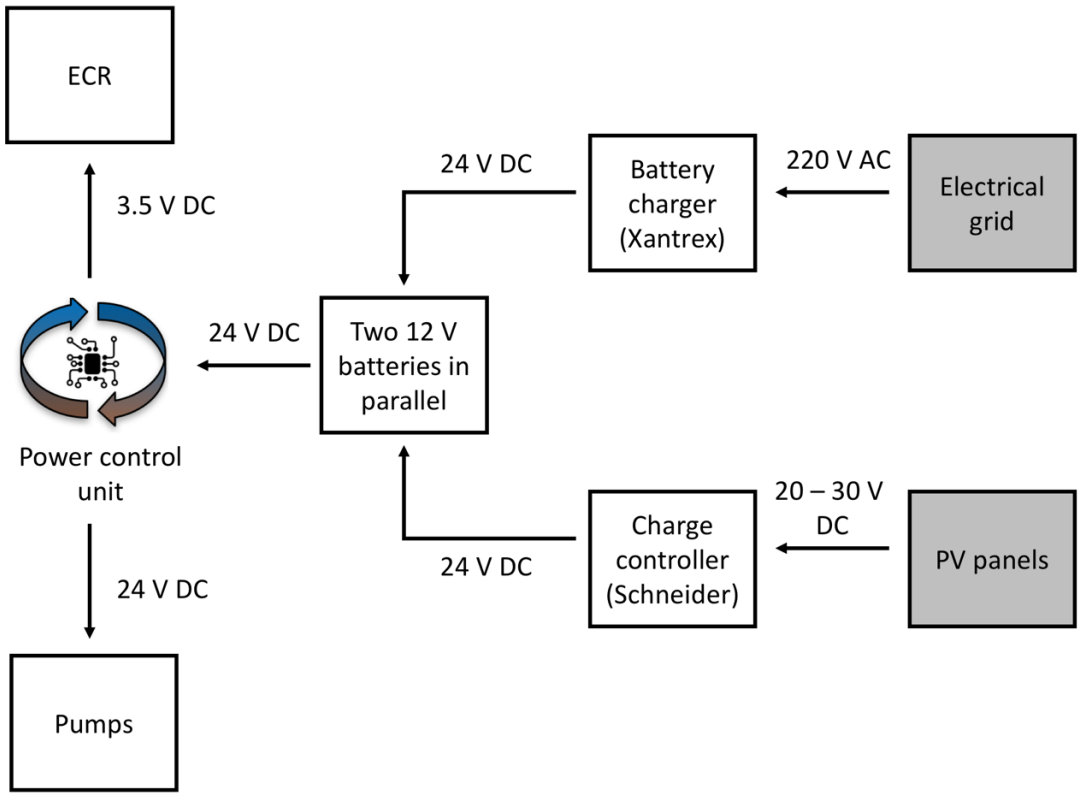

Figure S2.3: Simplified electrical energy flow diagram of the Caltech Solar Toilet.

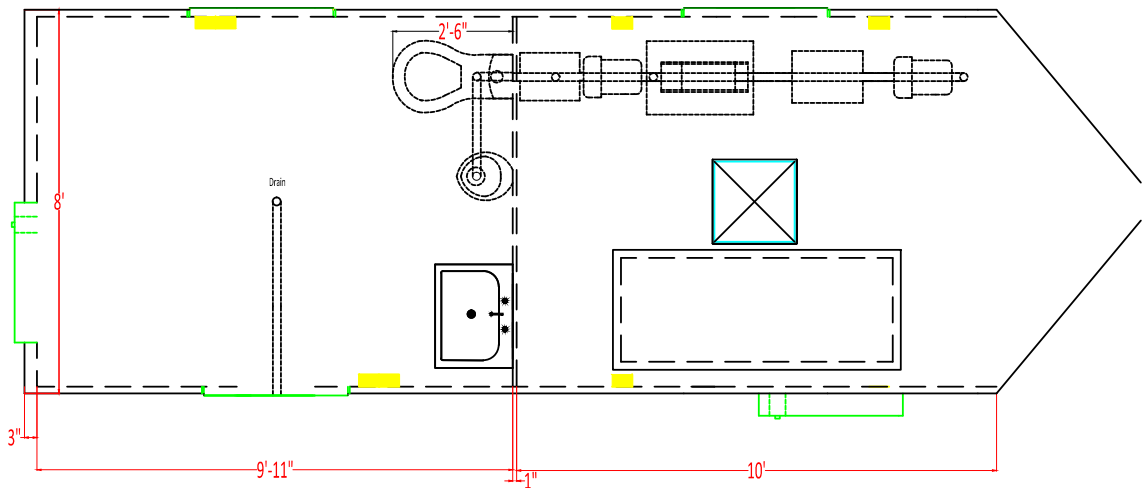

Figure S2.4: Typical layouts of the self-contained electrochemical treatment systems with a dedicated bathroom located on the left side and a treatment room on the right side.

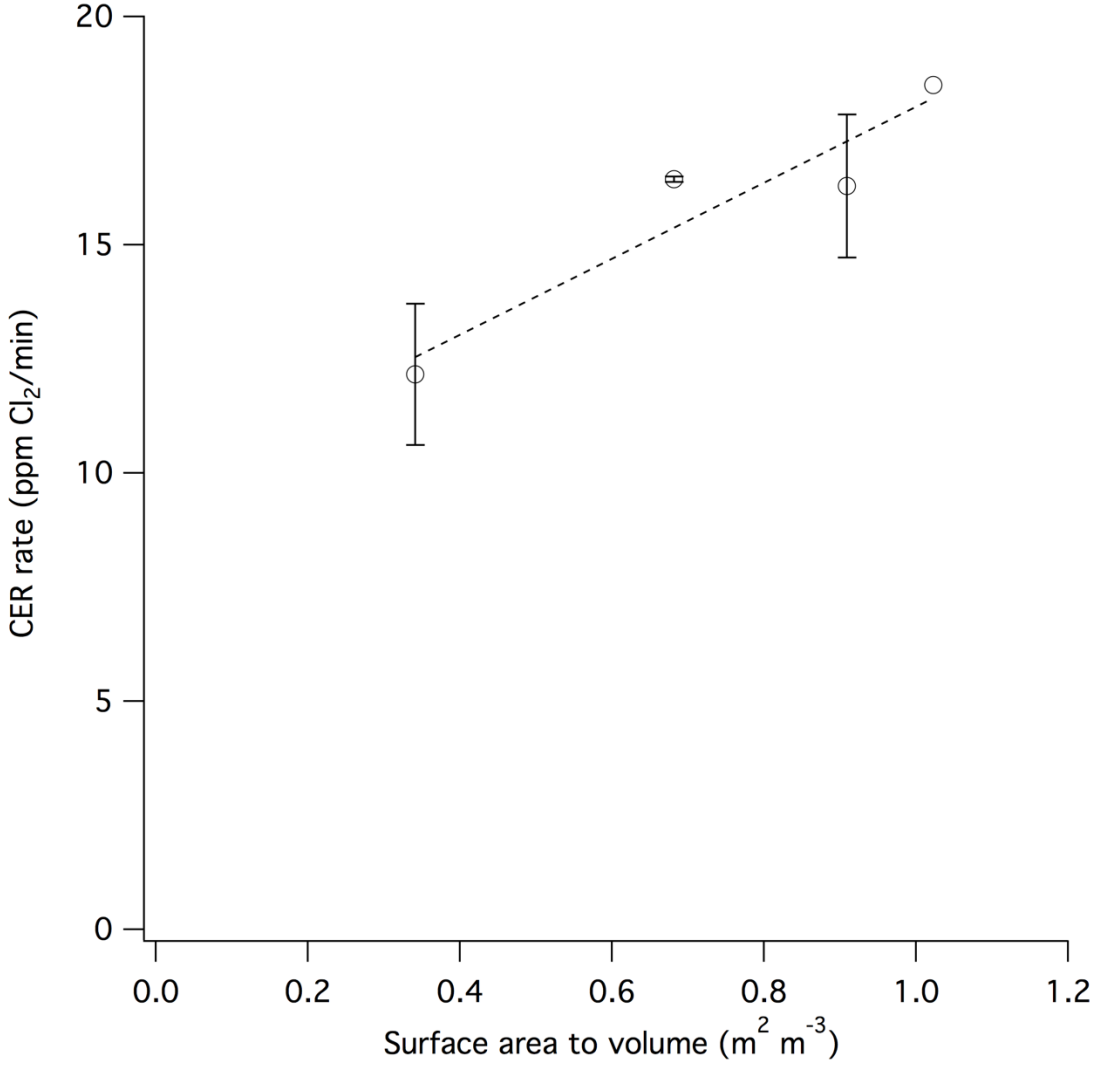

Figure S2.5: Measured CER rate (ppm Cl_2/min) in 22 L of 20 mM NaCl solution as a function of electrodes surface to reactor active volume (m^2 m^{-3}). Linear regression equation: CER = 8.3*x* + 9.7 (R^2 = 0.89), *x* is the electrode surface area to solution volume ratio. Error bars represent ± one standard deviation of 3 replicates.

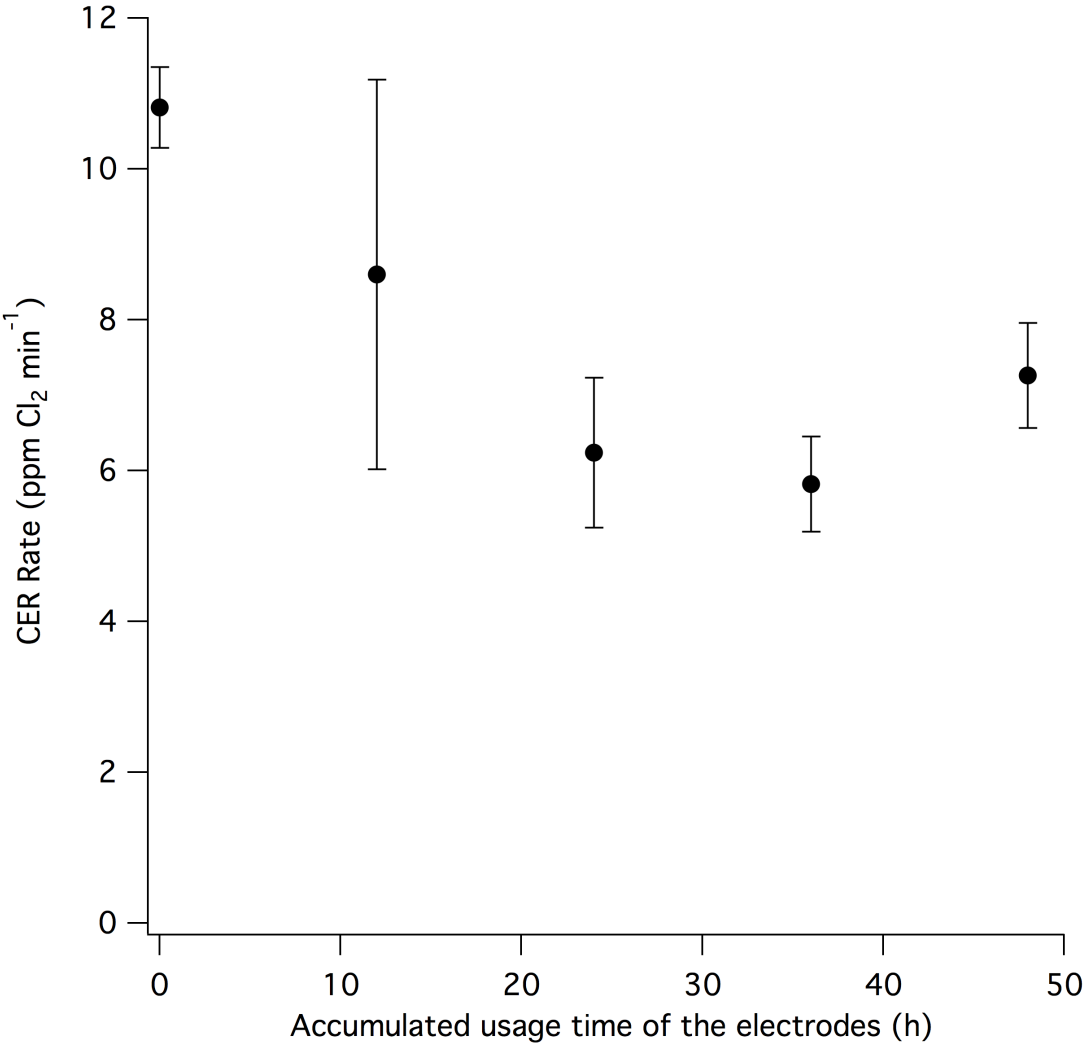

Figure S2.6: CER rate determined in 20 mM NaCl after usage of the electrodes for toilet wastewater treatment.

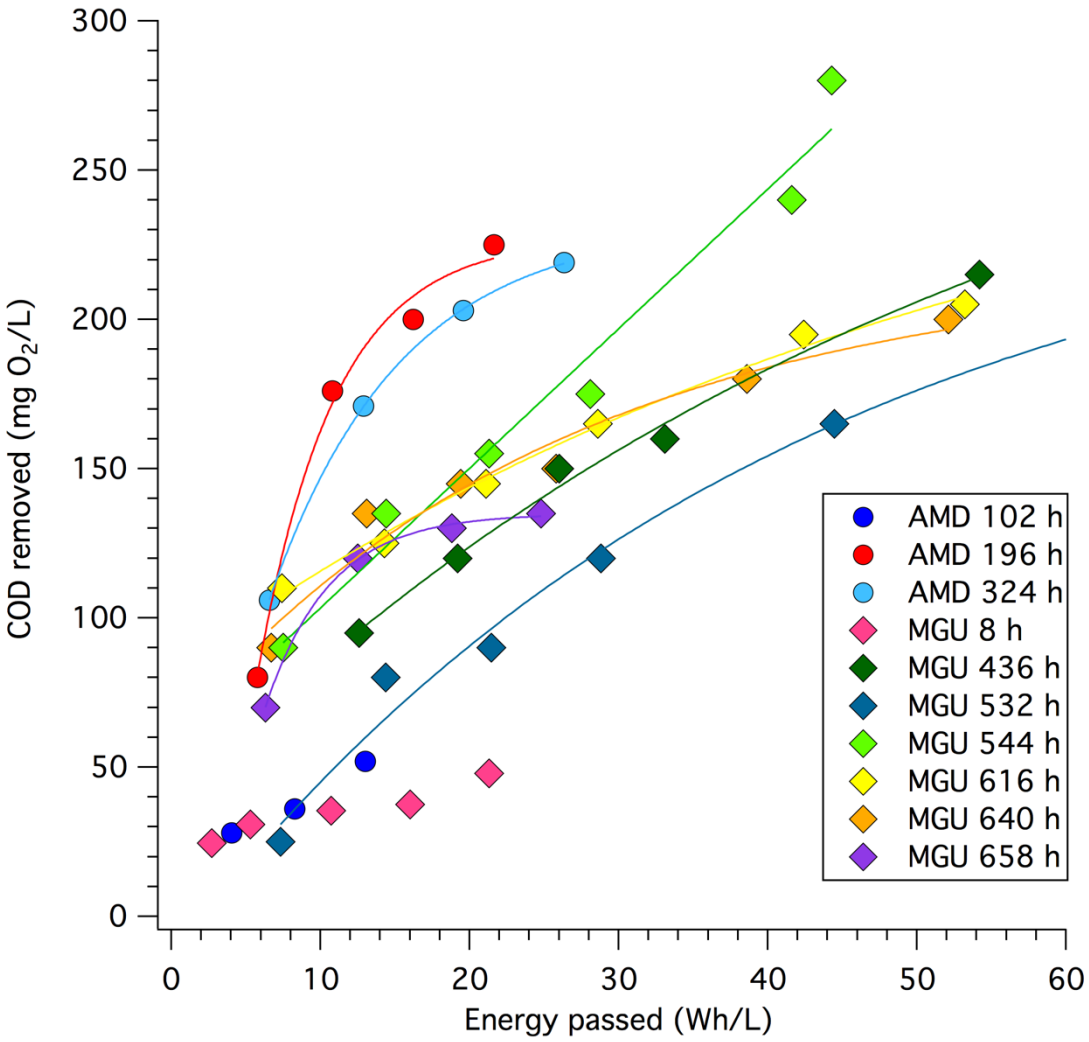

Figure S2.7: COD removed per Wh L^{-1} during a treatment cycle (4 h to 6 h) after specific acumulated toilet wastewater electrolysis time.

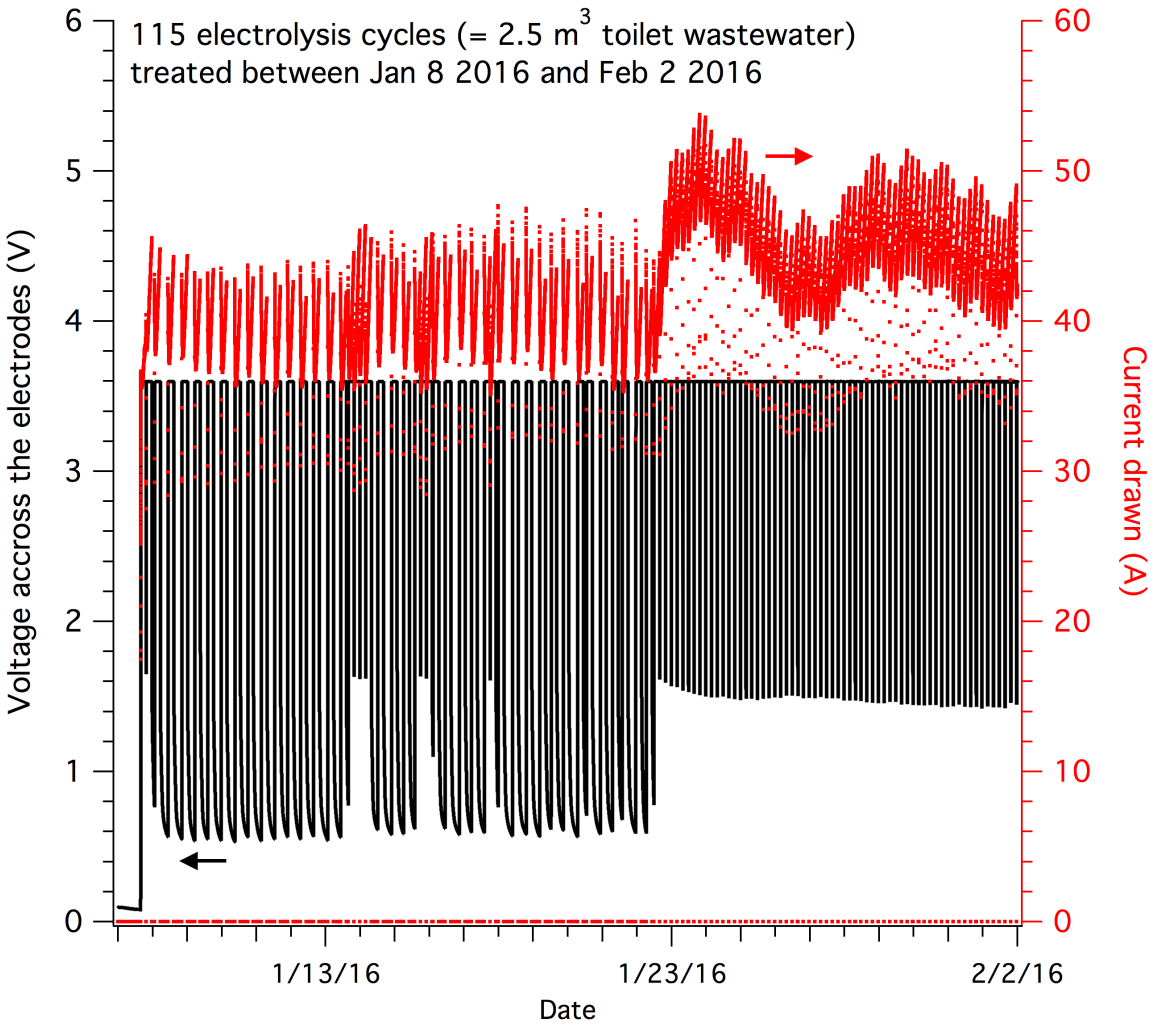

Figure S2.8: Recorded electrolysis voltage and current of the ECR during a typical month of full usage of AMD prototype. Variations in cycles are due to ECR turning off and on following the automation mechanism Figure 2.3.

Table S2.1: Coefficients obtained by computational fit obtained by Igor Pro 6.37 (Wavemetrics) with equation (S1) of the COD removal data measured after the specific acumulated electrolysis times (Figure S2.7). σ_0, σ_1, and σ_2 correspond to ± one standard deviation of C_0, C_1, and C_2 respectively.

AET* (h)	C_0	C_1	C_2	A_0	σ_0	σ_1	σ_2
196	227	-147	5.16	5.77	14.4	16.5	1.58
324	232	-126	8.75	6.56	1.27	1.29	0.22
344	188	-78.3	7.82	5.27	-	-	-
436	320	-224	55.2	12.6	83.7	81	29.6
532	255	-224	40.7	7.33	48.3	44.9	15.6
544	3.03E+05	-3.02E+05	6.46E+04	7.50	3.23E+08	3.23E+08	6.9E+07
616	286	-178	55.5	7.40	47.5	45.7	21.8
640	218	-122	26.4	6.70	30.6	28.2	13.5
658	135	-64.9	4.32	6.30	1.79	2.43	0.49

*Accumulated Electrolysis Time

$$\text{COD (removed)} = C_0 + C_1 \exp(-(x - A_0)/A_2) \quad \text{(S1)}$$

2.9. References

American Society of Civil Engineers. (2013). *Failure to act: the impact of current infrastructure investments on America's economic future*. Retrieved from

Atlas, R. M. (1984). Sanitation and Disease-Health Aspects of Excreta and Waste-water Management. *JAWRA Journal of the American Water Resources Association, 20*(5), 803-803.

Augusto, O., & Miyamoto, S. (2011). Oxygen Radicals and Related Species. In K. Pantopoulos & H. M. Schipper (Eds.), *Principles of Free Radical Biomedicine* (Vol. 1).

Baumann, E. R., & Ludwig, D. D. (1962). Free Available Chlorine Residuals for Small Nonpublic Water Supplies. *Journal - American Water Works Association, 54*(11), 1379-1388.

Beal, C., Gardner, E., & Menzies, N. (2005). Process, performance, and pollution potential: A review of septic tank–soil absorption systems. *Soil Research, 43*(7), 781-802.

Boon, A. G. (1995). Septicity in sewers: Causes, consequences and containment. *Water Science and Technology, 31*(7), 237-253. doi:10.1016/0273-1223(95)00341-J

Burian, S. J., & Edwards, F. G. (2002). *Historical perspectives of urban drainage.* Paper presented at the 9th International Conference on Urban Drainage.

Cho, K., & Hoffmann, M. R. (2014). Urea Degradation by Electrochemically Generated Reactive Chlorine Species: Products and Reaction Pathways. *Environmental science & technology, 48*(19), 11504-11511. doi:10.1021/es5025405

Cho, K., & Hoffmann, M. R. (2015). BixTi1–xOz Functionalized Heterojunction Anode with an Enhanced Reactive Chlorine Generation Efficiency in Dilute Aqueous Solutions. *Chemistry of Materials, 27*(6), 2224-2233. doi:10.1021/acs.chemmater.5b00376

Cho, K., Qu, Y., Kwon, D., Zhang, H., Cid, C. A., Aryanfar, A., & Hoffmann, M. R. (2014). Effects of Anodic Potential and Chloride Ion on Overall Reactivity in Electrochemical Reactors Designed for Solar-Powered Wastewater Treatment. *Environmental science & technology, 48*(4), 2377-2384. doi:10.1021/es404137u

Comninellis, C. (1994). Electrocatalysis in the electrochemical conversion/combustion of organic pollutants for waste water treatment. *Electrochimica Acta, 39*(11–12), 1857-1862. doi:10.1016/0013-4686(94)85175-1

Comninellis, C., & Chen, G. (2009). *Electrochemistry for the Environment*.

Corcoran, E., Nellemann, C., Baker, E., Bos, R., Osborn, D., & Savelli, H. (2010). Sick Water? The central role of wastewater management in sustainable development. .

De Feo, G., Antoniou, G., Fardin, H., El-Gohary, F., Zheng, X., Reklaityte, I., . . . Angelakis, A. (2014). The Historical Development of Sewers Worldwide. *Sustainability, 6*(6), 3936-3974. doi:10.3390/su6063936

Deborde, M., & von Gunten, U. (2008). Reactions of chlorine with inorganic and organic compounds during water treatment—Kinetics and mechanisms: A critical review. *Water Research, 42*(1–2), 13-51. doi:10.1016/j.watres.2007.07.025

Dzwairo, B., Hoko, Z., Love, D., & Guzha, E. (2006). Assessment of the impacts of pit latrines on groundwater quality in rural areas: A case study from Marondera district, Zimbabwe. *Physics and Chemistry of the Earth, Parts A/B/C, 31*(15-16), 779-788. doi:10.1016/j.pce.2006.08.031

Eiswirth, M., & Hötzl, H. (1997). The impact of leaking sewers on urban groundwater. *Groundwater in the urban environment, 1*, 399-404.

Gandy, M. (1999). The Paris sewers and the rationalization of urban space. *Transactions of the Institute of British Geographers, 24*(1), 23-44.

Graham, J. P., & Polizzotto, M. L. (2013). Pit latrines and their impacts on groundwater quality: a systematic review. *Environ Health Perspect, 121*(5), 521-530. doi:10.1289/ehp.1206028

Huang, X., Qu, Y., Cid, C. A., Finke, C., Hoffmann, M. R., Lim, K., & Jiang, S. C. (2016). Electrochemical disinfection of toilet wastewater using wastewater electrolysis cell. *Water Research, 92*, 164-172. doi:10.1016/j.watres.2016.01.040

Hynds, P. D., Thomas, M. K., & Pintar, K. D. (2014). Contamination of groundwater systems in the US and Canada by enteric pathogens, 1990-2013: a review and pooled-analysis. *PLoS One, 9*(5), e93301. doi:10.1371/journal.pone.0093301

ISO 16075-1. (2012). Guidelines for Treated Wastewater Use for Irrigation Projects—Part 1: General.

Jasper, J. T., Shafaat, O. S., & Hoffmann, M. R. (2016). Electrochemical Transformation of Trace Organic Contaminants in Latrine Wastewater. *Environ Sci Technol, 50*(18), 10198-10208. doi:10.1021/acs.est.6b02912

Kaika, M., & Swyngedouw, E. (2000). Fetishizing the modern city: the phantasmagoria of urban technological networks. *International Journal of Urban and Regional Research, 24*(1), 120-138.

Kesselman, J. M., Weres, O., Lewis, N. S., & Hoffmann, M. R. (1997). Electrochemical production of hydroxyl radical at polycrystalline Nb-doped TiO2 electrodes and estimation of the partitioning between hydroxyl radical and direct hole oxidation pathways. *The Journal of Physical Chemistry B, 101*(14), 2637-2643.

Li, W.-W., Yu, H.-Q., & He, Z. (2014). Towards sustainable wastewater treatment by using microbial fuel cells-centered technologies. *Energy & Environmental Science, 7*(3), 911-924.

Lin, J., Aoll, J., Niclass, Y., Velazco, M. I., Wünsche, L., Pika, J., & Starkenmann, C. (2013). Qualitative and Quantitative Analysis of Volatile Constituents from Latrines. *Environmental science & technology, 47*(14), 7876-7882. doi:10.1021/es401677q

Martinez-Huitle, C. A., & Ferro, S. (2006). Electrochemical oxidation of organic pollutants for the wastewater treatment: direct and indirect processes. *Chemical Society Reviews, 35*(12), 1324-1340. doi:10.1039/B517632H

Mayer, P. W., & DeOreo, W. B. (1999). *Residential End Uses of Water*. Retrieved from

Metcalf, & Eddy. (2014). *Wastewater Engineering: Treatment and Resource Recovery*: McGraw-Hill international ed.

Ministry of Home Affairs, G. o. I. (2011). HH-01 Normal Households By Household Size. In I. Office of the Registrar General & Census Commissioner (Ed.).

Montgomery, M. A., & Elimelech, M. (2007). Water And Sanitation in Developing Countries: Including Health in the Equation. *Environmental science & technology, 41*(1), 17-24. doi:10.1021/es072435t

Panizza, M., & Cerisola, G. (2009). Direct And Mediated Anodic Oxidation of Organic Pollutants. *Chemical Reviews, 109*(12), 6541-6569. doi:10.1021/cr9001319

Park, H., Choo, K.-H., Park, H.-S., Choi, J., & Hoffmann, M. R. (2013). Electrochemical oxidation and microfiltration of municipal wastewater with simultaneous hydrogen production: Influence of organic and particulate matter. *Chemical Engineering Journal, 215–216*(0), 802-810. doi:10.1016/j.cej.2012.11.075

Park, H., Vecitis, C. D., Choi, W., Weres, O., & Hoffmann, M. R. (2008). Solar-powered production of molecular hydrogen from water. *Journal of Physical Chemistry C, 112*(4), 885-889. doi:10.1021/jp710723p

Park, H., Vecitis, C. D., & Hoffmann, M. R. (2008). Solar-powered electrochemical oxidation of organic compounds coupled with the cathodic production of molecular hydrogen. *The Journal of Physical Chemistry A, 112*(33), 7616-7626.

Pletcher, D., & Walsh, F. C. (1990). *Industrial Electrochemistry*.

Putnam, D. F. (1971). Composition and concentrative properties of human urine. *NASA Contractor Report CR-1802*.

Radjenovic, J., & Sedlak, D. L. (2015). Challenges and Opportunities for Electrochemical Processes as Next-Generation Technologies for the Treatment of Contaminated Water. *Environmental science & technology, 49*(19), 11292-11302. doi:10.1021/acs.est.5b02414

Sadowsky, M. J., & Whitman, R. L. (2010). *The Fecal Bacteria*.

Sharma, M. K., Tyagi, V. K., Saini, G., & Kazmi, A. A. (2016). On-site treatment of source separated domestic wastewater employing anaerobic package system. *Journal of Environmental Chemical Engineering, 4*(1), 1209-1216. doi:10.1016/j.jece.2016.01.024

Starkl, M., Stenström, T., Roma, E., Phansalkar, M., & Srinivasan, R. (2013). Evaluation of sanitation and wastewater treatment technologies: case studies from India. *Journal of Water Sanitation and Hygiene for Development, 3*(1), 1-11.

U.S. Environmental Protection Agency. (1986). Method 9132: Total Coliform: Membrane-filter technique.

U.S. Environmental Protection Agency. (1999). Alternative disinfectants and oxidants guidance manual. *Environmental Protection Agency Publication 815 R 999014.*

U.S. Environmental Protection Agency. (2010a). Method 1103.1: Escherichia coli (E. coli) in Water by Membrane Filtration Using membrane-Thermotolerant Escherichia coli Agar (mTEC).

U.S. Environmental Protection Agency. (2010b). Method 1680: Fecal Coliforms in Sewage Sludge (Biosolids) by Multiple-Tube Fermentation Using Lauryl Tryptose Broth (Ltb) and Ec Medium. *Washington, DC, US EPA*.

Water Environmental Federation, W., & American Public Health Association, A. (2005). Standard methods for the examination of water and wastewater. *American Public Health Association (APHA): Washington, DC, USA*.

Weres, O. (2009). U.S. Patent 7,494,583.

Weres, O., & O'Donnell, H. E. (2003). U.S. Patent 6,589,405. U.S. Patent.

Whelan, B. R., & Titamnis, Z. V. (1982). Daily chemical variability of domestic septic tank effluent. *Water, Air, and Soil Pollution, 17*(2), 131-139. doi:10.1007/bf00283296

White, G. C. (1999). *The handbook of chlorination and alternative disinfectants*.

Wignarajah, K., Litwiller, E., Fisher, J. W., & Hogan, J. (2006). Simulated Human Feces for Testing Human Waste Processing Technologies in Space Systems. *SAE Technical Papers*.

World Health Organization. (2006). *Guidelines for the Safe Use of Wastewater, Excreta and Greywater: Policy and regulatory aspects* (Vol. 1).

World Health Organization. (2015). *Progress on sanitation and drinking water: 2015 update and MDG assessment*.

Wydeven, h., & Morton A. Golub. (1990). *Generation Rates and Chemical Compositions of Waste Streams in a Typical Crewed Space Habitat*. Retrieved from

Yang, Y., Shin, J., Jasper, J. T., & Hoffmann, M. R. (2016). Multilayer Heterojunction Anodes for Saline Wastewater Treatment: Design Strategies and Reactive Species Generation Mechanisms. *Environmental science & technology, 50*(16), 8780-8787.

Yates, M. V. (1985). Septic Tank Density and Ground-Water Contamination. *Ground water, 23*(5), 586-591.

Yates, M. V. (1987). *Septic tank siting to minimize the contamination of ground water by microorganisms*. Retrieved from

Yin, Z. Q., Hoffmann, M., & Jiang, S. (2018). Sludge disinfection using electrical thermal treatment: The role of ohmic heating. *Science of The Total Environment, 615*, 262-271. doi:10.1016/j.scitotenv.2017.09.175

Chapter 3

URINE MICROBIAL FUEL CELLS IN A SEMI-CONTROLLED ENVIRONMENT FOR ONSITE URINE PRE-TREATMENT AND ELECTRICITY PRODUCTION

Clément A. Cid[1]

in collaboration with

Andrew Stinchcombe[2], Ioannis Ieropoulos[2], and Michael R. Hoffmann[1]

[1]Linde-Robinson Laboratories, California Institute of Technology, Pasadena, CA

[2]Bristol BioEnergy Centre, Bristol Robotics Laboratory, University of the West of England, BS16 1QY, UK

Prepared for submission to

Energy & Environmental Science

C. A. C. is the principal and coordinating author of the manuscript. C. A. C. designed the study, performed the sampling, and analyzed and interpreted the data. C. A. C. performed the DNA extraction and purification. H. Y. graciously scheduled the DNA sequencing and C. A. C. analyzed the data. I. I. provided the MFC system prototypes and remote and in-person support on their operation. M. R. H. provided intellectual and writing contributions.

3.1. Abstract

Microbial fuel cell (MFC) systems have the ability to oxidize organic matter and transfer electrons to an external circuit as electricity at voltage levels of <1V. Urine has been shown to be an excellent feedstock for various MFC systems, particularly MFCs inoculated with activated sludge and with a terracotta ceramic membrane separating carbon-based electrodes. In this article, we studied a MFC system composed of two stacks of 32 individual cells each sharing the same anolyte. By combining the current produced by the 32 cells connected in parallel and by adding the potential of both stacks connected in series, an average power density of 23 mW m^{-2} was produced at an effective current density of 65 mA m^{-2} for more than 120 days. [NH_3], TIC, COD, and TOC levels were monitored frequently to understand the chemical energy conversion to electricity as well as to determine the best electrical configuration of the stacks. Archaeal and bacterial populations on selected anode felts and in the anolyte of both stacks were investigated as well. Indicator microorganisms for bacterial waterborne diseases were measured in anolyte and catholyte compartments to evaluate the risk of reusing the catholyte in a non-regulated environment.

Keywords

Microbial fuel cell; electricity generation; urine treatment

3.2. Introduction

Energy-recovery from waste is a major challenge at a time in which the Earth's resources are increasingly strained by human exploitation (Walther, 2013). For instance, a 2012 special issue of *Science* focused on "Working with Waste" to minimize the use of raw materials (Wigginton, Yeston, & Malakoff, 2012). One attractive way to recover part of the estimated $1.5 \cdot 10^{11}$ kWh of chemical and physical energy lost from the wastewater rejected annually in the United States, is through the use of respiration of microbes in microbial electrochemical technologies (Bruce E. Logan & Rabaey, 2012) such as microbial fuel cells (MFCs). However, efficiently recovering useful amounts of energy from sewage at large scale treatment plants, is —at present— a suboptimal process because the nutrients containing most of the chemical energy of the wastewater have been highly diluted in the sewers (Jiang et al., 2011). The key is then to recover the chemical energy close to the source (*e.g.*, the toilet) before dilution. Urine-diversion toilets, with urine collection systems, have been employed in certain parts of the World, but even though urine is pathogen-free for healthy individuals, its potential contamination with fecal material (Höglund, Stenström, & Ashbolt, 2002) and its high ammonia and mineral content often prevent it from safe and user-friendly nutrient recovery in peri-urban and urban communities (Bischel, Schertenleib, Fumasoli, Udert, & Kohn, 2015). It has previously been reported that urine can successfully be used as a direct feedstock for certain microbes (Ieropoulos, Greenman, & Melhuish, 2012) that will oxidize some of its nutrients and transfer electrons to an inert substrate via direct or indirect processes as the anodic part of a MFC system (Lovley, 2012; Schroder, 2007). This direct energy recovery and

conversion to electricity from urine has shown promising results in standalone MFC systems (Ieropoulos et al., 2012; Salar-García et al., 2017) with a high power production per biomass for terracotta ceramic MFCs (Greenman & Ieropoulos, 2017). Such systems can also be installed in an onsite self-contained human waste treatment system relying on electrolysis to remove nitrogen, chemical oxygen demand (COD), pathogens, and to recover phosphorus (Hoffmann et al., 2013). MFC systems can also be used as a pre-treatment for COD and TOC removal of urine coming from waterless urinals (Figure S3.1). In this article, we investigate the operation of a MFC system for the pre-treatment of human urine by anodic microorganisms with electrical energy recovery. While this usage of MFC can lower the energy cost for treating human waste, it can also recover electrical energy in order to divert the urine flow, making this approach an overall energy gain for the entire onsite self-contained human waste treatment system.

3.3. Materials and methods

3.3.1. MFC stacks

Two versions of a similar design of MFC stacks were employed in this study. The differences in the design are highlighted when necessary. Version A was used for the bacterial cross-over and current efficiency characterizations. Version B was used for long term monitoring with electrical energy harvesting.

Two MFC stacks for each version consisted each of 32 individual cells per stack (Figure 3.1 a) separated evenly and suspended in a rectangular tank connected to a water-free urinal (Figure 3.1 b). A gravity-driven cross-flow through each stack was made possible by placing the input and output connection at the outermost parts of the rectangular tank (Figure 3.1 c). In normal operation, the input of the top stack was connected to an equalization tank equipped with a level sensor commanding a pump. About 3.5 L of the urine drained from the water-free urinal were pumped when the level of urine in the equalization tank reached a certain height. The residence time of urine in the equalization tank could vary from few hours to few days as shown by the recorded feeding intervals in Figure 3.2. The output of the top stack was connected to the input of the bottom stack with two 90º bent pipes to minimize cross-over between the top and the bottom stack. The output of the bottom stack drained by gravity into a tank for further processing.

The cells in both versions A and B were similar to the ones described by Salar-García *et al.* (Salar-García et al., 2017): each cell had a terracotta tubular ceramic tube of 150 mm length and 42 mm internal diameter (50 mm outer diameter) with an unknown pore size (Weston Mill Pottery, Newark, United Kingdom) open to air in its

center and acting as an ion-conductive separator between anode and cathode. Each anode was 1000 mm by 260 mm carbon veil (loading 20 g m^{-2}, PRF Composite Materials, Dorset, UK) folded in half along its length to make 1000 mm by 130 mm and wrapped around the outside surface of the terracotta tubular ceramic tube. This was held in place by a stainless-steel wire. The wire was physically holding the electrode against the terracotta tube and acted as a current collector connected directly to the other anodes via alligator clips and metal wires (version A) or through an electrical bus bar attached to the stack acting as the anodic current collector (version B). The cathode was a 140 mm by 130 mm carbon veil with micro pores described elsewhere (Papaharalabos et al., 2013). The cloth was rolled along its length (140 mm) and placed inside the terracotta tube in a manner intended to maximize the contact with the ceramic wall while reaching the bottom of the tube. Alligator clips connected to each other (version A) or to a metal bus bar cathodic current collector (version B) were used for electrical contact with the cathode cloth.

The inoculation period was similar for version A and version B and lasted approximately 24 days. Each stack was first inoculated with 10 L of a 1:1 solution of human urine and activated sludge from a local domestic wastewater treatment plant treating mostly domestic wastewater (San José Creek Water Reclamation Plant, Whittier, California, USA) for 3 days. After the initial addition, 3 to 6 L of urine were added to each stack at regular intervals (Figure S3.2). The stacks were drained of the same volume before urine addition. During the inoculation, the anodes and cathodes were connected to a 4 Ω load, and voltage across the load was recorded on a continuous basis via an automatic data logger, *vide infra*. The inoculation period was

stopped when the voltage across the resistor stabilized (not taking into account diurnal variations) (Figure S3.2).

3.3.2. Electronics for performance monitoring and energy harvesting

The wires (version A) or metal bus bar (version B) from each stack were connected directly to a power harvester. The power harvester did not contain any active electrical components but facilitated connecting the stacks in series or parallel. The electrical energy of each stack was dissipated by the 'Joule effect' through an adjustable load with a potentiometer of 1 to 25 Ω range with 0.2 Ω precision (Digikey, USA). The electrical potential across the load was measured and recorded every ten seconds by a two-channel data logger (Programmed Scientific Instruments, Arcadia California) connected to a Panel PC PPC-L62T (Advantech, China) with a dedicated software package (Program Scientific Instruments, Arcadia CA). The potentiometers and the data logger electrical connections were adjusted to fit an independent, series, or parallel wiring between the two stacks.

3.3.3. Solution sampling and chemical analyses

Grab samples were taken from approximately 10 cm below the surface of each stack through a hole drilled as close to the inlet/outlet as possible. A 50-mL plastic syringe (BD, Franklin Lakes, NJ) connected to a 15-cm piece of Tygon tube (Saint-Gobain, France) was used to collect between 10 mL and 20 mL of the solution. The syringe and the tube were rinsed with ultrapure water and dried multiple times with several suction/injection movements between each sampling. After the last sample was taken, the syringe and the tube were cleaned with a 10% solution of bleach and

rinsed several times with ultrapure water and then allowed to dry until the next sampling.

Sampled solutions were filtered through a 25-mm Acrodisc Syringe Filters with a 0.45-µm GHP membrane (Pall Corporation, Port Washington NY) and diluted appropriately with ultrapure water before storage at 4 ºC and analysis.

COD was measured in duplicates and triplicates via the colorimetric method Hach 8000 (Hach Company, Loveland CO). Ammonia [NH_3] (measured as [NH_4^+]) was determined by ion chromatography (Dionex ICS 2000; AS19G anions, CS12A cations). TOC and TIC concentrations were measured with an Aurora 1030W TOC Analyzer (OI Analytical, College Station TX) using the heated persulfate wet oxidation technique.

3.3.4. Coulombic efficiency

Coulombic efficiency ε for COD removal (%) was determined using equation (1) proposed by Logan *et al.* (Bruce E Logan et al., 2006) with the approximation that the MFC stacks were receiving an average daily flow q = 1 L day^{-1}. Other parameters were M the molar mass of oxygen (M = 32 g mol^{-1}), $\boldsymbol{\mathcal{F}}$ the Faraday's constant ($\boldsymbol{\mathcal{F}}$ = 96,500 C mol^{-1}), and b the number of electrons exchanged per mole of oxygen reduced (b = 4). I (A) was the averaged current going through the MFC stack as determined by Ohm's law ($E = RI$, E being the potential (V) across the resistor R (Ω) and I the current flowing through R). Δ_{COD} (mg O_2 L^{-1}) was the difference in COD values between influent and effluent.

$$\varepsilon = \frac{MI}{\boldsymbol{\mathcal{F}} b q \Delta_{COD}} \cdot 100 \qquad (1)$$

3.3.5. Analyses of biomass in suspension

Three catholyte compartments from the top stack (C1, C2, and C3, Figure 3.1 c) were sampled as well as inside the anolyte compartment of the top and the bottom stacks. The sampling of the anolyte was performed close to the inlet and the outlet of the top stack and close to the outlet of the bottom stack. The samples were taken with a similar apparatus previously described.

Bacterial cross-over between anolyte and catholyte was assessed by estimating the quantity of indicator organisms *E. Coli*, *Total Coliforms*, and *Enterococcus* with the following respective EPA methods: 1103.1 (U.S. Environmental Protection Agency, 2010), 9132 (U.S. Environmental Protection Agency, 1986), and 1600 (U.S. Environmental Protection Agency, 2002) with appropriate dilutions.

3.3.6. Biological analyses of the anodes

Bacterial population estimates on the sampled carbon veils that were used as anodes for 4.5 months were determined by staining a small portion of a carbon veil anode using a LIVE/DEAD BacLight Bacterial Viability Kit L7012 (Molecular Probes, Eugene OR). The kit contained an appropriate mixture of SYTO 9 (excitation at about 480 nm, emission in green at about 500 nm) and propidium iodide (excitation at about 490 nm, emission in red at about 635 nm). The carbon veil was infused with enough volume of the dye mixture to cover all the veil sample following the manufacturer's recommendations. The dyed veil was then placed on a glass slide and observed under a fluorescent light microscope (Leica DMi 8, Leica Microsystems, Wetzlar, Germany) controlled by LAS X Expert software and equipped with the

following fluorescence filter cubes: DAPI (blue color), FITC (green color), and RHOD (red color).

16S rRNA metagenomic sequencing was performed on selected anode and anolyte samples based on the analytical method developed by Kozich *et al.* (Kozich, Westcott, Baxter, Highlander, & Schloss, 2013) DNA was extracted using a Mo Bio PowerWater DNA isolation kit (QIAGEN, Germantown, MD) following a modified extraction method described in the Supplementary Information section.

3.4. Results and Discussion

3.4.1. Stabilization of MFC performance

The electricity produced from two separated MFC stacks (version B) connected in series was monitored continuously over the course of 160 days (Figure 3.2). Input and output [NH_3], TIC, COD, and TOC levels for both stacks were measured on a regular basis during the same period of time (Figure 3.3).

After the initial feeding and inoculation period of 24 days (Figure S3.2) described earlier, voltage across the potentiometer for each stack remained between 280 mV and 350 mV (Figure 3.2) with increases of 30 ± 10 mV appearing soon after some feeding events. This is in contrast to the rapid increase in cell voltage of approximately 100 mV (Figure S3.2), observed soon after a feeding event during the first seven days of the inoculation process. The lowering of the potential rise over the course of the 160 days of testing can be explained by the stabilization of the biological community of the MFC stacks as observed with various MFC systems in the literature (Paitier et al., 2017).

This stabilization is also observed relative to some of the chemical parameters measured, particularly [NH_3] and TIC (Figure 3.3 a and b): after the initial inoculation period, [NH_3] stabilizes at 210 ± 20 mM with limited variation between the two stacks. This concentration is nearly half of the molar equivalent of Total Kjeldahl Nitrogen (TKN) present in urine. After 80 days, [NH_3] in the bottom stack was found to be 40 mM higher than that in the top stack. This difference in [NH_3] is probably due to two factors: the evaporation of NH_3 happening in both stacks not necessarily at the

same rate (the top stack is open to air while the bottom stack partially sealed under the top stack, see

Figure 3.1 b) and the slow hydrolysis of urea that occurs preferentially in the bottom stack after a longer retention time (Udert, Larsen, Biebow, & Gujer, 2003). The TIC in the top stack was slightly higher (0.2 ± 0.1 g C L^{-1} = 22 mM C) than in the bottom stack. This was most likely due to the formation of HCO_3^- from urea hydrolysis, which also partially accounted for the 40 mM increase in [NH_3] between top and bottom stacks.

Contrary to the stability of [NH_3], the variability in COD levels over the 160-day period was more pronounced (Figure 3.3, c): in the top stack the COD level was higher than in the bottom stack by 2 g O_2 L^{-1} to 5 g O_2 L^{-1}, on average. This indicated active mechanisms for COD removal linked with the presence of microbial communities that were feeding on organic compounds from urine. Furthermore, the difference between inlet and outlet values of the top stack of 2.4 ± 1.2 g O_2 L^{-1} (*e.g.*, days 55, 71, 96, 150 and 157) and less than 1 g O_2 L^{-1} for the bottom stack indicates that the COD removal activity in the top stack is not as uniform as in the bottom stack. Finally, the difference in COD value between the outlet of the top stack and the inlet of the bottom stack is due to the fact that despite being connected hydraulically in series, the two stacks did not share fluids continuously: the overflow of the top stack drops to the bottom stack only when it was filled, which occurred after a urine feed event as recorded on Figure 3.3, a). The rise in COD values near 140 days could be explained by a more frequent number of feeding events or a decrease in microbial activity in the top stack, the latter being the least probable because the voltage of the top stack did not drop (Figure 3.2).

The variation in TOC values follows closely the same pattern as the COD values with the difference between inlet and outlet values of the top and bottom stacks of 0.75 ± 0.25 g C L^{-1} on different days, indicating a non-uniform oxidation of organic matter across both stacks. TOC levels were significantly higher in the top stack than in the bottom stack for the majority of the samples except for two sampling days: day 71 and day 150. The drop in the TOC value measured on these two days did not seem to be part of a trend and might be due to sampling error. The sustained difference between TOC levels from top to bottom stacks indicates a relatively high mineralization process and is consistent with microbial respiration.

The 12-day controlled feeding test, performed between day 96 and 107 (Figure 3.4) with frequent chemical monitoring of the same parameters as previously cited, confirmed the limited impact of a single feeding event on [NH_3] and TIC (Figure 3.4 a and b): [NH_3] remained at 210 ± 10 mM at the outlet of the top stack and 175 ± 5 mM in the bottom stack over the 12-day test period with moderate changes due to feeding events. The highest variation in [NH_3] occurred at the inlet port of the top stack: [NH_3] increased after 4 days of fasting to 220 mM and then decreased to 200 mM between day 4 and 7 of the test. This pattern reappeared in a similar fashion after the second feeding. This slight jump in [NH_3] was probably due to hydrolysis of urea present in a higher concentration at the inlet (when fresh urine entered the system) than at the outlet with slight changes (± 0.1 g C L^{-1}) of similar pattern in TIC concentration in the top stack. This increase in [NH_3] and TIC levelled off across the entire stack through diffusion.

Contrary to [NH_3] and TIC, the difference in COD and TOC levels between feeding events (Figure 3.4 c) and among top and bottom stacks is more consequential: all the inlet and outlet values showed a decrease short after the feeding followed by an increase a few days later. The highest drop in COD levels was observed at the outlet of the stacks: during the first 3 days after feeding, the COD level at the outlet of the top stack decreased by 50% from 8 g O_2 L^{-1} and less than 20% at the inlet of the same stack. An even more drastic decrease of close to 90% from 4.2 g O_2 L^{-1} occurs at the outlet and the inlet of the bottom stack. After reaching their respective minima, the COD levels increased by 4 g O_2 L^{-1} for the top stack outlet and by 2 g O_2 L^{-1} for the other sampling ports. TOC values followed the same trend but with less drastic changes. The increase in COD and TOC levels followed by a decrease is typical of microbial oxidation of organic waste as observed in wastewater treatment batch processes (Metcalf & Eddy, 2014). Thus, the oxidation of organics by the microbial community appeared to be the key driver for electricity production in both MFC stacks.

The differences in the microbial community on the anodes and in the anolyte were determined qualitatively by fluorescence microscopy (Figure 3.6) and quantitatively by 16S rRNA metagenomic sequencing and sorting into operational taxonomic units (OTUs, Figure 3.7). Fluorescence microscopy pictures of the anode felt show a large amount of dead and live microorganisms (Figure 3.6 a), with live microorganisms preferentially arranged along the fibers (Figure 3.6 b) in groups. Dead microorganisms are also present in similar areas, thus showing an active microbial biota on the anodes. The metagenomics analysis of the biota on the anodes and in the

unfiltered anolyte showed different OTUs in the anolyte of the two MFC stacks as well as within the same anode (Figure 3.7).

There were no significant differences between the composition of the OTUs at the outlet and the inlet of a specific MFC stack except for the following groups: *Archea* and *Clostridia* units were present at a higher levels in the anolyte of the bottom stack than in the top, whereas *Gamma Proteobacteria* and *Bacili* units were found at higher levels in the anolyte of the top stack than in the bottom. These differences in population might have been due to an adaptation of the biota in suspension to the different types of nutrient mixtures entering the stacks, since the top stack inlet received urine while the bottom stack inlet received the anolyte (spent urine) from the top stack outlet. Furthermore, the sampled anodes from the top stack had large differences in distribution of OTUs whether they were sampled close to the inlet (C1) or close to the outlet (C3,

Figure 3.1 c) or whether they were sampled at the bottom, middle, or top of the anode along its vertical axis: for instance, bottom samples for C1 and C3 had the lowest *Bacteroidia* percentage and the highest *Clostridia* percentage of their respective anode, while bottom and middle parts of C1 and C3 had higher *Bacili* levels than the top of their respective anode.

Comparing the anodes and the anolyte showed no single emergent microorganism that could exclusively be linked to the electron-transfer mechanisms between bacteria and electrode. Nevertheless, the amounts of *Gammaproteobacteria* and *Clostridia* OTUs on the anodes higher than in the top anolyte could be linked to those mechanisms. Furthermore, the observed differences in microbial populations

revealed an adaptation of the microbial community to its location along the vertical axis and that adaptation was probably due to a non-uniformity of the nutrient concentration, dissolved oxygen concentration, and current density along or close to the anode. A deeper understanding of the microbial communities and their role in organics oxidation in a urine medium could potentially lead to greater energy production and COD removal.

3.4.2. Energy recovery to electricity

Three electrical configurations for MFC stacks (version A) were tested for optimal electricity generation and COD removal: an independent configuration in which each stack was connected to a potentiometer of resistance R = 12.5 Ω for 14 days, a series configuration in which both stacks were connected in series with a potentiometer of resistance R = 25 Ω for two periods of 7 days each, and a parallel configuration in which both stacks were connected in parallel to a potentiometer of resistance R = 12.5 Ω for 14 days. The external resistance values should have been different for the three electrical configurations, and this was due to practical limitations and connection error. It may, nonetheless help to explain the variation in the observed behavior of the two stacks.

The highest electrical power density averaging 24 mW m^{-2} for each stack was produced when the two stacks are electrically separated (Figure 3.5, top graph). This value was within range of what has been found in the literature for similar configuration (Liu & Logan, 2004; Rabaey & Verstraete, 2005). In this case, there was no potential or current limitation that occurred when stacks were connected in series (19 mW m^{-2}) or parallel (9 mW m^{-2}) configurations. The overall COD removal

obtained with the stacks connected independently or in series (Figure 3.5, bottom graph) had the following pattern: the COD removal in the top stack was around 25 ± 5% irrespectively of the electrical configuration while the COD removal in the bottom stack was of 70% when the stacks were independent and 35% when they were in series. Moreover, the overall COD removal of the MFC system was 80% when the stacks were independent, 70% when the stacks were in parallel, and less than 50% when the stacks were connected in series.

Combined with power density measurements, Coulombic Efficiency ε for COD removal was dependent on electrical configuration of the stacks: the lowest overall ε was obtained when the stacks were connected in parallel ($\varepsilon \approx 3\%$) while the maximum overall ε was obtained when the stacks were connected in series ($\varepsilon \approx 15\%$). These results are in agreement with those of Oliot *et al.* on smaller scale systems (Oliot, Etcheverry, Mosdale, & Bergel, 2017); they concluded that configuring MFC stacks in series was a good compromise between COD removal, power density, and Coulombic Efficiency. In addition, connecting the two stacks in series allowed for a higher output voltage and a more effective usage of the electrical energy by minimizing conversion losses for voltage ramp-up to charge a battery.

Had the stacks been connected to the correct resistance values, then the power output of the second and third configurations (series and parallel) would have been roughly double that of the individual stacks when running independently; the series connection would have produced the same current but double the voltage, and the parallel connection would have produced the same voltage but double the current. Both parameters have been shown to affect COD, efficiency, and even killing efficacy

of MFCs, when studied from a principal component analysis (PCA) perspective (Ieropoulos, Pasternak, & Greenman, 2017). This could have been a key factor in changing the MFC behavior and will form part of our near-term experiments to corroborate.

3.4.3. Bacterial cross-over

Catholytes were monitored for bacterial cross-over from the anolyte that contains urine and activated sludge to the catholyte compartments of the cells. Table 3.1 summarizes the occurrence of four common indicator microorganisms: *E. Coli.*, *Total Coliforms*, *Fecal Coliforms*, and *Enterococcus* in selected catholytes and anolytes in four electrical configurations of the stacks as follows: 1) at open circuit for 7 days, 2) independently connected to a load, 3) connected in series, 4) or in parallel to the same load. In all electrical configurations, the levels of detected microorganisms in the anolyte were too numerous to count in most instances. This is consistent with the fact that bacteria derived from activated sludge should be present in the anolyte at all time.

All indicator microorganisms were detected in all three catholyte samples when the MFC stacks were at open circuit for 7 days. When the stacks were electrically connected in series or in parallel for 14 days, only *Total Coliform* tests appeared positive while the other indicator organisms were not detected. The independent connection of the stacks for 7 days showed mix results with *Enterococcus* and *Fecal Coliform* below detection limits; *E. Coli.* at or above 1 CFU mL^{-1} in two out of three catholytes. *Total Coliform* tests appeared positive in all instances.

Since no catholyte is intentionally placed in contact with the activated sludge and urine mixture of the anolyte compartment, bacterial diffusion through the terracotta membrane is the probable reason why all the indicator microorganisms are detected in the catholyte compartment. Furthermore, for stacks at open circuit, there is no electrical potential gradient between anode and cathode and diffusion through the terracotta occurs because of drying on the cathode (open to air).

When anodes and cathodes are connected to a load, the cathodic reduction of oxygen to water (eqn 2) increases the pH in the catholyte (Kumar & Mungray, 2017) observed in this type of MFCs (Gajda, Greenman, Melhuish, & Ieropoulos, 2016), making the catholyte less favorable for bacteria to grow (Thorn, Lee, Robinson, Greenman, & Reynolds, 2012).

$$O_2 + 4\ e^- + 4\ H^+ \rightarrow 2\ H_2O \qquad (2)$$

There is no significant difference between the electrochemical potentials at each electrode whether the stacks are electrically connected independently or in series to the same load: the difference in concentration of indicator organisms in the catholytes between independent connection and parallel or series might be simply due to a longer period of time at which the system was run with oxygen reduction at the cathode.

The minimal bacterial cross-over during operation could imply that water present in the catholyte compartment could be used beneficially; however, the high level of *Total Coliforms* indicate that the catholyte water may contain pathogens. Direct contact usage would not be recommended but indirect usage such as heavy metals precipitation could be applied (Gajda, Stinchcombe, Greenman, Melhuish, &

Ieropoulos, 2017). The low bacterial-load reduction of the anolyte makes the presence of a post-treatment option such as electrochemical oxidation compulsory.

3.5. Conclusions

- Continuous averaged power density of 23 mW m^{-2} at a current density of 65 mA m^{-2} was produced for more than 120 days.
- COD and TOC removal was observed concomitantly with power production via anodic oxidation.
- Bacterial cross-over between anolyte and catholyte was observed at open circuit, but fewer micro-organisms are detected when MFC stacks are electrically connected in series or parallel.
- A large diversity of microorganisms was observed on the anodes and in solution; however, electricity production could not be linked to a single genus.

3.6. Acknowledgments

The authors acknowledge Dr. Hank Yu from the Orphan research group and Dr. Nathan Dalleska from the Environmental Analysis Center at the California Institute of Technology. Dr. Yu helped on DNA extraction, 16S rRNA gene sequencing, and processing. Dr. Nathan Delleska provided access and guidance for Ion Chromatography and Total Organic/Inorganic Carbon analyses. This research was supported by the Bill and Melinda Gates Foundation under RTTC Grants OPP 1069500 and OPP 1111246 for CAC and MRH, and GCE Grant OPP1094890 for AS and II.

Table 3.1: Bacterial count (CFU per ml) of Total Coliform, Fecal Coliform, Escerichia Coli., and Enterococcus indicator microogranisms for different electrical configurations of the stacks in the following sequence: open circuit (7 days), independent (7 days), series (14 days), and parallel (14 days).

Configuration & Sample type	*Total Coliform*	*Fecal Coliform*	*Escerichia Coli*	*Enterococcus*
Urine	n.d.*	n.d.	n.d.	n.d.
Open circuit				
Top stack IN	TNTC#	TNTC	TNTC	TNTC
Top stack OUT	TNTC	TNTC	TNTC	TNTC
Bottom stack OUT	TNTC	TNTC	TNTC	2.2
Catholyte 1	n.d.	22	6.0	39
Catholyte 2	4.0	12	5.0	29
Catholyte 3	1.0	10	2.0	3.4
Independent				
Top stack IN	TNTC	n.d.	TNTC	TNTC
Top stack OUT	TNTC	n.d.	TNTC	TNTC
Bottom stack OUT	TNTC	TNTC	TNTC	8.0
Catholyte 1	>1.0	n.d.	1.0	n.d.
Catholyte 2	TNTC	n.d.	n.d.	n.d.
Catholyte 3	TNTC	n.d.	37	n.d.
Series				
Top stack IN	6.0	n.d.	n.d.	TNTC
Top stack OUT	n.d.	n.d.	n.d.	TNTC
Bottom stack OUT	TNTC	n.d.	n.d.	n.d.
Catholyte 1	n.d.	n.d.	n.d.	n.d.
Catholyte 2	TMTC	n.d.	n.d.	n.d.
Catholyte 3	n.d.	n.d.	n.d.	n.d.
Parallel				
Top stack IN	TNTC	TNTC	TNTC	TNTC
Top stack OUT	TNTC	TNTC	TNTC	n.d.
Bottom stack OUT	TNTC	n.d.	n.d.	n.d.
Catholyte 1	0	n.d.	n.d.	n.d.
Catholyte 2	TNTC	n.d.	n.d.	n.d.
Catholyte 3	3.0	-	-	-

* non detected; # too numerous to count

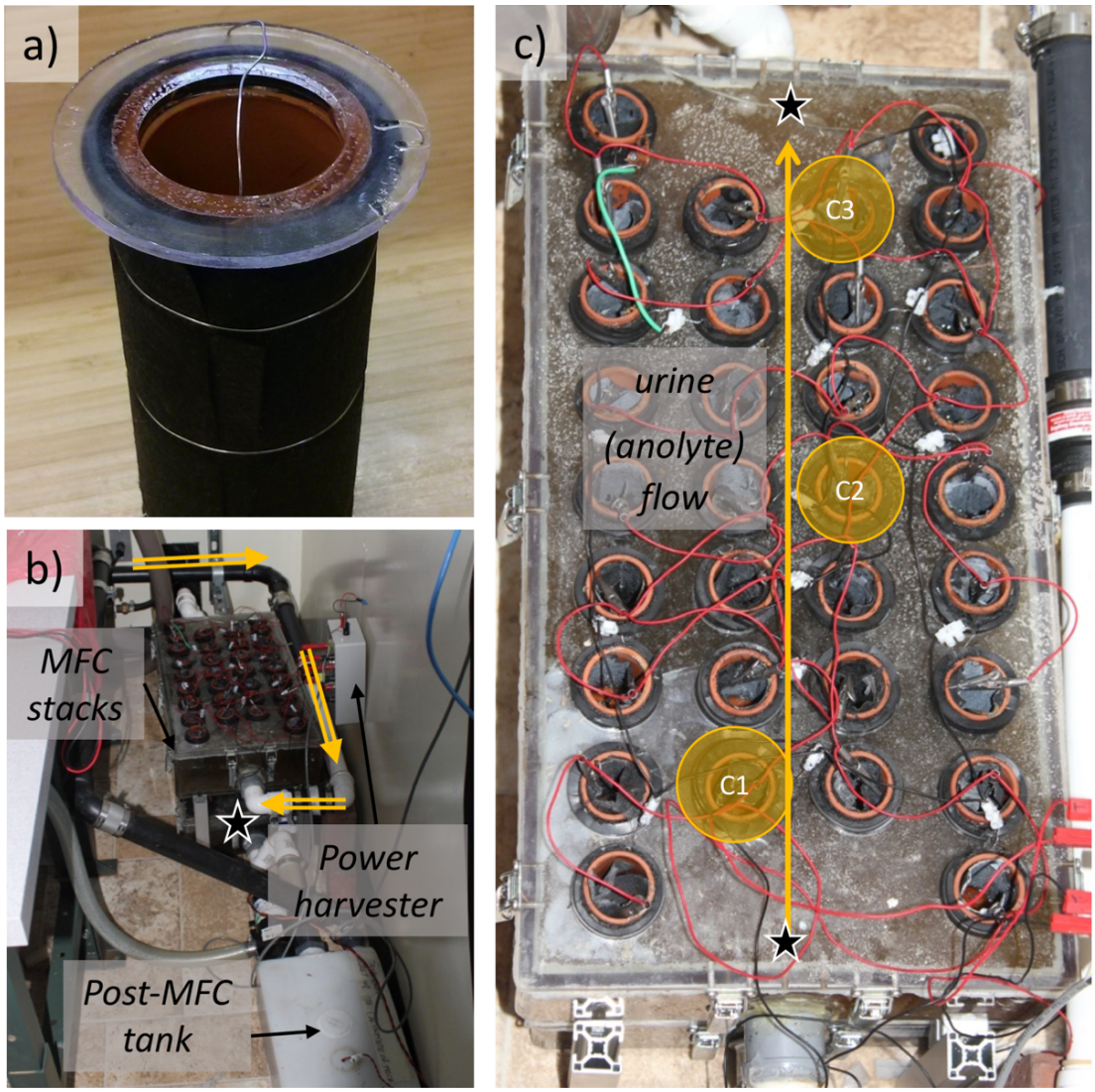

Figure 3.1: a) Picture of an empty terracotta microbial fuel cell with the anode supported by a nickel-chromium wire. b) Two MFC stacks on top of each other fed by gravity and installed behind a water-free urinal on Caltech campus. c) Top view of the MFC stacks (version A) with direction of the gravity-fed urine flow through the system. Cells C1, C2, and C3 used for catholyte sampling for microbial testing (Table 3.1) are highlighted. Sampling points for the anolyte in top and bottom stacks are marked with a star.

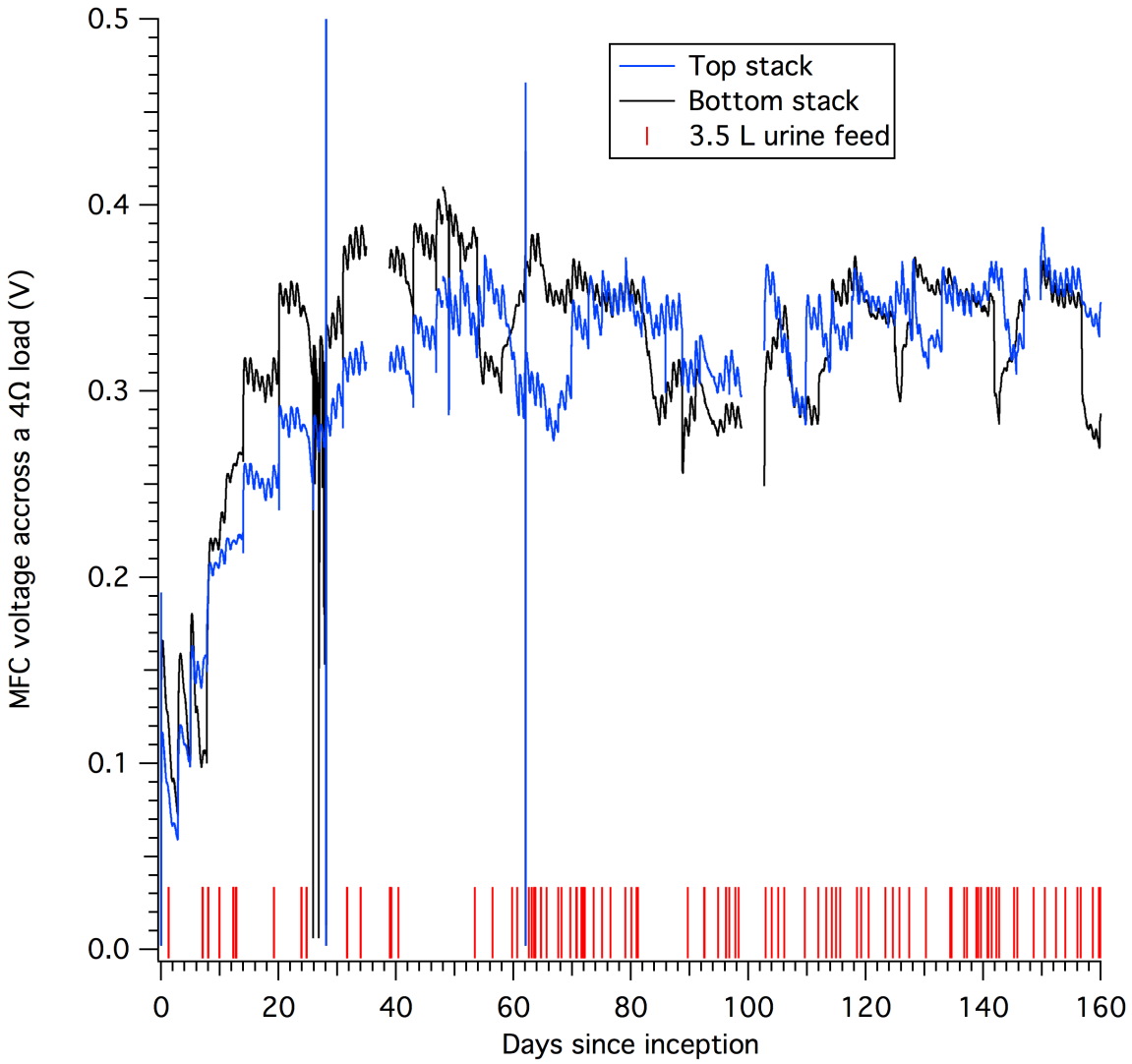

Figure 3.2: Voltage across the bottom and top stack (version B), each connected to a separate 4Ω individual load. Recorded urine feeding events are represented with vertical red bars.

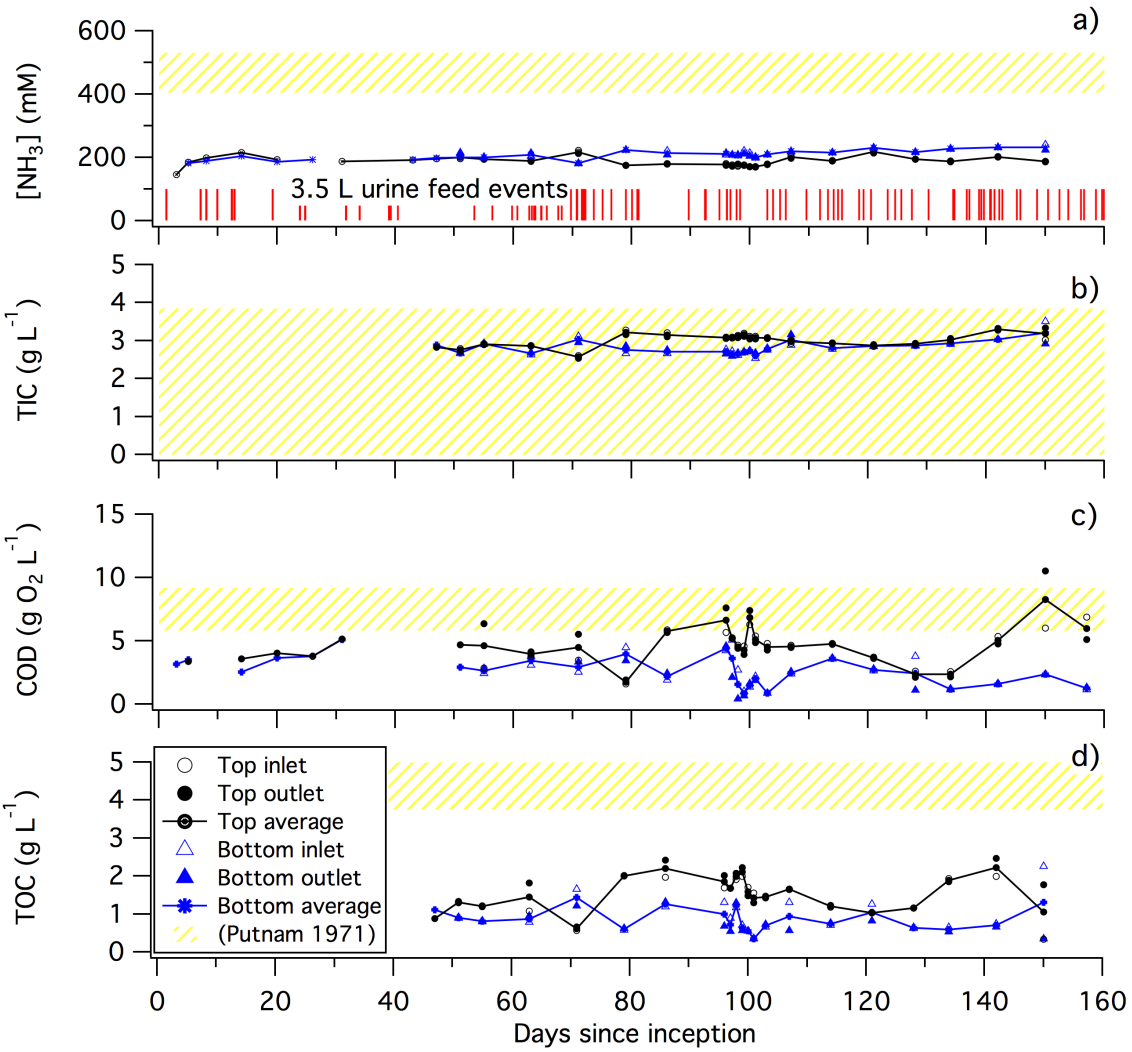

Figure 3.3: a) [NH_3], b) TIC, c) COD, and d) TOC levels at the inlet, outlet, and averaged for each MFC stacks. Recorded urine feeding events are represented with vertical red bars. Range of values measured in urine samples by Putnam *et al.* are reproduced in a yellow pattern. [NH_3] pattern is based of Total Kjehdal Nitrogen (TKN).

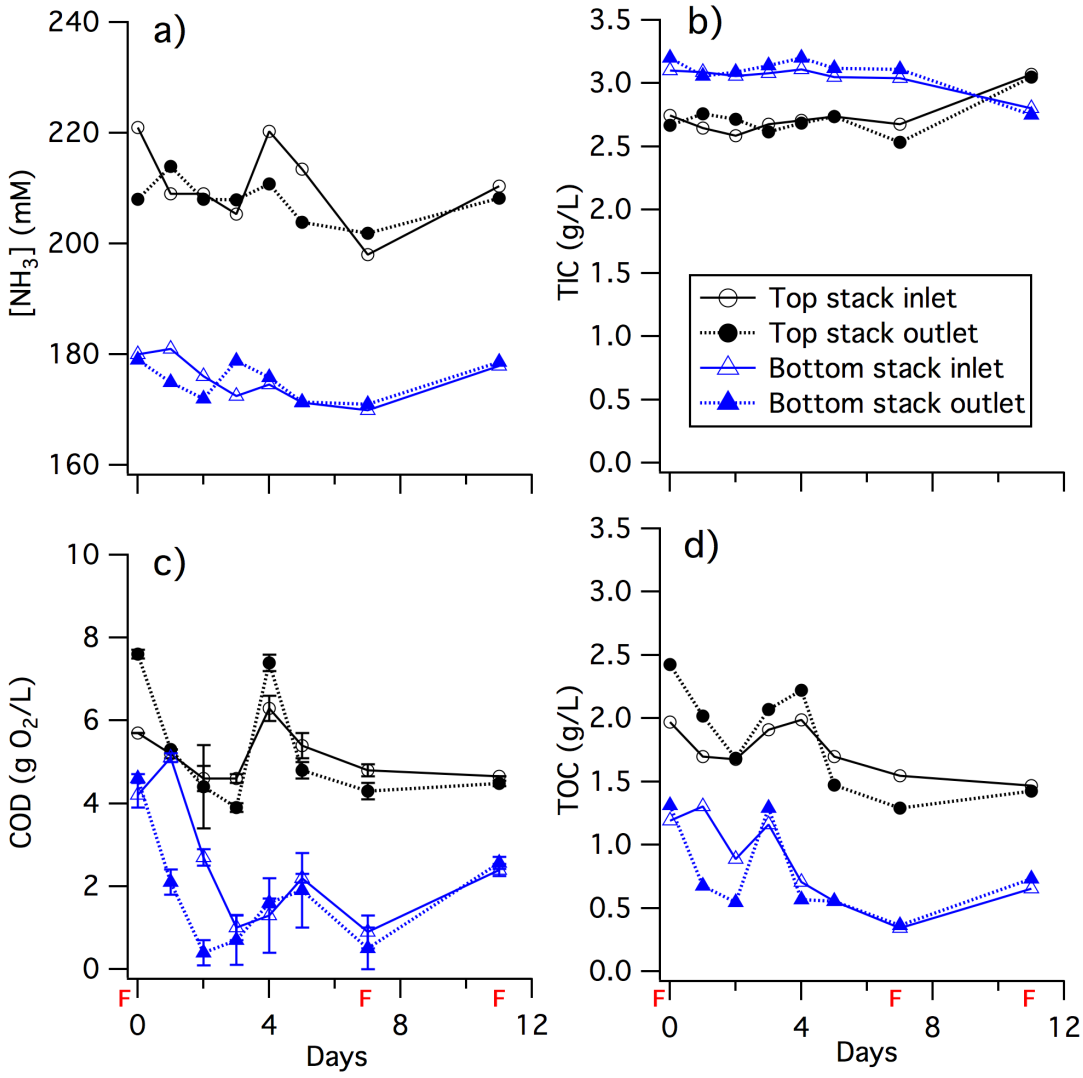

Figure 3.4: Evolution of chemical parameters a) [NH_3], b) TIC, c) COD, and e) TOC, over the course of 12 days with three distinctive "feeding events" (marked "F") in which 3.5 ± 0.25 L of fresh urine entered from the top MFC stack inlet.

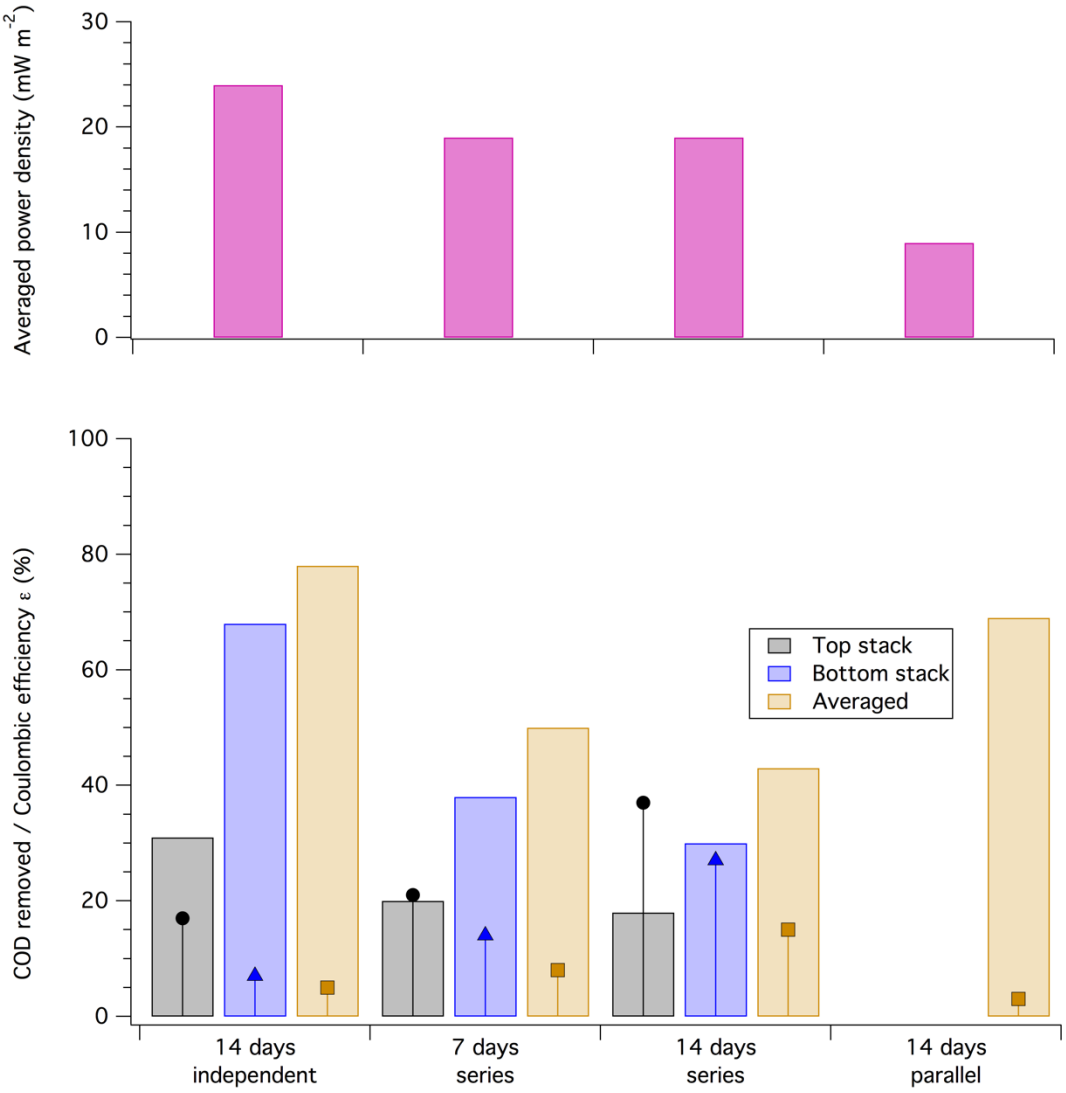

Figure 3.5: Top: specific power density (top, mW m^2) and bottom: COD removal afficiency (bars, %) and Coulombic efficiency ε (sticks and markers, %) for different electrical configurations of the MFC stacks (version A): independent for 14 days (R = 12.5 Ω), in series for 7 and 14 days (R = 12.5 Ω), and in parallel for 14 days (R = 25 Ω).

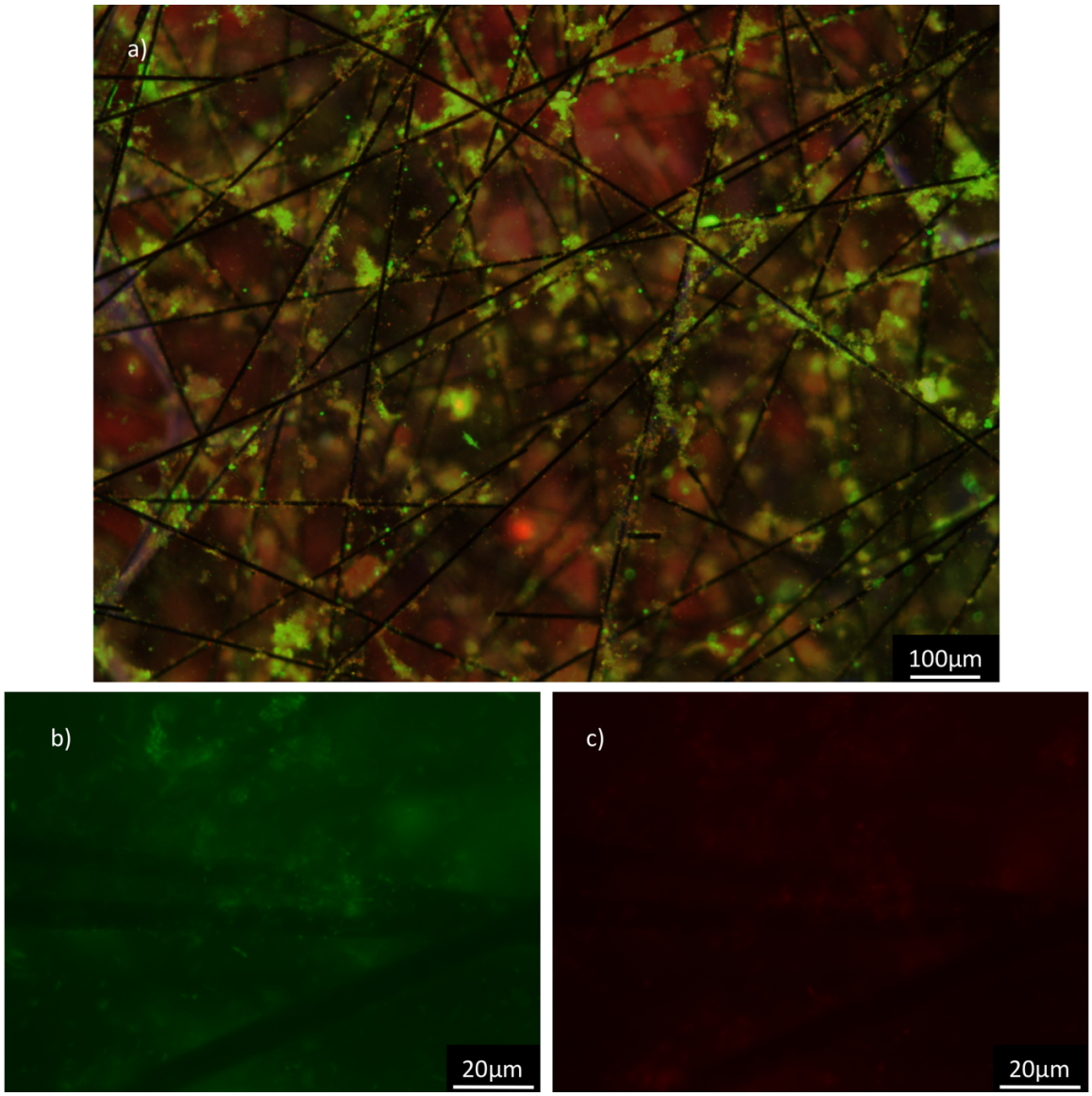

Figure 3.6: Middle section of a stained anode (see Materials and methods section) revealed under fluoresence miroscopy after several months of operation in the top MFC stack: a) FITC and RHOD channels combines, b) FITC and c) RHOD channels at higher magnification with same contrast and brightness.

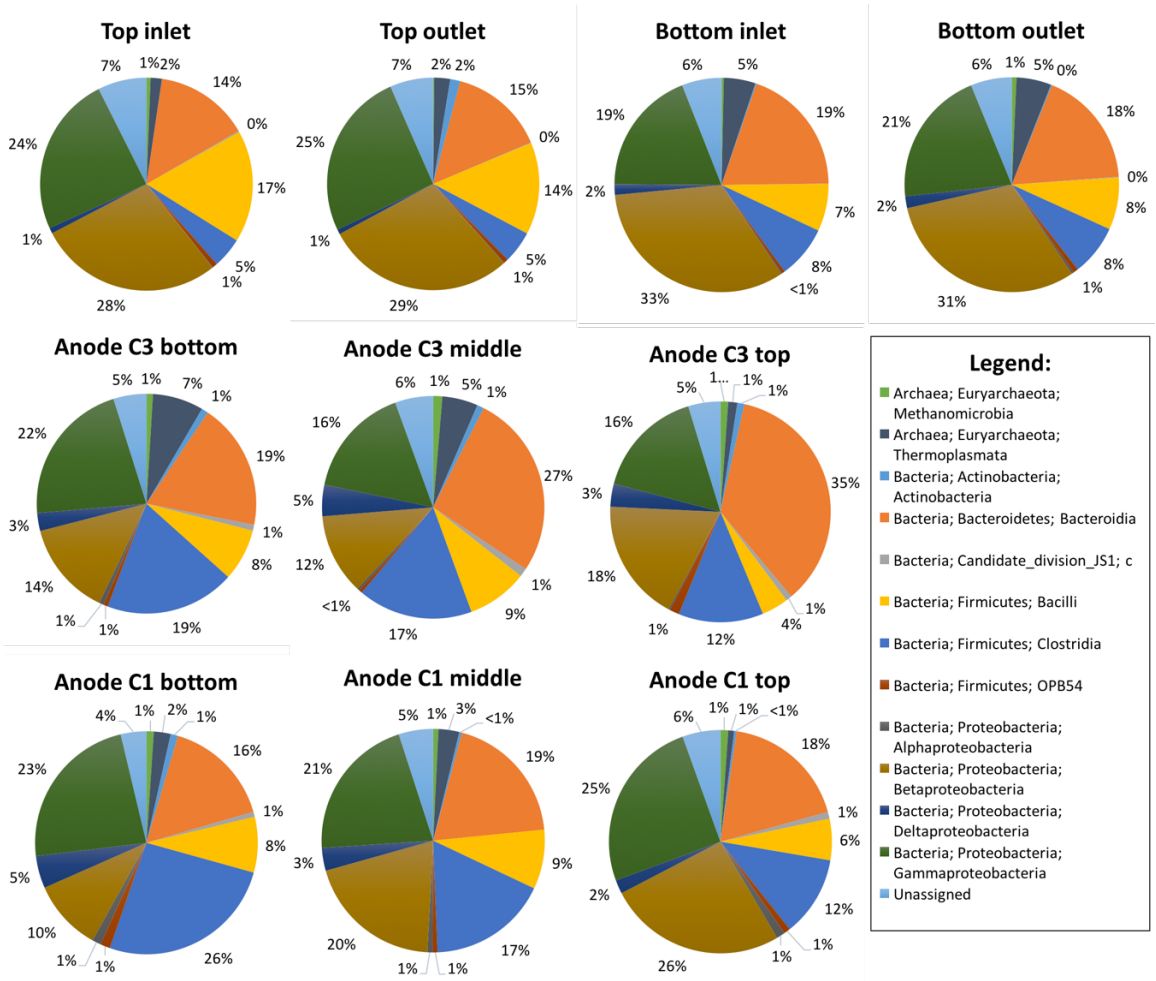

Figure 3.7: Proportion of archeal and bacterial population assigned by 16S rDNA taxonomy analysis into operational taxonomic units (OTU). Only OTUs with a minimum of 1% occurance for any sample are represented. See Supporting Information for details on the DNA extraction method.

3.7. Supplementary figures

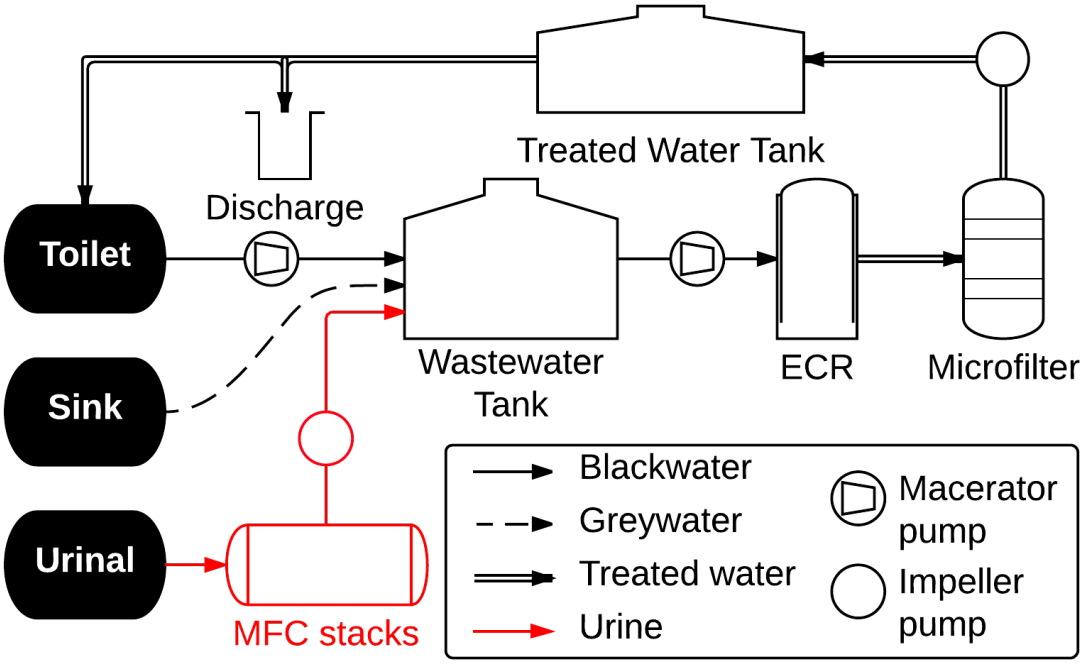

Figure S3.1: Integration of the MFC stacks within the treatment scheme of the self-contained wastewater treatment and recycling system developed by Hoffmann *et al.* (Hoffmann et al., 2013).

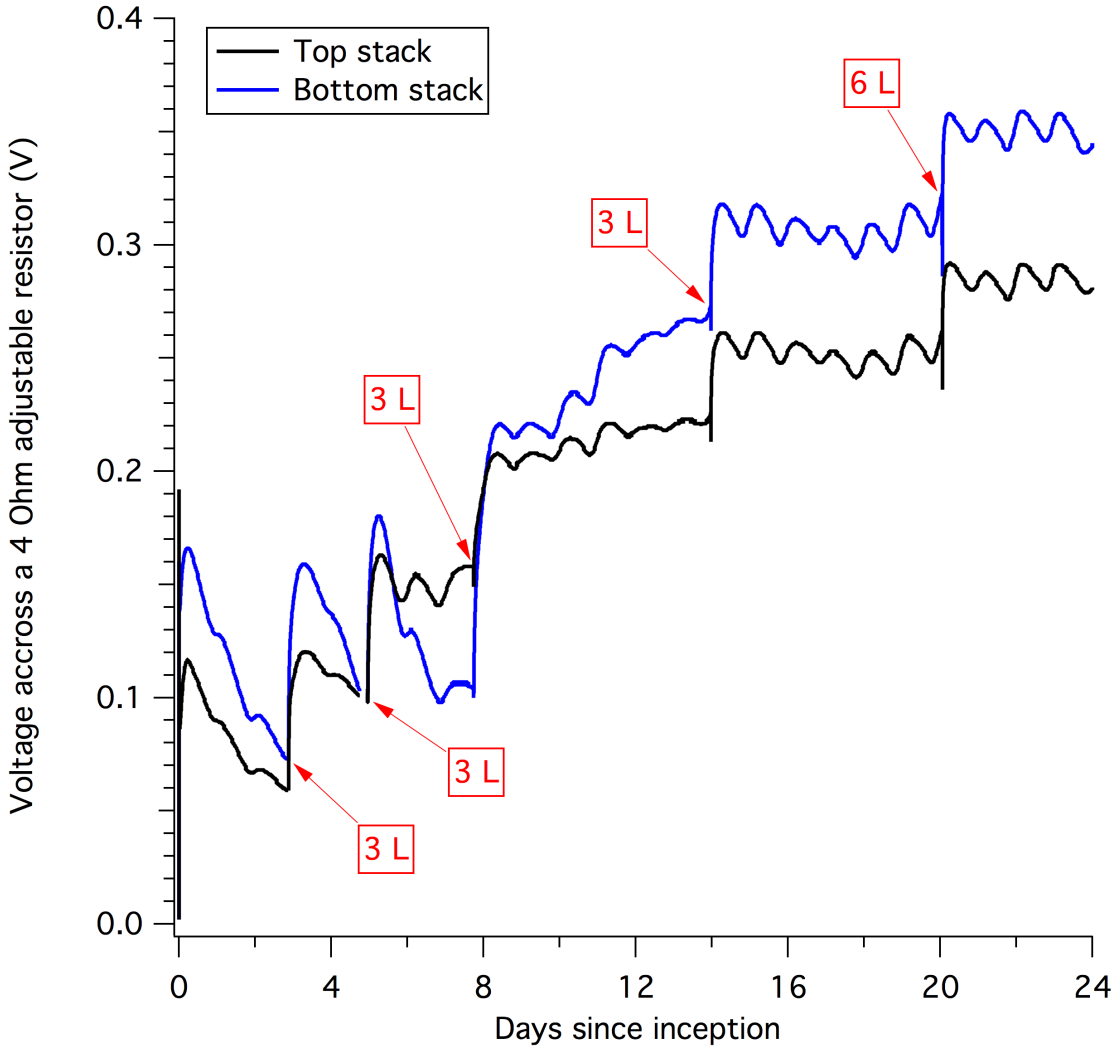

Figure S3.2: Potential measured across a 4 Ω resistor for each independent stack. The red arrows indicate a feeding event: each stack was slowly drained of the anolyte volume written and replaced by the same quantity of fresh urine.

3.8. Supplementary information: protocols

3.8.1. Genomic DNA extraction protocol (based on Mo Bio and modified by the Orphan research group at the California Institute of Technology):

Anode felts were cut in pieces of 0.5 cm by 1 cm. Each felt was placed in a 15-mL conical centrifuge tube with 10 mL of a 70% ethanol solution in an ice bath. The mixture was sonicated for three sessions of 10 s each at 5 W power with 30 s break between sessions. After sonication, the felt was discarded and the remaining mixture was quickly filtered using a disposable filter funnel system with 0.45 μm filter membrane. Anolyte samples were directly filtered on a similar disposable filter funnel.

After filtration, the filter membrane was carefully inserted in the 5-mL Mo Bio PowerWater® Bead Tube with the top (cell) side of the membrane facing inwards. After adding 1 mL of Mo Bio PowerWater® PW 1 solution at 65 ºC, the tube was briefly vortexed and incubated at 65 ºC for 10 min in a heat block. At the end of the incubation period, the tube was attached vertically using Mo Bio Vortex Adapter and vortexed at maximum speed for 5 min. The tube and its content were then centrifuged at 4,000•*g* force for 1 min so all the supernatant could be transferred to an autoclaved 2-mL centrifuge tube and centrifuged at 13,000•*g* force for 1 min. The rest of the protocol was identical to steps 11 through 24 of the Experienced User Protocol published by Mo Bio (Mo Bio, 2015).

3.8.2. 16S rRNA gene sequencing and processing from Case *et al.* (Case et al., 2015):

Preparation for sequencing of the V4 region of the 16S rRNA gene was performed with universal primers according to the protocol recommended by the Earth Microbiome Project (http://www.earthmicrobiome.org/emp-standard-protocols/16s/) (J Gregory Caporaso et al., 2012; J. Gregory Caporaso et al., 2011), with minor modifications described elsewhere (Mason et al., 2015). Raw sequences were generated on an Illumina MiSeq platform at Laragen, Inc. (Los Angeles, CA). In-house data processing was completed in QIIME1.8.0 and included joining paired ends, quality trimming, chimera checking, 97% OTU clustering, singleton removal, PCR contaminant removal, 0.01% relative abundance threshold removal, and rarefaction to 16,051 sequences per sample. Taxonomic assignments were generated according to an appended version of the Silva 115 database (for details, see (Mason et al., 2015)).

3.9. References

Bischel, H. N., Schertenleib, A., Fumasoli, A., Udert, K. M., & Kohn, T. (2015). Inactivation kinetics and mechanisms of viral and bacterial pathogen surrogates during urine nitrification. *Environmental Science: Water Research & Technology, 1*(1), 65-76. doi:10.1039/C4EW00065J

Caporaso, J. G., Lauber, C. L., Walters, W. A., Berg-Lyons, D., Huntley, J., Fierer, N., . . . Bauer, M. (2012). Ultra-high-throughput microbial community analysis on the Illumina HiSeq and MiSeq platforms. *The ISME journal, 6*(8), 1621-1624.

Caporaso, J. G., Lauber, C. L., Walters, W. A., Berg-Lyons, D., Lozupone, C. A., Turnbaugh, P. J., . . . Knight, R. (2011). Global patterns of 16S rRNA diversity at a depth of millions of sequences per sample. *Proceedings of the National Academy of Sciences, 108*(Supplement 1), 4516-4522. doi:10.1073/pnas.1000080107

Case, D. H., Pasulka, A. L., Marlow, J. J., Grupe, B. M., Levin, L. A., & Orphan, V. J. (2015). Methane seep carbonates host distinct, diverse, and dynamic microbial assemblages. *MBio, 6*(6), e01348-01315.

Gajda, I., Greenman, J., Melhuish, C., & Ieropoulos, I. A. (2016). Electricity and disinfectant production from wastewater: Microbial Fuel Cell as a self-powered electrolyser. *Sci Rep, 6*, 25571. doi:10.1038/srep25571

Gajda, I., Stinchcombe, A., Greenman, J., Melhuish, C., & Ieropoulos, I. (2017). Microbial fuel cell – A novel self-powered wastewater electrolyser for electrocoagulation of heavy metals. *International Journal of Hydrogen Energy, 42*(3), 1813-1819. doi:10.1016/j.ijhydene.2016.06.161

Greenman, J., & Ieropoulos, I. A. (2017). Allometric scaling of microbial fuel cells and stacks: The lifeform case for scale-up. *Journal of Power Sources, 356*, 365-370. doi:10.1016/j.jpowsour.2017.04.033

Hoffmann, M. R., Aryanfar, A., Cho, K., Cid, C. A., Kwon, D., & Qu, Y. (2013).

Höglund, C., Stenström, T. A., & Ashbolt, N. (2002). Microbial risk assessment of source-separated urine used in agriculture. *Waste Management & Research, 20*(2), 150-161. doi:10.1177/0734242x0202000207

Ieropoulos, I., Greenman, J., & Melhuish, C. (2012). Urine utilisation by microbial fuel cells; energy fuel for the future. *Physical Chemistry Chemical Physics, 14*(1), 94-98. doi:10.1039/C1CP23213D

Ieropoulos, I., Pasternak, G., & Greenman, J. (2017). Urine disinfection and in situ pathogen killing using a Microbial Fuel Cell cascade system. *PLoS One, 12*(5), e0176475.

Jiang, D., Curtis, M., Troop, E., Scheible, K., McGrath, J., Hu, B., . . . Li, B. (2011). A pilot-scale study on utilizing multi-anode/cathode microbial fuel cells (MAC MFCs) to enhance the power production in wastewater treatment. *International Journal of Hydrogen Energy, 36*(1), 876-884. doi:10.1016/j.ijhydene.2010.08.074

Kozich, J. J., Westcott, S. L., Baxter, N. T., Highlander, S. K., & Schloss, P. D. (2013). Development of a Dual-Index Sequencing Strategy and Curation Pipeline for Analyzing Amplicon Sequence Data on the MiSeq Illumina Sequencing Platform. *Applied and Environmental Microbiology, 79*(17), 5112-5120. doi:10.1128/AEM.01043-13

Kumar, P., & Mungray, A. K. (2017). Microbial fuel cell: optimizing pH of anolyte and catholyte by using taguchi method. *Environmental Progress & Sustainable Energy, 36*(1), 120-128. doi:10.1002/ep.12459

Liu, H., & Logan, B. E. (2004). Electricity Generation Using an Air-Cathode Single Chamber Microbial Fuel Cell in the Presence and Absence of a Proton Exchange Membrane. *Environmental science & technology, 38*(14), 4040-4046. doi:10.1021/es0499344

Logan, B. E., Hamelers, B., Rozendal, R., Schröder, U., Keller, J., Freguia, S., . . . Rabaey, K. (2006). Microbial fuel cells: methodology and technology. *Environmental science & technology, 40*(17), 5181-5192.

Logan, B. E., & Rabaey, K. (2012). Conversion of Wastes into Bioelectricity and Chemicals by Using Microbial Electrochemical Technologies. *Science, 337*(6095), 686-690. doi:10.1126/science.1217412

Lovley, D. R. (2012). Electromicrobiology. *Annu Rev Microbiol, 66*, 391-409. doi:10.1146/annurev-micro-092611-150104

Mason, O. U., Case, D. H., Naehr, T. H., Lee, R. W., Thomas, R. B., Bailey, J. V., & Orphan, V. J. (2015). Comparison of archaeal and bacterial diversity in methane seep carbonate nodules and host sediments, Eel River Basin and Hydrate Ridge, USA. *Microbial Ecology, 70*(3), 766-784.

Metcalf, & Eddy. (2014). *Wastewater Engineering: Treatment and Resource Recovery*: McGraw-Hill international ed.

Mo Bio. (2015). PowerWater® DNA Isolation Kit Sample. Retrieved from https://mobio.com/media/wysiwyg/pdfs/protocols/14900-S.pdf

Oliot, M., Etcheverry, L., Mosdale, R., & Bergel, A. (2017). Microbial fuel cells connected in series in a common electrolyte underperform: Understanding why and in what context such a set-up can be applied. *Electrochimica Acta, 246*, 879-889. doi:10.1016/j.electacta.2017.06.114

Paitier, A., Godain, A., Lyon, D., Haddour, N., Vogel, T. M., & Monier, J. M. (2017). Microbial fuel cell anodic microbial population dynamics during MFC start-up. *Biosens Bioelectron, 92*, 357-363. doi:10.1016/j.bios.2016.10.096

Papaharalabos, G., Greenman, J., Melhuish, C., Santoro, C., Cristiani, P., Li, B., & Ieropoulos, I. (2013). Increased power output from micro porous layer (MPL) cathode microbial fuel cells (MFC). *International Journal of Hydrogen Energy, 38*(26), 11552-11558. doi:10.1016/j.ijhydene.2013.05.138

Rabaey, K., & Verstraete, W. (2005). Microbial fuel cells: novel biotechnology for energy generation. *Trends in Biotechnology, 23*(6), 291-298. doi:10.1016/j.tibtech.2005.04.008

Salar-García, M. J., Ortiz-Martínez, V. M., Gajda, I., Greenman, J., Hernández-Fernández, F. J., & Ieropoulos, I. A. (2017). Electricity production from human urine in ceramic microbial fuel cells with alternative non-fluorinated polymer binders for cathode construction. *Separation and Purification Technology, 187*, 436-442. doi:10.1016/j.seppur.2017.06.025

Schroder, U. (2007). Anodic electron transfer mechanisms in microbial fuel cells and their energy efficiency. *Physical Chemistry Chemical Physics, 9*(21), 2619-2629. doi:10.1039/B703627M

Thorn, R. M. S., Lee, S. W. H., Robinson, G. M., Greenman, J., & Reynolds, D. M. (2012). Electrochemically activated solutions: evidence for antimicrobial efficacy and applications in healthcare environments. *European Journal of Clinical Microbiology & Infectious Diseases, 31*(5), 641-653. doi:10.1007/s10096-011-1369-9

U.S. Environmental Protection Agency. (1986). Method 9132: Total Coliform: Membrane-filter technique.

U.S. Environmental Protection Agency. (2002). Method 1600: Enterococci in Water by Membrane Filtration Using membrane-Enterococcus Indoxyl-$-D-Glucoside Agar (mEI).

U.S. Environmental Protection Agency. (2010). Method 1103.1: Escherichia coli (E. coli) in Water by Membrane Filtration Using membrane-Thermotolerant Escherichia coli Agar (mTEC).

Udert, K. M., Larsen, T. A., Biebow, M., & Gujer, W. (2003). Urea hydrolysis and precipitation dynamics in a urine-collecting system. *Water Research, 37*(11), 2571-2582. doi:10.1016/S0043-1354(03)00065-4

Walther, J. V. (2013). *Earth's Natural Resources*: Jones & Bartlett Learning.

Wigginton, N., Yeston, J., & Malakoff, D. (2012). More Treasure Than Trash. *Science, 337*(6095), 662.

Chapter 4

PHOSPHATE RECOVERY FROM HUMAN WASTE VIA THE FORMATION OF HYDROXYAPATITE DURING ELECTROCHEMICAL WASTEWATER TREATMENT

Clément A. Cid[1]

in collaboration with

Justin T. Jasper[1] and Michael R. Hoffmann[1]

[1]Linde-Robinson Laboratories, California Institute of Technology, Pasadena, CA

Published in

ACS Sustainable Chemistry & Engineering

C. A. C. is the principal and coordinating author of the manuscript. C. A. C. and J. T. J. planned the study, performed the laboratory experiments, and analyzed and interpreted the data. C. A. C. performed the SEM/EDS imaging, XRD measurements, and thermogravimetric analysis. J. T. J. performed the simulations for total phosphate removal.

4.1. Abstract

Electrolysis of toilet wastewater with TiO_2-coated semiconductor anodes and stainless steel cathodes is a potentially viable onsite sanitation solution in parts of the world without infrastructure for centralized wastewater treatment. In addition to treating toilet wastewater, pilot-scale and bench-scale experiments demonstrated that electrolysis can remove phosphate by cathodic precipitation as hydroxyapatite at no additional energy cost. Phosphate removal could be predicted based on initial phosphate and calcium concentrations, and up to 80% total phosphate removal was achieved. While calcium was critical for phosphate removal, magnesium and bicarbonate had only minor impacts on phosphate removal rates at concentrations typical of toilet wastewater. Optimal conditions for phosphate removal were 3 to 4 h treatment at about 5 mA cm^{-2} (~3.4 V), with greater than 20 m^2 m^{-3} electrode surface area to reactor volume ratios. Pilot-scale systems are currently operated under similar conditions, suggesting that phosphate removal can be viewed as an ancillary benefit of electrochemical wastewater treatment, adding utility to the process without requiring additional energy inputs. Further value may be provided by designing reactors to recover precipitated hydroxyapatite for use as a low solubility phosphorus-rich fertilizer.

Keywords

Electrochemical precipitation; phosphorous; phosphate removal; wastewater; onsite sanitation

4.2. Introduction

Discharge of phosphorus-containing wastewater to surface waters can cause algal blooms, leading to growth of toxic cyanobacteria, hypoxia, and disruption of food webs (Conley et al., 2009; Correll, 1998). At the same time, phosphorus is a limited resource with an average price that has nearly tripled between 2005 and 2015 (World Bank, 2015), making the recovery of phosphorus from waste crucial (Karunanithi et al., 2016). Toilet and domestic wastewater are an important source of phosphorus, as up to 22% of the world's consumption of phosphorus could be recovered from human urine and feces (Cordell, Rosemarin, Schröder, & Smit, 2011; Mihelcic, Fry, & Shaw, 2011). Recovery of phosphorus from toilet wastewater or septic systems could therefore reduce phosphorus pollution as well as reduce dependency on imported mineral phosphate in countries where access to affordable fertilizers is limited (Simons, Solomon, Chibssa, Blalock, & Lehmann, 2014).

Enhanced Biological Phosphorus Removal (EBPR) may provide effective phosphorus recovery in centralized wastewater treatment processes (de-Bashan & Bashan, 2004), but in rural communities, small onsite sanitation systems (*e.g.*, septic tanks, latrines, or cesspools) make this technology challenging without engineered processes to maintain the correct microbial population (Oehmen et al., 2007). Phosphorus recovery in rural communities can be accomplished via forced precipitation as struvite ($NH_4MgPO_4 \cdot 6H_2O$) or hydroxyapatite ($Ca_5(PO_4)_3OH$), but these strategies typically require separation of urine and feces, addition of chemicals, or use of sacrificial electrodes that further complicates and increases the cost of

existing wastewater treatment strategies (Fumasoli, Etter, Sterkele, Morgenroth, & Udert, 2016; Hug & Udert, 2013; Morse, Brett, Guy, & Lester, 1998).

Electrochemical systems have previously been suggested for phosphorus removal from wastewater. Electrochemical coagulation of phosphate from synthetic wastewater has been achieved using sacrificial aluminum or iron anodes (Lacasa, Cañizares, Sáez, Fernández, & Rodrigo, 2011; Tran, Drogui, Blais, & Mercier, 2012), as well as magnesium anodes, which allowed for struvite recovery from ammonium-containing solutions (Kruk, Elektorowicz, & Oleszkiewicz, 2014). However, this type of electrode is depleted by oxidation and needs to be replaced on a regular basis. Alternatively, an alkaline catholyte chamber separated from the anode by a cation exchange membrane has been incorporated into an electrochemical system to homogeneously precipitate phosphate as hydroxyapatite from synthetic wastewater (Gorni-Pinkesfeld, Shemer, Hasson, & Semiat, 2013). Electrochemical deposition of struvite directly onto a nickel cathode has been demonstrated in synthetic solutions containing magnesium, ammonium, and phosphate, due to the increased pH near the cathode surface (Wang, Hao, Guo, & van Loosdrecht, 2010). However, these systems provided phosphorus removal alone and none of these studies investigated authentic toilet wastewater or utilized a system that was practical for toilet wastewater treatment.

Onsite electrochemical wastewater treatment is an appealing technology for small- and medium-sized treatment and recycling systems, providing treatment without requiring construction of traditional wastewater infrastructure (Comninellis & Chen, 2010). One promising electrochemical treatment system under development

by Hoffmann *et al.* (Hoffmann et al., 2013) couples stainless steel cathodes to stable layered-layered semiconductor anodes ($[Bi_2O_3]_z[TiO_2]_{1-z}/Ir_xTa_yO_2/Ti$) (Cho & Hoffmann, 2014, 2015; Yang, Shin, Jasper, & Hoffmann, 2016) treating the toilet wastewater in a sequential batch reactor at constant potential (3.5 ± 0.25 V) with a typical residence time of 3 to 4 h. Bench-scale experiments and long-term field-testing have shown effective wastewater disinfection due to generation of hypochlorous acid from the oxidation of chloride, as well as reduction of chemical oxygen demand, transformation of trace organic chemicals, and removal of ammonium via breakpoint chlorination (Cho & Hoffmann, 2014; Cho et al., 2014; Huang et al., 2016; J. T. Jasper, Shafaat, & Hoffmann; Yang et al., 2016).

The purpose of this study was to evaluate the potential for phosphate removal from human wastewater during electrochemical treatment using the same combined anode-cathode system previously shown to provide efficient wastewater treatment (Cho & Hoffmann, 2014; Cho et al., 2014; Huang et al., 2016). Phosphate-containing precipitates were identified and phosphate removal efficiencies were measured in authentic and synthetic toilet wastewater. Experiments in synthetic wastewater allowed quantification of the effects of ion composition, buffering capacity, current density, and electrode surface area to volume ratio on phosphate removal kinetics and equilibria.

4.3. Materials and methods

4.3.1. Materials

All reagents were of analytical grade or higher purity. Solutions were prepared using 18 MΩ Milli-Q water from a Millipore system.

Toilet (human) wastewater containing an uncontrolled mixture of urine, feces, and flushing water was taken from a previously described public recycling wastewater treatment system located on the California Institute of Technology campus (Pasadena, CA) via a macerator pump (J. T. Jasper et al., 2016). The residence time in the wastewater tank was approximately 160 d. Synthetic wastewater was formulated to replicate the ionic composition and pH (8.3) of the toilet wastewater (Table 4.1) by dissolving the following salts in water: NaCl (17.1 mM), $NaHCO_3$ (4.7mM), $NaH_2PO_4{\cdot}H_2O$ (0.6 mM), Na_2SO_4 (2.1 mM), $MgCl_2{\cdot}6H_2O$ (0.8 mM), $CaCl_2{\cdot}2H_2O$ (1 mM), KCl (3.6 mM), $(NH_4)_2SO_4$ (0.9 mM), NH_4HCO_3 (12.1 mM), and KOH (2.5 mM). Ion concentrations were adjusted to test the effect of individual ions on phosphate removal rates.

Electrode arrays consisted of mixed metal oxide anodes ($(Bi_2O_3)_z[TiO_2]_{1-z}/Ir_xTa_yO_2/Ti$) and stainless steel cathodes (Nanopac, Korea) and were similar to those developed by Weres (Weres, 2009; Weres & O'Donnell, 2003) and used in previous electrochemical wastewater treatment studies (Cho & Hoffmann, 2014; Cho et al., 2014; Huang et al., 2016; J. T. Jasper et al., 2016; Justin T. Jasper, Yang, & Hoffmann, 2017).

4.3.2. Pilot-scale experiments

Pilot-scale experiments were performed in batch mode in a 40-L acrylic reactor (22 L working volume) mixed with a circulation pump (10 L min^{-1}), as described previously (Hoffmann et al., 2013; Huang et al., 2016). Electrode arrays (7 anodes and 8 cathodes) were sandwiched with a 3 mm separation. The active geometric anodic surface area was 1.8 m^2, giving a surface area to effective volume ratio of 80 m^2 m^{-3}. Pilot-scale experiments were conducted using a potentiostatic power supply coupled with a data logger (Program Scientific Instruments, USA) with a potential set between 3.3 V and 3.5 V. Ion recoveries as precipitate were calculated in select experiments by calculating ion masses in the formed precipitate (Figure S4.1) using the average precipitate composition and comparing those masses to ion removal from the aqueous phase.

4.3.3. Bench-scale experiments

Bench-scale experiments were conducted to study the role of ionic composition, buffering capacity, and current density on phosphate removal kinetics and equilibria using anode and cathode pieces cut from a pilot-scale array. The electrode spacing (3 mm) and electrode surface area to volume ratio (~35 m^2 m^{-3}) were comparable to the pilot-scale system. The electrode array was either operated potentiostatically (typically 3.5 V between anode and cathode) or galvanostatically (~10 mA cm^{-2}; 3.75 mA mL^{-1}) using a battery cycler (Neware, China). Experiments were conducted in open beakers with magnetic stirring (600 rpm).

The role of wastewater composition was studied by varying calcium, magnesium, phosphate, and bicarbonate concentrations over the range of values expected in toilet

wastewater (i.e., typical values present in human waste diluted approximately 10 times by flushing; Table S4.1 and Figure S4.2). The role of buffering capacity was studied by adding borate (0 - 100 mM) to synthetic wastewater at pH 8.3. No ion interactions with borate were predicted by Visual MINTEQ 3.1 software (Gustafsson, 2014). The effects of wastewater volume to electrode surface area ratios (~10 – 35 $m^2\ m^{-3}$) were studied by adjusting the solution volume while using the same size electrodes. The effects of current density were investigated by increasing the current density galvanostatically (~3 - 55 mA cm^{-2}; 1 - 20 mA mL^{-1}). Energy efficiency of phosphate removal was calculated based on the final phosphate concentration and the total amount of electrical energy consumed.

4.3.4. Precipitate solubility measurements

Precipitate scraped from the stainless-steel cathodes or collected from the pilot-scale reactor bottom was rinsed with deionized water and dried at 70 °C overnight before being ground for analysis. The solubility product constant (K_{sp}) of the collected precipitate was measured in dilute phosphoric acid solutions (~0.1 mM) adjusted to pH 6 with sodium hydroxide, as described previously (McDowell, Gregory, & Brown, 1977). Precipitate (0.1 g) was added to vials (25 mL) capped with minimal headspace. Vials were mixed on a rotisserie for 8 d at 22 °C and solid precipitate remained at the end of the experiment. The K_{sp} for hydroxyapatite was calculated according to:

$$K_{sp} = (Ca^{2+})^5(PO_4^{3-})^3(OH^-) \quad (1)$$

Solubility indices (SI), as defined by equation 2, and ion activity products (IAP) were calculated using Visual MINTEQ 3.1 software (Gustafsson, 2014), accounting for ion pairs (*e.g.*, $CaPO_4^-$). Equilibrium calculations and supersaturated conditions for

various minerals were determined using the same software, taking into consideration ion concentrations listed in Table 4.1.

$$SI = \log IAP - \log K_{sp} \quad (2)$$

4.3.5. Analytical methods

X-ray powder diffraction spectra (Philips PANalytical X'Pert Pro X-ray) were collected for crystal phase analysis. Thermogravimetric analysis was conducted for moisture content determination and qualitative mineral identification (Perkin Elmer STA 6000). Scanning electron microscope imaging and energy dispersive spectrometry (SEM/EDS; Zeiss 1550VP Field Emission with Oxford X-Max SDD X-ray) were used for surface topography and elemental analysis. A “site” represented an indistinguishable agglomerate of amorphous or crystallized material.

The chloride, sulfate, nitrate, phosphate, ammonium, potassium, calcium, and magnesium contents of collected precipitates were determined by dissolution in 1 M sulfuric acid or 1 M nitric acid and analysis by ion chromatography (Dionex ICS 2000; AS19G anions, CS12A cations) (American Public Health, 1995). Precipitate carbonate content was determined by manometric carbon dioxide measurement following dissolution in acid (6 M HCl) (Loeppert & Suarez, 1996).

Samples for aqueous ion concentrations were diluted (10 - 25x) and measured by ion chromatography as described above.

4.4. Results and Discussion

4.4.1. Phosphate removal during pilot-scale treatment

Electrolysis of collected toilet wastewater in the pilot-scale onsite treatment system resulted in removal of total phosphate, magnesium, and calcium over the 5 h treatment cycle (Figure 4.1; 50% total PO_4^{3-} ($PO_4^{3-}{}_T$), 89% Mg^{2+}, 42% Ca^{2+} removed). Total phosphate removal was similar to predictions based on initial calcium and phosphate concentrations (see below). Breakpoint chlorination was achieved in approximately 4 h with complete ammonia removal (White, 2010) and subsequent production of free chlorine (Figure S4.3). Concurrent with electrolysis, a greyish precipitate flaked off the stainless-steel cathodes into solution (Figure S4.1). Precipitate recovered from the cathodes and the bottom of the reactor after treatment accounted for more than 90% of the calcium and total phosphate removed based on the measured precipitate composition. Pilot-scale phosphorus removal was therefore primarily attributed to electrochemically-induced precipitation.

4.4.2. Characterization of precipitated hydroxyapatite

Precipitate collected from the pilot-scale electrochemical reactor was primarily composed of hydroxyapatite ($Ca_5(PO4)_3OH$), based on X-ray diffraction spectroscopy (Figure 4.2). The crystallinity of the precipitate was found to be significantly higher than hydroxyapatite formed by homogeneous precipitation in synthetic dairy manure wastewater (Cao & Harris, 2007), as evidenced by resolution of peaks at 2Θ values of 28°, 29°, 31°, and 32°.

In addition to phosphate (30 ± 2% by mass) and calcium (18 ± 1% by mass), the precipitate was composed of chemically-bound water (8 - 20% by thermogravimetry;

Figure S4.4), magnesium (6 ± 1%), carbonate (6 ± 1%), silicate (9 ± 3%), and undissolvable material (3 - 6%; Table 4.2). Magnesium and carbonate are commonly observed to substitute for calcium and hydroxide, respectively, in hydroxyapatite (Amjad, Koutsoukos, & Nancollas, 1984; Cao & Harris, 2007; Golubev, Pokrovsky, & Savenko, 1999; Ito, Maekawa, Tsutsumi, Ikazaki, & Tateishi, 1997) and may affect precipitation kinetics. Silicate is known to substitute for phosphate in hydroxyapatite ($Ca_{10}(PO_4)_{6-x}(SiO_4)_x(OH)_{2-x}$) (Gibson, Best, & Bonfield, 1999) and was only observed in reactors sealed with silicon grease. Chloride, sulfate, nitrate, ammonium, potassium, and sodium were not present in collected precipitates in significant amounts (less than 1% by mass), as expected for hydroxyapatite.

SEM/EDS mapping of collected precipitate revealed a homogeneous distribution of elements with phosphorous, calcium, and magnesium in all deposits (Figure S4.5). Scanning of several particles showed ratios of Ca/P = 1.5 ± 0.3, Mg/P = 1.0 ± 0.2, and O/P = 5.0 ± 1.6. The low Ca/P ratios observed as compared to pure hydroxyapatite (Ca/P = 1.67) could be explained by substitution of magnesium for calcium and silicate for phosphate ((Ca+Mg)/(Si+P) = 1.7 ± 0.2).

The measured K_{sp} of the electrochemically deposited hydroxyapatite ($5.0 \pm 0.5 \times 10^{-47}$) was significantly larger than literature values for pure hydroxyapatite ($3.04 \pm 0.25 \times 10^{-59}$) (McDowell et al., 1977), likely due to incorporation of magnesium, carbonate, and silicate (Sprio et al., 2008). For example, incorporation of a similar mass percentage of carbonate (i.e., ~4% by mass) into hydroxyapatite can increase hydroxyapatite's K_{sp} by more than 8 orders of magnitude (Ito et al., 1997). Electrochemically deposited hydroxyapatite solubility may also have

been lower than that of pure hydroxyapatite, since it was not completely crystalline (Figure 4.2).

Although no precipitation was observed before electrolysis (Dai, Lu, Peng, Yang, & Zhsssu, 2017), the collected toilet wastewater (Table 4.1) was supersaturated with respect to aragonite and calcite (SI ≈ 0.9 and 1.1), disordered and ordered dolomite (SI ≈ 1.7 and 2.2) (Spanos & Koutsoukos, 1998), α and β tricalcium phosphate (SI ≈ 2.2 and 2.9), tetracalcium phosphate (SI ≈ 2.3), and pure hydroxyapatite (SI ≈ 12), which was the thermodynamically favored mineral phase. However, toilet wastewater was slightly below saturation with respect to the measured solubility of the electrochemically-formed precipitate (SI = -0.2).

4.4.3. Phosphate removal equilibria and kinetics

4.4.3.1. Phosphate removal in synthetic versus authentic wastewater

Synthetic wastewater was used to determine the effect of wastewater composition ($[Ca^{2+}]$, $[Mg^{2+}]$, $[HCO_3^-]$, and $[PO_4^{3-}]_T$), buffering capacity, and current density on phosphate removal (Figure S4.6). Despite the lack of organic matter in synthetic wastewaters, which may reduce hydroxyapatite formation rates (Cao, Harris, Josan, & Nair, 2007), calcium, magnesium, and total phosphate removal was found to be comparable to that observed with authentic toilet wastewater (Figure 4.3). In both cases, the collected precipitate exhibited similar compositions to precipitate formed in the pilot-scale reactor (data not shown). The XRD spectrum of a stainless steel cathode after consecutive synthetic wastewater electrolysis cycles also exhibited similar peaks as the precipitate formed in the pilot-scale reactor (Figure S4.7). The majority of the phosphate removed was recovered as a precipitate

on the cathode (70-100%), indicating that phosphate removal was primarily due to hydroxyapatite formation. Synthetic wastewater was therefore taken to be a good proxy for genuine toilet wastewater for these experiments.

4.4.3.2. Extent of phosphate removal

In synthetic wastewater, percent phosphate removal at equilibrium (~3 - 4 h) could typically be predicted (Figure 4.4) based on initial calcium and phosphate concentrations by solving the simultaneous equations for the hydroxyapatite solubility product (equation 1) and the mass balance for calcium and phosphate removal (equation 3) at a cathodic pH of about 9.4 (Table S4.1).

$$\frac{5}{3}\left([PO_4^{3-}]_{T,0} - [PO_4^{3-}]_{T,fin}\right) = \left([Ca^{2+}]_0 - [Ca^{2+}]_{fin}\right) \quad (3)$$

However, for low ratios of calcium to total phosphate, phosphate removal was greater than predicted. This may have been due to precipitation of calcium-phosphate minerals poor in calcium, such as amorphous calcium phosphate ($Ca_3(PO_4)_2 \cdot nH_2O$; $K_{sp} = 2.49 \times 10^{-7}$), dicalcium phosphate dihydrate ($CaHPO_4 \cdot 2H_2O$; $K_{sp} = 1.26 \times 10^{-7}$), and others (Cao et al., 2007). Other deviations between predicted and observed percent phosphate removal could be explained by the presence of magnesium or variations in the applied current density (see below).

Based on equations 1 and 3, high phosphate removal is predicted at high initial calcium concentrations and high initial ratios of calcium to phosphate concentrations (Figure 4.5). Reliance on high calcium concentrations for efficient phosphate removal is a limitation of this technology. However, urine in toilet wastewater typically contains sufficient calcium to achieve greater than 50% phosphate removal (i.e., ~1 mM following ~10x dilution by flushing) (Putnam, 1971).

4.4.3.3. Electrochemical phosphate precipitation rates

In synthetic wastewater initial electrochemical phosphate precipitation rates (k_{ini}) were determined based on calcium and phosphate concentrations during the first 3 h of treatment (Figure S4.6). Initial phosphate precipitation rates increased from about 0.05 to 0.25 mM h^{-1} with the product $[Ca^{2+}][PO_4^{3-}]$ (Figure 4.6), as expected based on a homogeneous hydroxyapatite precipitation model previously developed by Inskeep and Silvertooth (Inskeep & Silvertooth, 1988):

$$\frac{d[\mathrm{HAP}]}{dt} = k_f[Ca^{2+}][PO_4^{3-}] \approx k_{ini} \quad (4)$$

Above $[Ca^{2+}][PO_4^{3-}]$ values of 0.4 mM^2, however, initial phosphate removal rates were constant at about 0.25 mM h^{-1}, suggesting that initial precipitation was mass limited only at low calcium and phosphate concentrations. In all cases, though, removal rates were sufficient to reach equilibrium within 3 to 4 h, which is a typical treatment cycle for disinfection and ammonium removal during onsite electrochemical wastewater treatment in the system developed by Hoffmann *et al* (Cho & Hoffmann, 2015; Justin T. Jasper et al., 2017).

4.4.3.4. Effect of magnesium on phosphate removal

Adsorption of magnesium onto actively growing crystals during homogeneous hydroxyapatite precipitation, and subsequent substitution of magnesium for calcium, has been shown to reduce hydroxyapatite growth rates and increase hydroxyapatite solubility (Amjad et al., 1984; Fuierer, LoRe, Puckett, & Nancollas, 1994; Okazaki, Takahashi, & Kimura, 1986). However, effects were generally significant only at concentrations above 1 mM (TenHuisen & Brown, 1997), which is the maximum

magnesium concentration expected in toilet wastewater assuming about 10 times dilution by flushing water (Putnam, 1971).

As expected, electrochemical treatment of synthetic wastewater with 1 mM calcium, 0.6 mM phosphate, and varying magnesium concentrations up to 1 mM showed no significant change in initial phosphate removal rates (Figure 4.7a) or percent phosphate removal (Figure 4.8a). In fact, at calcium concentrations below 1 mM with 0.5 mM total phosphate, phosphate removal percentages were higher than predicted based on calcium concentrations alone in the presence of 1 mM magnesium (Figure 4.8b, compare experiments B, C, and D with 1 mM Mg^{2+} to F, K, and G with 0 mM Mg^{2+}). This may have been due to magnesium compensating for the deficiency in calcium. Magnesium is therefore not expected to hamper electrochemical phosphate removal at concentrations typical of toilet wastewater.

4.4.3.5. Effect of bicarbonate on phosphate removal

Toilet wastewater stored in onsite treatment systems will produce bicarbonate due to hydrolysis of urea (Udert, Larsen, & Gujer, 2006). Previous studies have reported reductions in homogeneous hydroxyapatite precipitation by more than 40% with addition of carbonate, due to reduced hydroxyapatite crystallinity (Cao & Harris, 2007; Cao et al., 2007; Kapolos & Koutsoukos, 1999). Bicarbonate may also reduce hydroxyapatite precipitation by increasing the buffering capacity (β) of wastewater, inhibiting the increased cathodic pH that initiates precipitation (Shirkhanzadeh, 1998).

As expected, phosphate removal was significantly reduced at high bicarbonate concentrations (i.e., 57 ± 3% removal at 60 mM HCO_3^- vs. ~70 - 75% removal at 16 to

30 mM HCO_3^-; Figure 4.8c). Phosphate removal rates were also slightly reduced at 60 mM bicarbonate (Figure 4.7b), although the difference was not significant (i.e., 0.13 ± 0.04 mM h^{-1} at 60 mM HCO_3^- vs. 0.17 - 0.23 mM h^{-1} at 16 - 30 mM HCO_3^-).

The effect of bicarbonate on phosphate removal was attributed to the increased solubility of carbonate-substituted hydroxyapatite, as bicarbonate is not predicted to increase buffering capacities sufficiently to affect phosphate removal at concentrations typical of toilet wastewater (i.e., <100 mM). This assertion was supported by experiments in buffered synthetic wastewater with buffering capacities ranging from 3.6 to 25 meq L^{-1} pH^{-1} (0 – 100 mM borate) at pH 8.3. Buffering capacity (β) was calculated by equation 5:

$$\beta = \sum_i \frac{2.3\ C_i\ K_{a,i}[H^+]}{(K_{a,i} + [H^+])^2} \quad (5)$$

where C_i and $K_{a,i}$ are the concentration and acid dissociation constant of species i, respectively. Phosphate removal rates were only affected at buffering capacities of 14.2 meq L^{-1} pH^{-1} and above (50 – 100 mM borate; Figure S4.8). This was considerably higher than the buffering capacity of toilet wastewater at elevated bicarbonate concentrations (i.e., 5.6 meq L^{-1} pH^{-1} at 60 mM HCO_3^-; 7.4 meq L^{-1} pH^{-1} at 100 mM HCO_3^-).

4.4.3.6. Effect of current density and treatment volume on phosphate removal

Increasing current density increases the rate of proton consumption at the cathode, and, depending on the buffering capacity of the wastewater, can therefore

increase the pH near the cathode (Dahms & Croll, 1965), favoring hydroxyapatite precipitation.

As expected, initial phosphate removal rates (Figure 4.7 c) and total phosphate removal (Figure 8 d) increased from about 50% with an initial rate of about 0.1 mM h^1 at 2.6 mA cm^{-2} to greater than 75% with an initial rate of about 0.25 mM h^{-1} at 15 mA cm^{-2}. Increases in surface area to synthetic wastewater volume ratio augmented the rate of phosphate removal (Figure 4.7 d) but did not change significantly affect the amount of energy required per volume of wastewater (Figure S4.9 inset). For example, achieving 60% total phosphate removal required 30 ± 5 kWh m^{-3} at all surface area to volume ratios tested, but occurred after about 7 h at 10 m^2 m^{-3} and after only 2 h at 34 m^2 m^{-3}.

4.4.4. Design and operation considerations

During pilot-scale experiments, electrochemical phosphate precipitation resulted in scaling on the cathode (Figure S4.1), which subsequently fell into solution as approximately 1 cm^2 flakes. Although cathodic scaling did not adversely affect wastewater treatment over short-term tests (i.e., less than 200 treatment cycles), complete cathode coverage by the precipitate during long-term operation may be problematic. Sustainable phosphate removal therefore requires electrode maintenance to remove and collect deposited precipitate. Although electrodes can be cleaned manually, this process could also be accomplished automatically by periodically polarizing the hydroxyapatite-coated stainless steel plates anodically. In addition, post-treatment hydroxyapatite collection could be automated, for example by incorporating a funnel into the bottom of electrochemical reactors, providing a

phosphorous-rich precipitate that could be used as a fertilizer at minimum cost.(Moriyama, Kojima, Minawa, Matsumoto, & Nakamachi, 2001)

In addition to human waste in onsite toilet treatment systems, electrochemical treatment would likely be effective for other phosphate-rich waste streams including agricultural wastes, such as animal husbandry wastewater. Dairy manure waste has a similar composition to toilet wastewater(Cao & Harris, 2007) and in addition to phosphate removal, electrochemical treatment provides disinfection, nitrogen removal, and chemical oxygen demand reduction with no additional electrochemical energy costs.

4.5. Acknowledgments

This research was supported by the Bill and Melinda Gates Foundation (Grants OPP 1069500 and OPP 1111246), and a Resnick Sustainability Postdoctoral Fellowship to JTJ.

Table 4.1: Composition of toilet wastewater in onsite wastewater treatment system and buffering capacity of relevant species

Component	Value [a]	Buffer capacity (β_i) [b]
Ca^{2+}	1.0 mM	0
Cl^-	24 mM	0
$HCO_3^- + CO_3^{2-}$	17 mM	0.79 meq L^{-1} pH^{-1}
K^+	6.1 mM	0
Mg^{2+}	0.8 mM	0
Na^+	27 mM	0
NH_4^+	13 mM	2.71 meq L^{-1} pH^{-1}
$PO_4^{3-}{}_T$ [c]	0.6 mM	0.09 meq L^{-1} pH^{-1}
SO_4^{2-}	3.0 mM	0
COD [d]	320 - 380 mg O_2/L	-
pH	8.3	-

[a] Collected after 180 d of operation. [b] At pH 8.3. [c] Total phosphate. [d] Chemical oxygen demand.

Table 4.2: Collected precipitate composition

Component	% Mass	Detection Method
Ca^{2+}	18-19%	IC; SEM-EDS
Mg^{2+}	5-7%	IC; SEM-EDS
$PO_4^{3-}{}_T$	27-32%	IC; SEM-EDS
CO_3^{2-}	6±1%	Acid digestion
SiO_4^{2-} [a]	9±3%	SEM-EDS, assuming Si is SiO_4
H_2O	8-20%	Vacuum oven; TGA
Organics; un-digested material	3-6%	Filter acid-dissolved precipitate solution
Total	72-103%	

[a] SiO_4^{2-} was only detected in samples collected from a silicon-grease sealed electrochemical reactor.

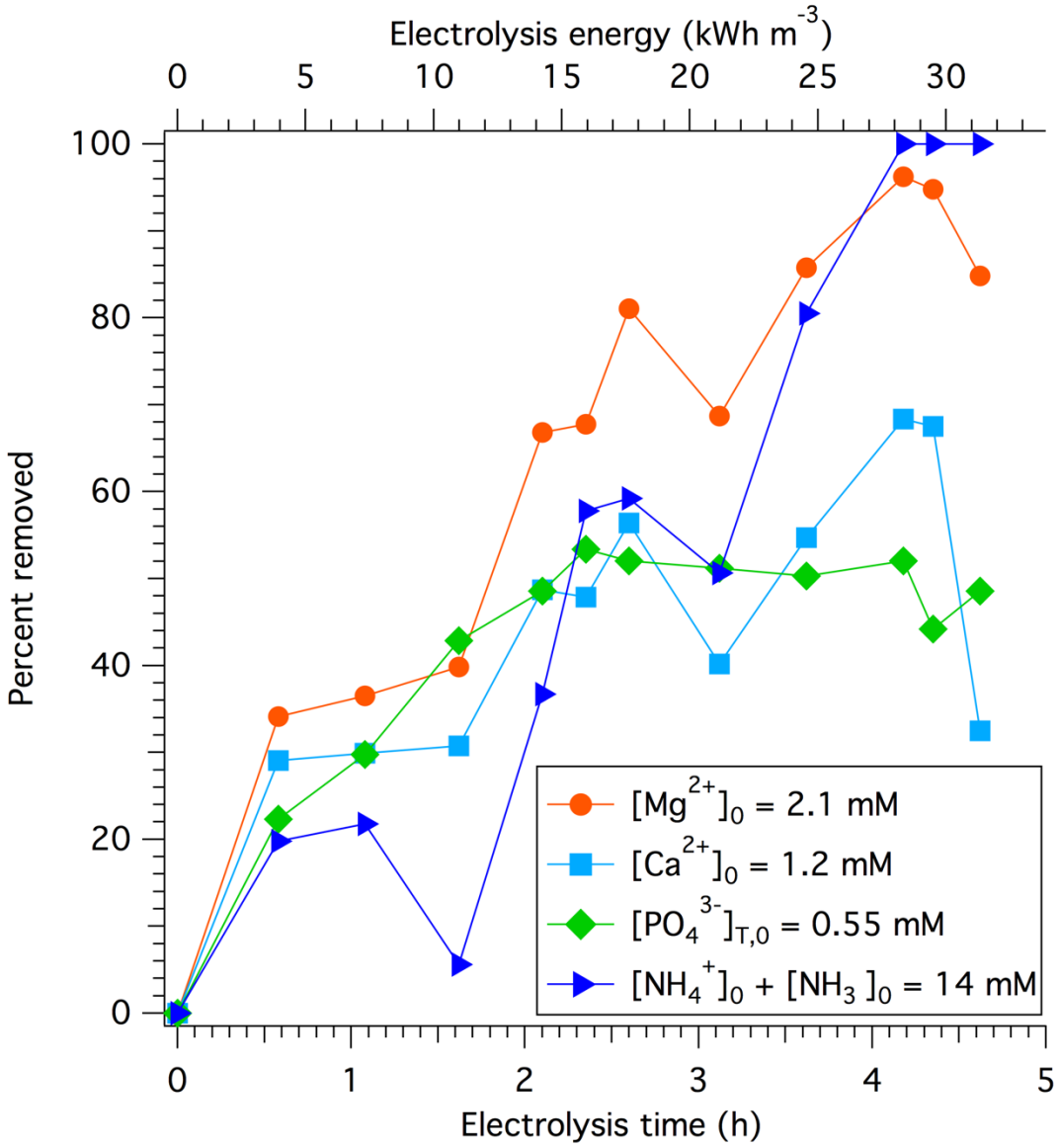

Figure 4.1: Mg^{2+}, Ca^{2+}, $PO_4^{3-}{}_T$, and ammonia (NH_4^+ + NH_3) percent removal during electrochemical treatment (3.3 V; 50 A) of toilet wastewater ([Cl^-] = 80 mM) in pilot-scale reactor. Initial ion concentrations are indicated in the legend.

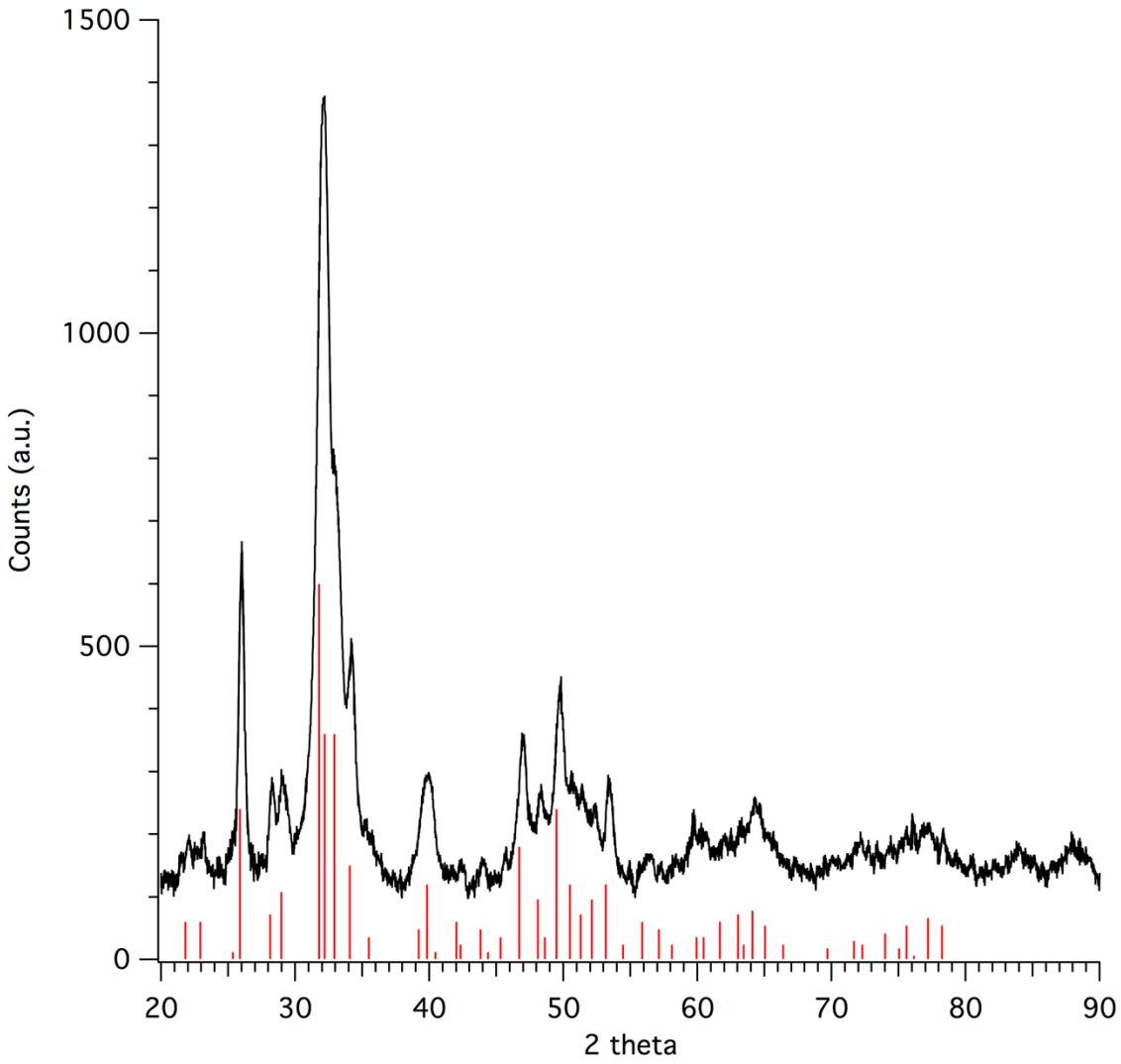

Figure 4.2: X-ray diffraction spectrum of collected precipitate. Overlay of pure hydroxyapatite with highest peak normalized to 600 a.u. (ICSD# 24240 and PDF# 01-073-1731) is in red sticks.

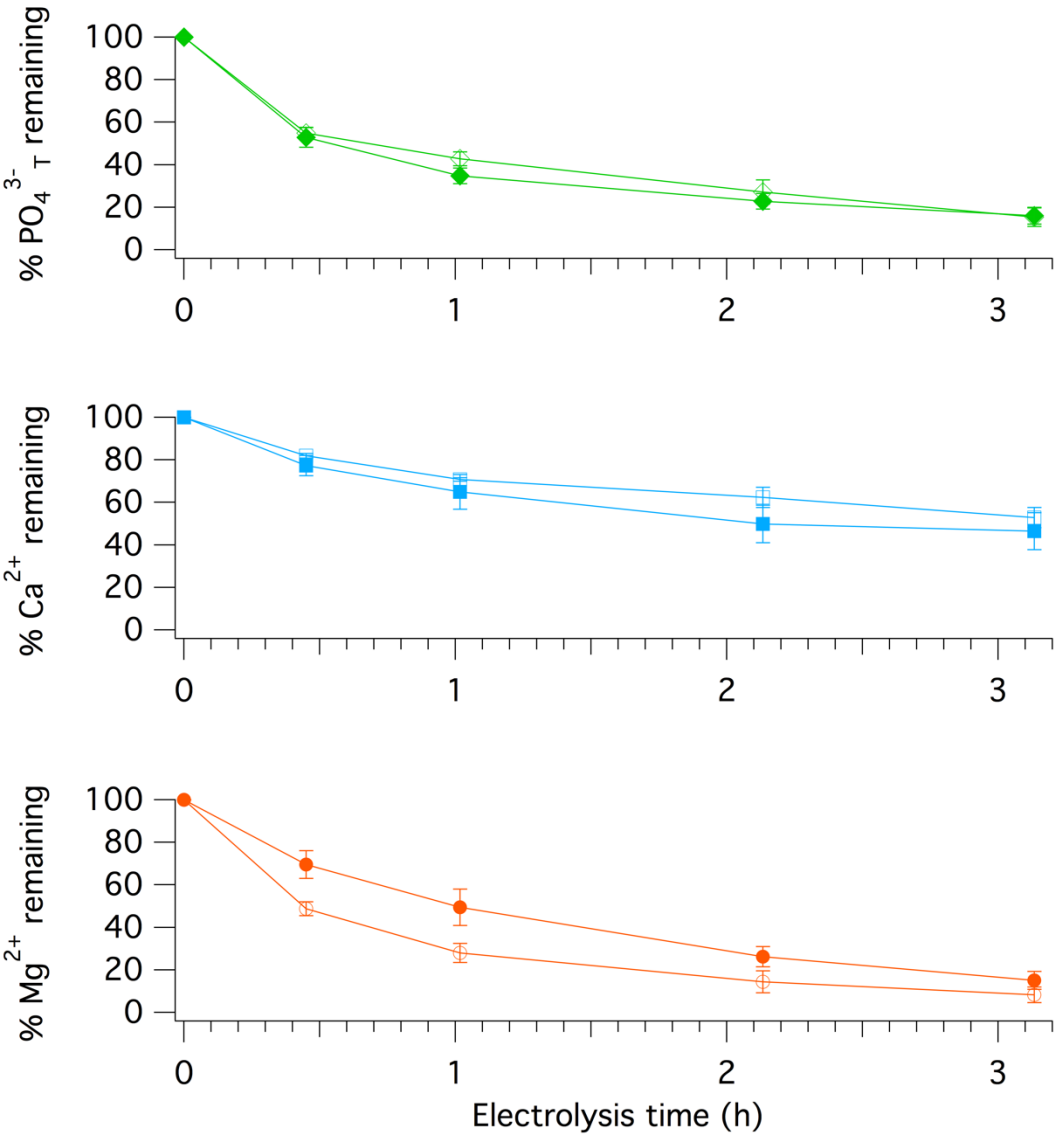

Figure 4.3: Percent $PO_4^{3-}{}_T$, Ca^{2+}, and Mg^{2+} remaining during potentiostatic electrochemical treatment (3.6 V; ~18 mA cm^{-2}) of genuine toilet wastewater (filled markers) and synthetic wastewater (empty markers) with similar ionic compositions. $[PO_4^{3-}]_{T,0} \approx 0.5$ mM; $[Ca^{2+}]_0 \approx 1.3$ mM; $[Mg^{2+}]_0 \approx 1.3$ mM. Error bars represent ± one standard deviation of 3 replicates.

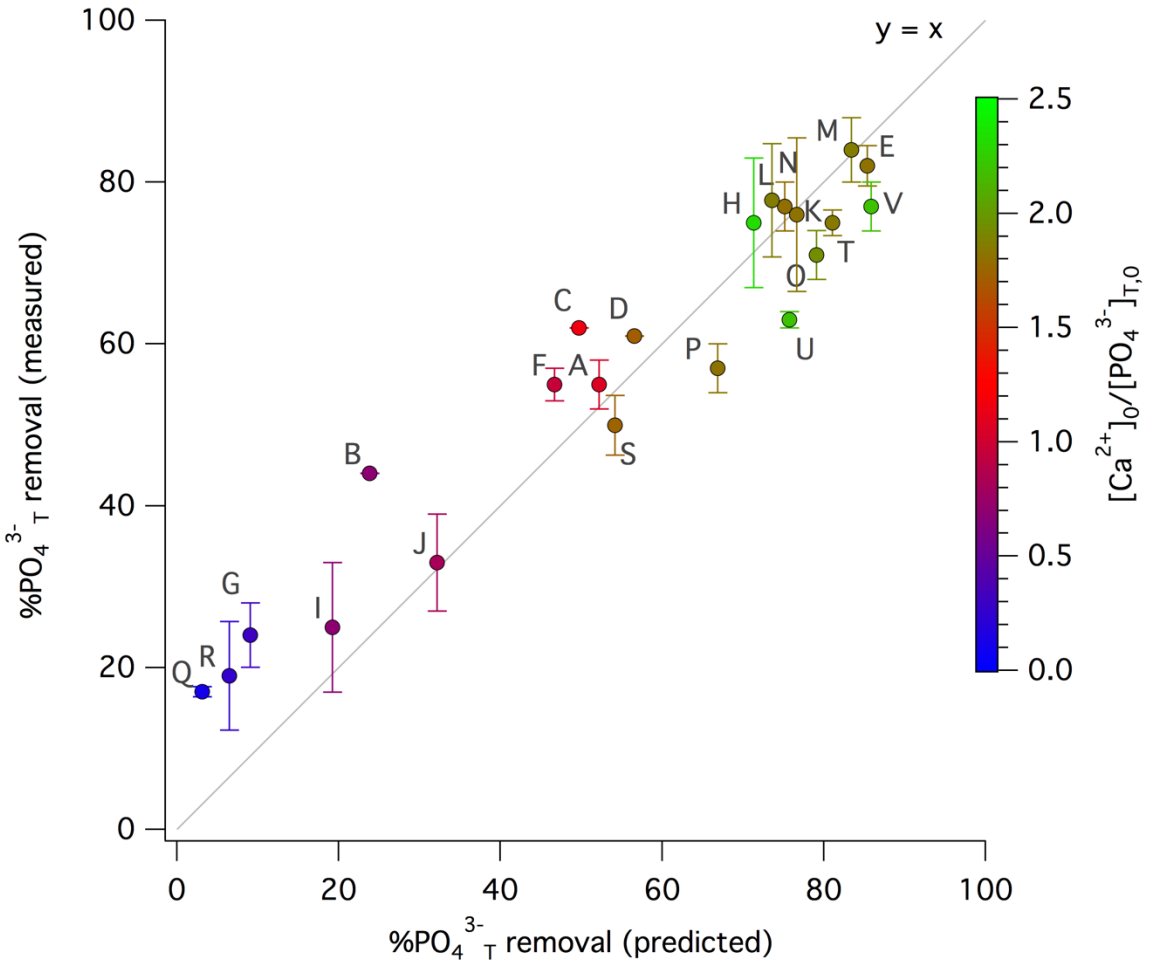

Figure 4.4: Measured vs. predicted percent total phosphate removal following galvanostatic electrolysis (4 h; 10 mA cm^{-2}). Error bars represent ± standard deviation of 3 replicates. Experiments are referenced by letter and are described in Table S4.1.

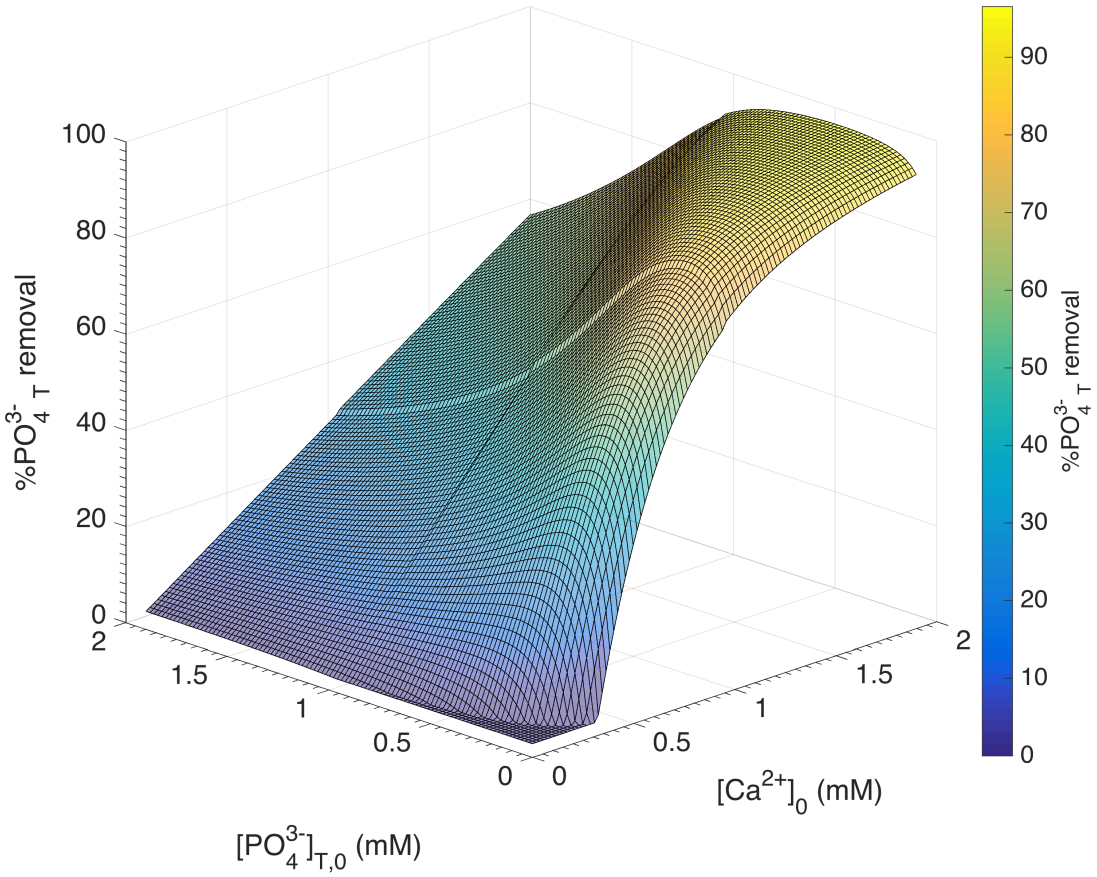

Figure 4.5: Predicted percent total phosphate removal. Predictions are based on solving the simultaneous equations 1 and 3 at varying initial total phosphate and calcium concentrations and a cathodic pH of 9.4.

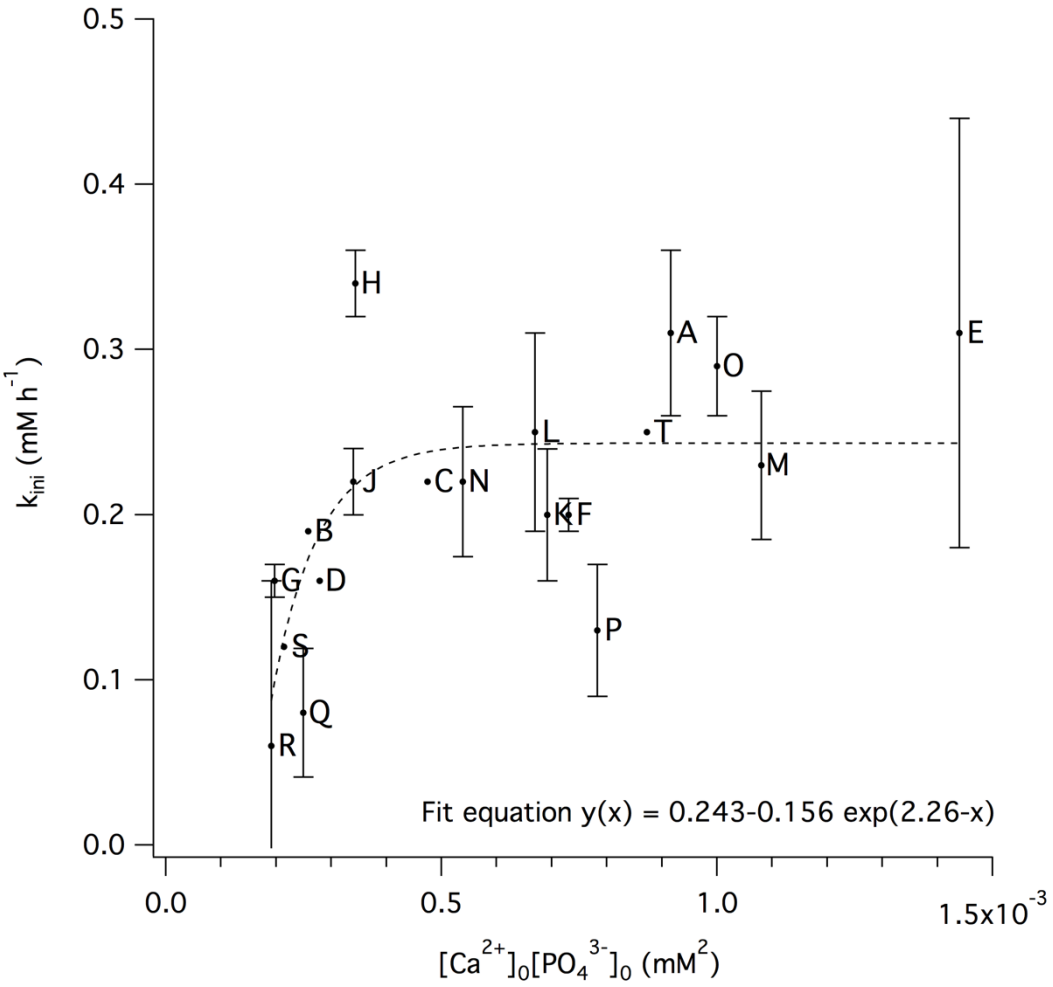

Figure 4.6: Initial rate constants (k_{ini}) for the formation of hydroxyapatite during galvanostatic electrolysis (10 mA cm^{-2}) as a function of $[Ca^{2+}]_0[PO_4^{3-}]_0$. The fit equation was determined empirically using Igor Pro 6.37 (Wavemetrics). Error bars represent ± standard deviation of 3 replicates. Experiments are referenced by letter and are described in Table S4.1.

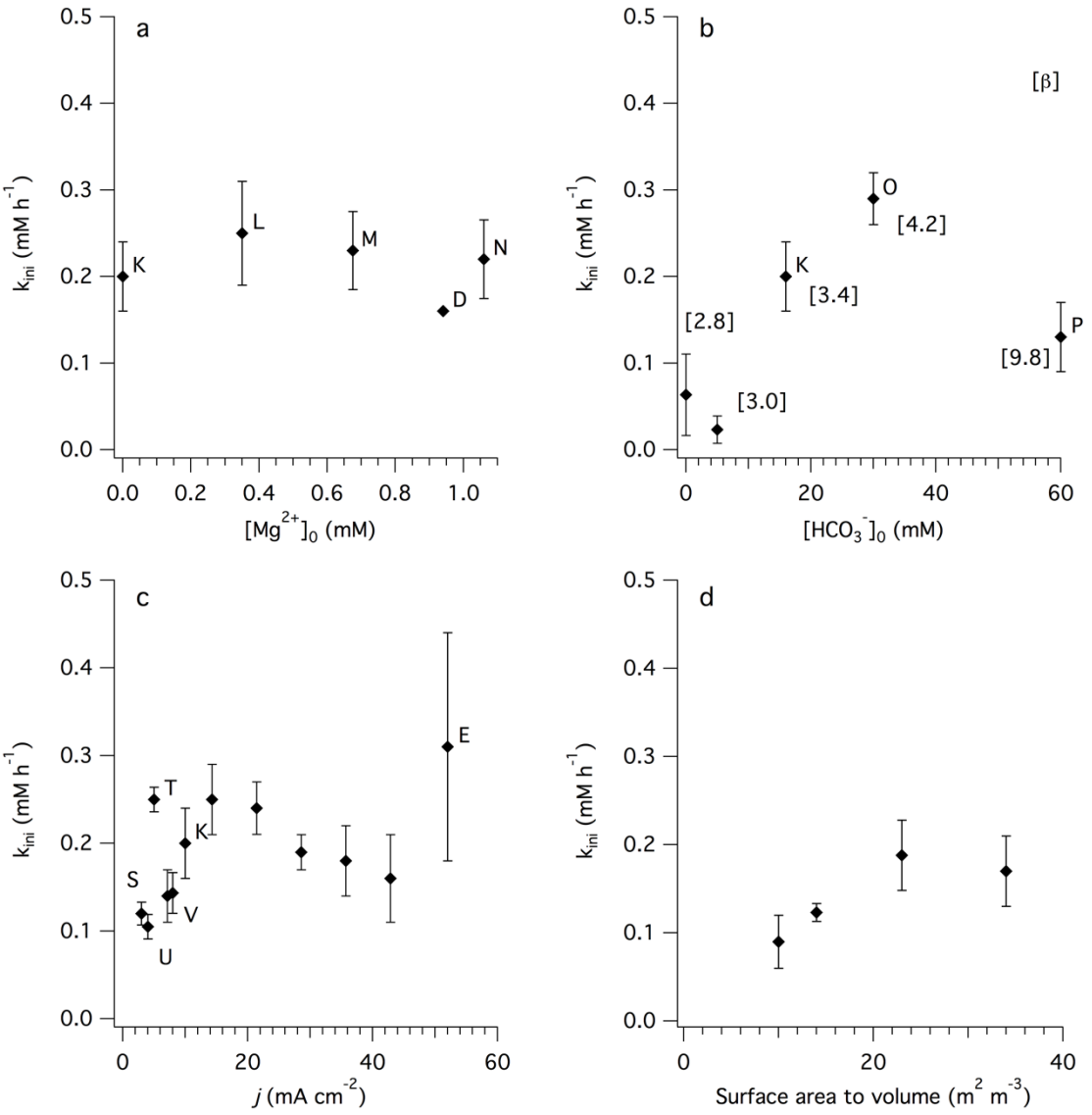

Figure 4.7: Intial phosphate removal rate following galvanostatic electrolysis (4 h; 10 mA cm^{-2} unless noted otherwise) as a function of (a) $[Mg^{2+}]_0$; (b) $[HCO_3^-]_0$; (c) electrolysis current density, *j*; and (d) electrode surface area to volume ratio. Error bars represent ± standard deviation of 3 replicates. Experiments are referenced by letter and are described in Table S4.1. (b): buffering capacity β (meq L^{-1} pH^{-1}) is noted in brackets.

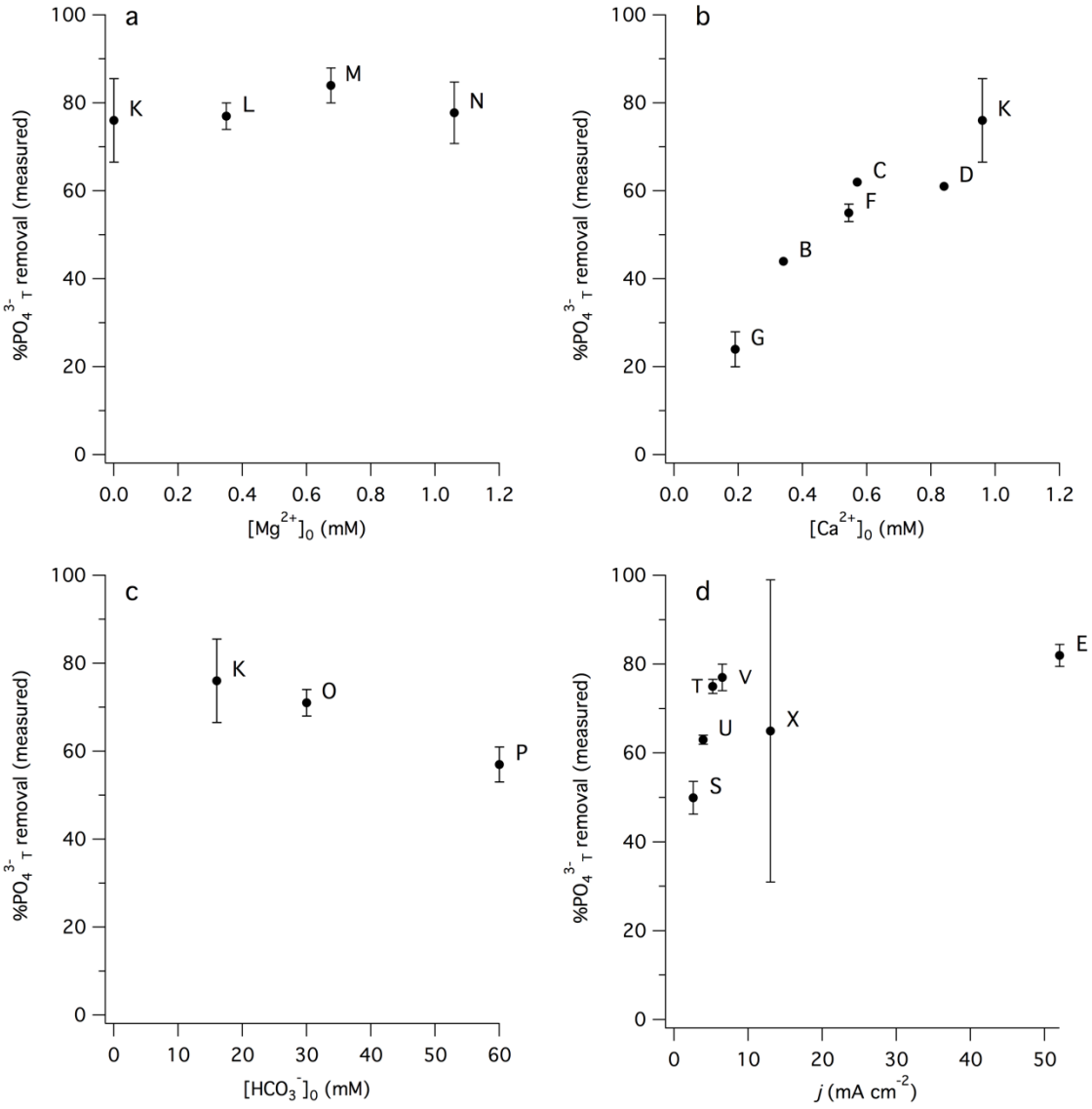

Figure 4.8: Measured percent total phosphate removal following galvanostatic electrolysis (4 h; 10 mA cm^{-2} unless noted otherwise) as a function of (a) $[Mg^{2+}]_0$; (b) $[Ca^{2+}]_0$; (c) $[HCO_3^-]_0$; and (d) electrolysis current density, *j*. Error bars represent ± standard deviation of 3 replicates. Experiments are referenced by letter and are described in Table S4.1 and Figure S4.2.

4.6. Supplementary figures and table

Figure S4.1: Dried stainless steel cathode after more than 800 h of toilet wastewater electrolysis. Most of the precipitate from the bottom of the electrode had fallen off during transporting and dismantelling the electrode array.

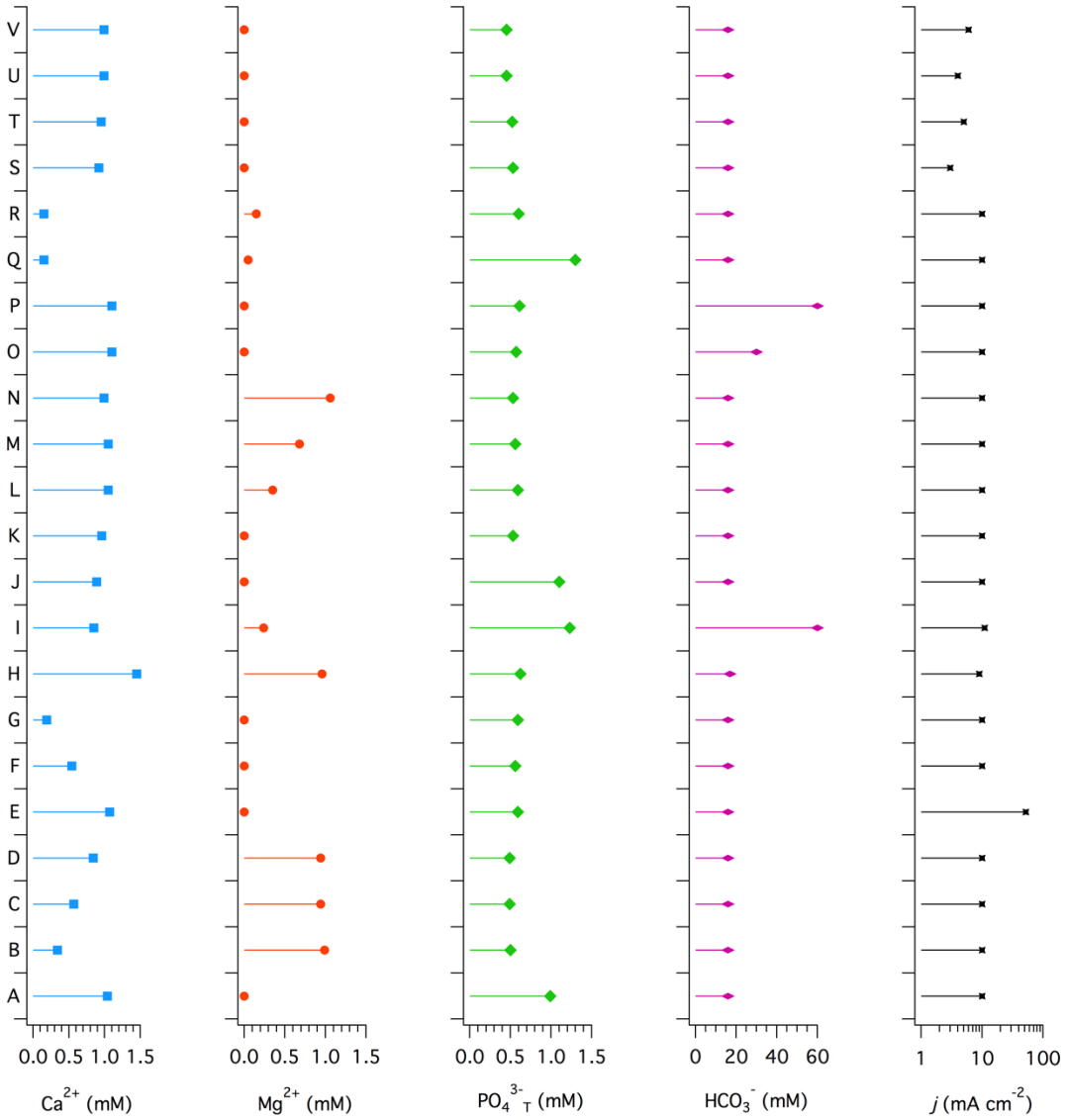

Figure S4.2: $[Ca^{2+}]_0$, $[Mg^{2+}]_0$, $[PO_4^{3-}]_{T,0}$, $[HCO_3^-]_0$, and current density *j* (log10 scale) for each set of triplicate experiments reported in Table S4.1.

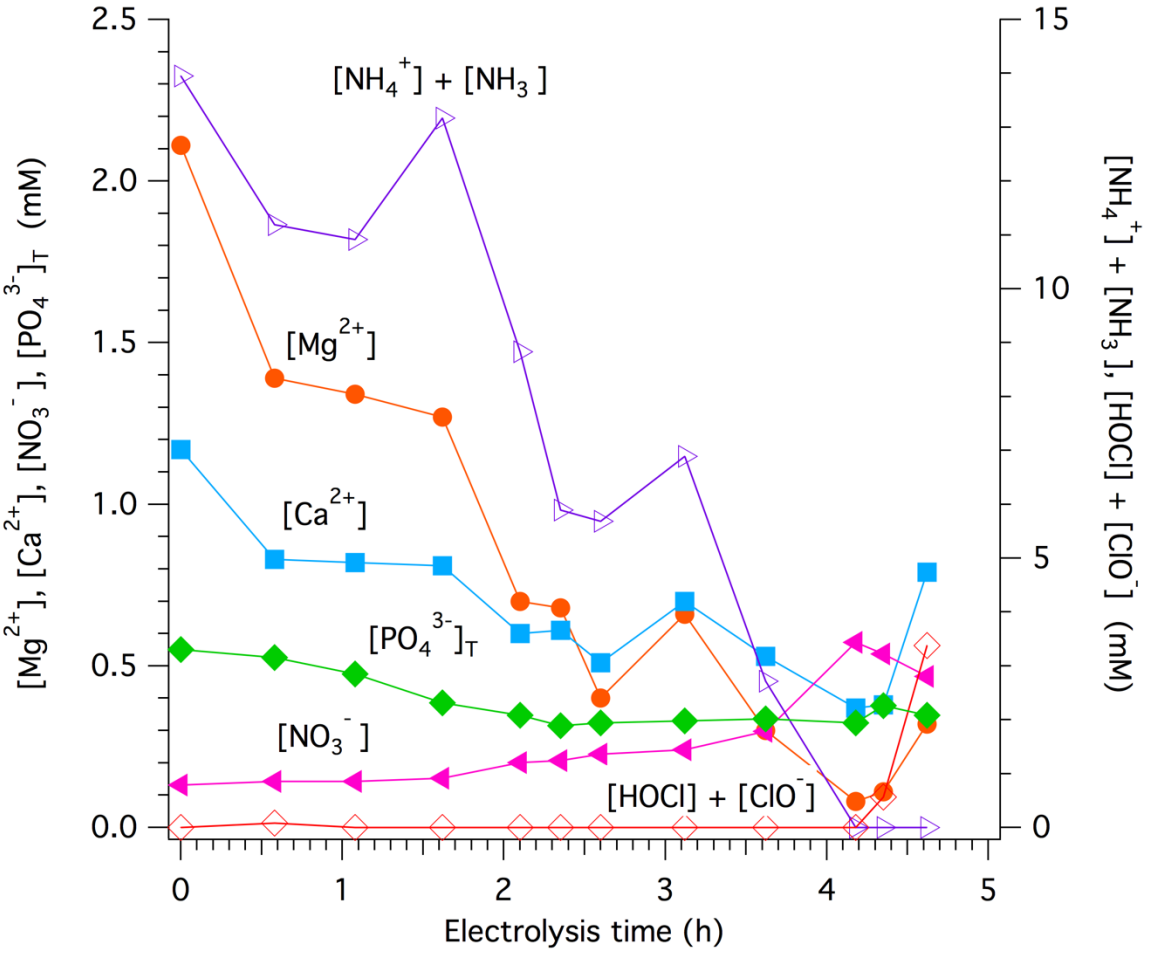

Figure S4.3: Ammonia ($NH_4^+ + NH_3$), Mg^{2+}, Ca^{2+}, total PO_4^{3-}, NO_3^-, and free chlorine ($HOCl + ClO^-$) concentrations during electrochemical treatment (3.3 V; 50 A) of toilet wastewater ($[Cl^-]$=80 mM) in pilot-scale reactor.

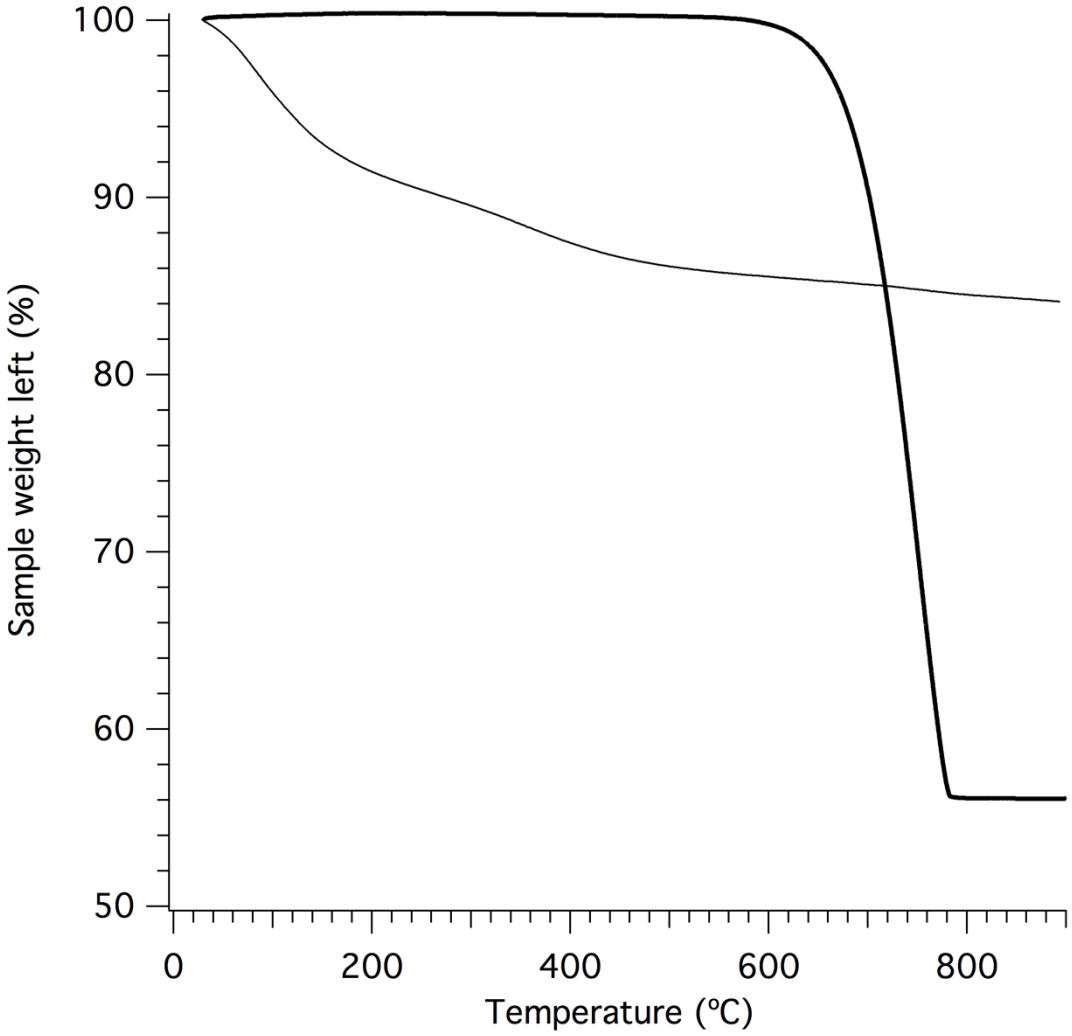

Figure S4.4: Thermogravimetric analysis of the precipitate collected from the electrochemical reactor (thin line) compared to calcium carbonate (thick line).

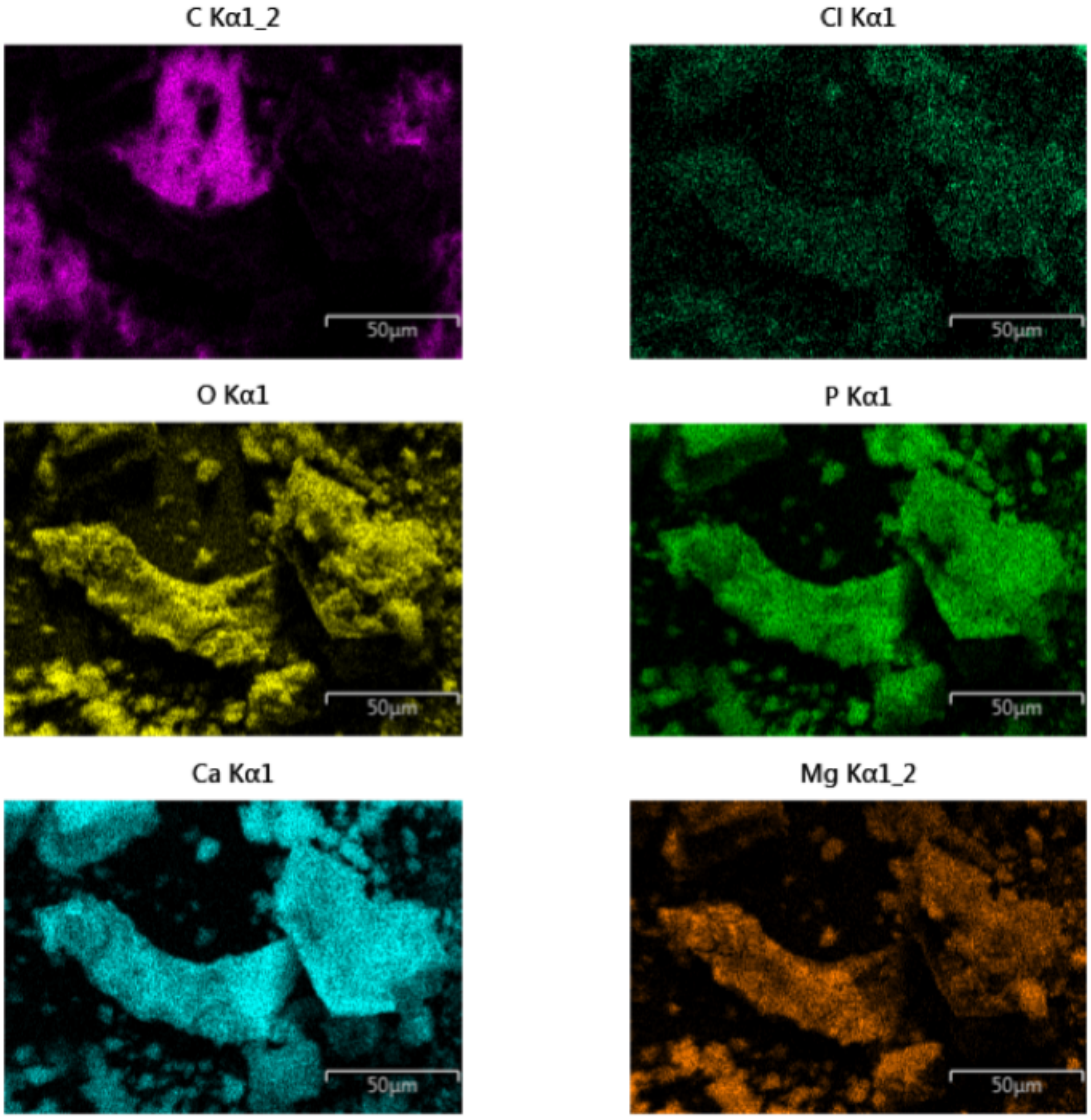

Figure S4.5: SEM/EDS mapping of precipitate collected from stainless steel cathodes after several cycles of toilet wastewater electrolysis.

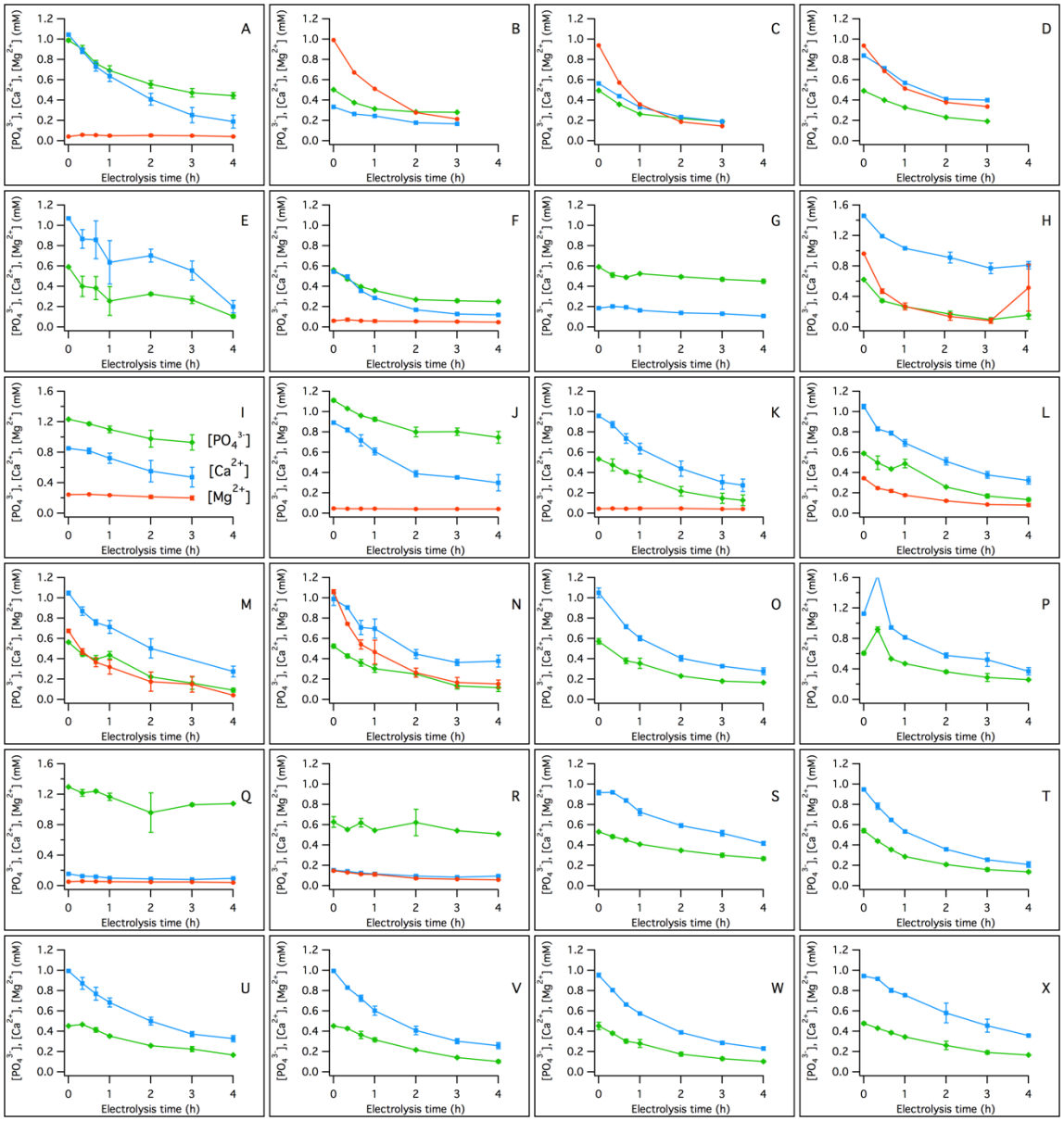

Figure S4.6: $[Ca^{2+}]$, $[Mg^{2+}]$, and $[PO_4^{3-}]_T$ during bench-scale synthetic wastewater electrolysis experiments. Experimental conditions for each test are detailed in Table S4.1. Error bars represent ± one standard deviation of 3 replicates.

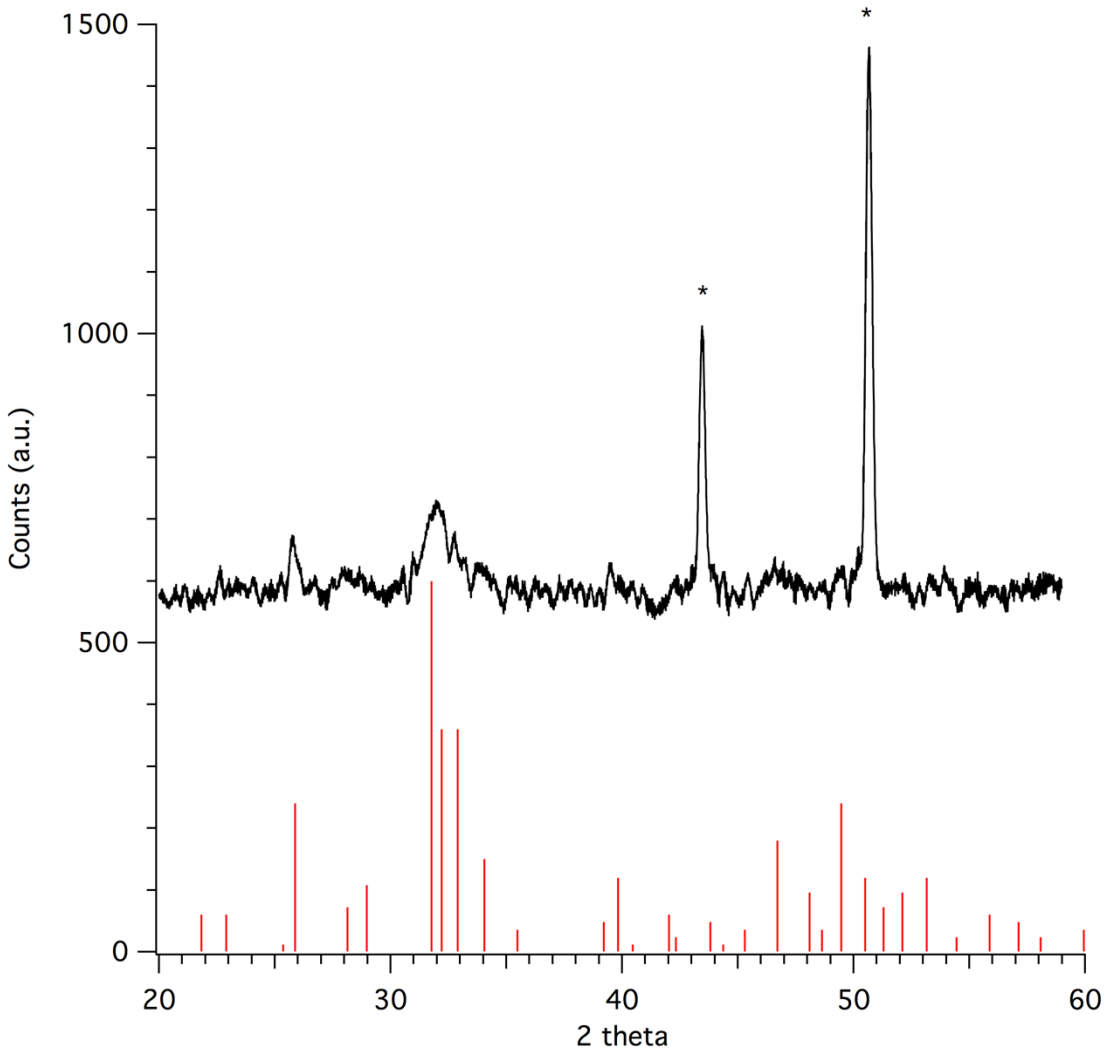

Figure S4.7: X-ray diffraction spectrum of a stainless steel cathode after four consecutive electrolyses of synthetic wasteater. Peaks with an asterisk are from the stainless steel. Overlaid red sticks shows pure hydroxyapatite with the highest peak normalized to 600 a.u. (ICSD# 24240 and PDF# 01-073-1731).

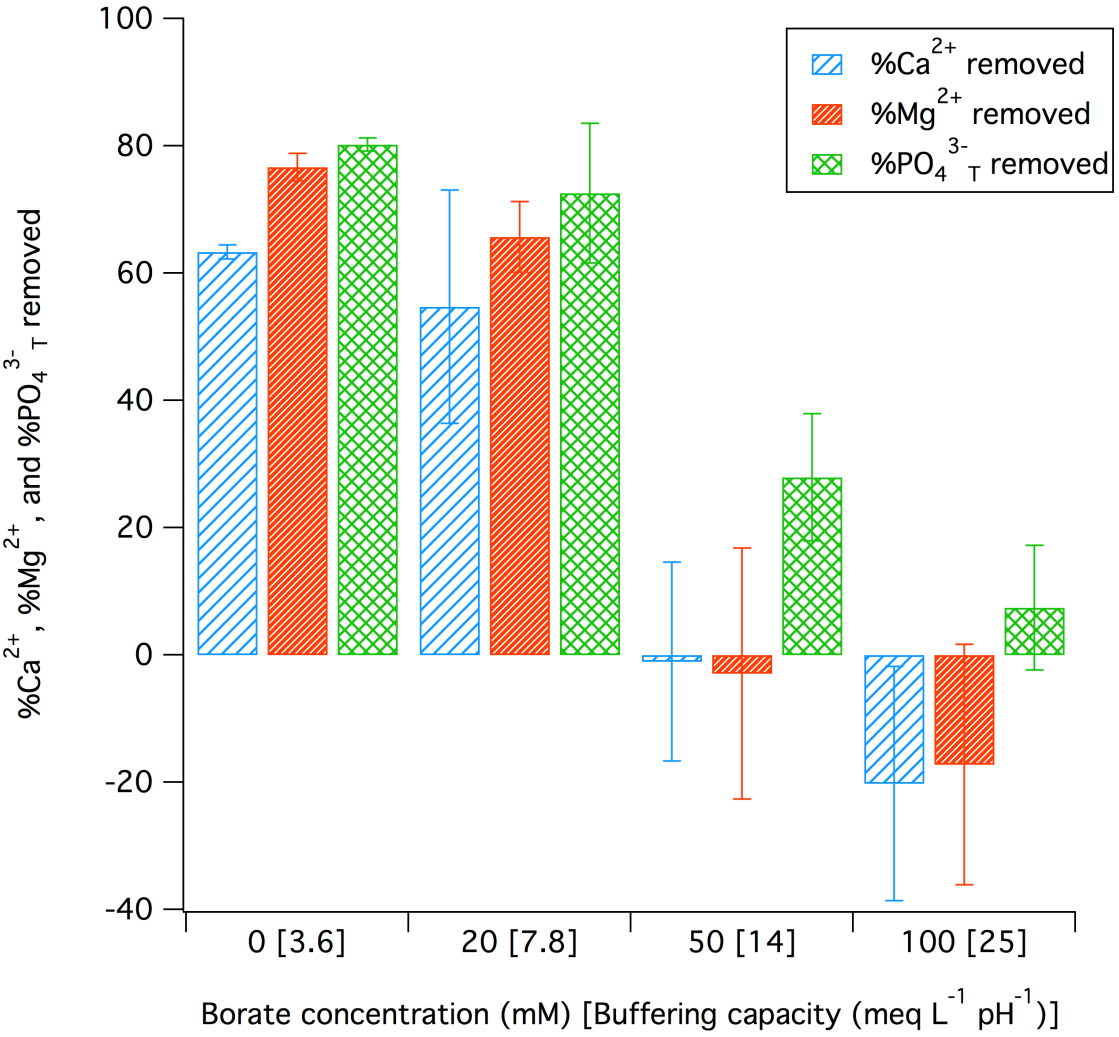

Figure S4.8: Percent Ca^{2+}, Mg^{2+}, and $PO_4^{3-}{}_T$ removal after potentiostatic treatment (3 h; 3.6 V; ~18 mA cm^{-2}) of synthetic wastewater buffered with sodium borate. Buffering capacities (β) of the solutions are noted in brakets. $[Ca^{2+}]_o \approx 1.0$ mM; $[Mg^{2+}]_o \approx 0.8$ mM; $[PO_4^{3-}]_o \approx 0.5$ mM; initial pH = 8.3. Error bars represent ± one standard deviation of 6 replicates.

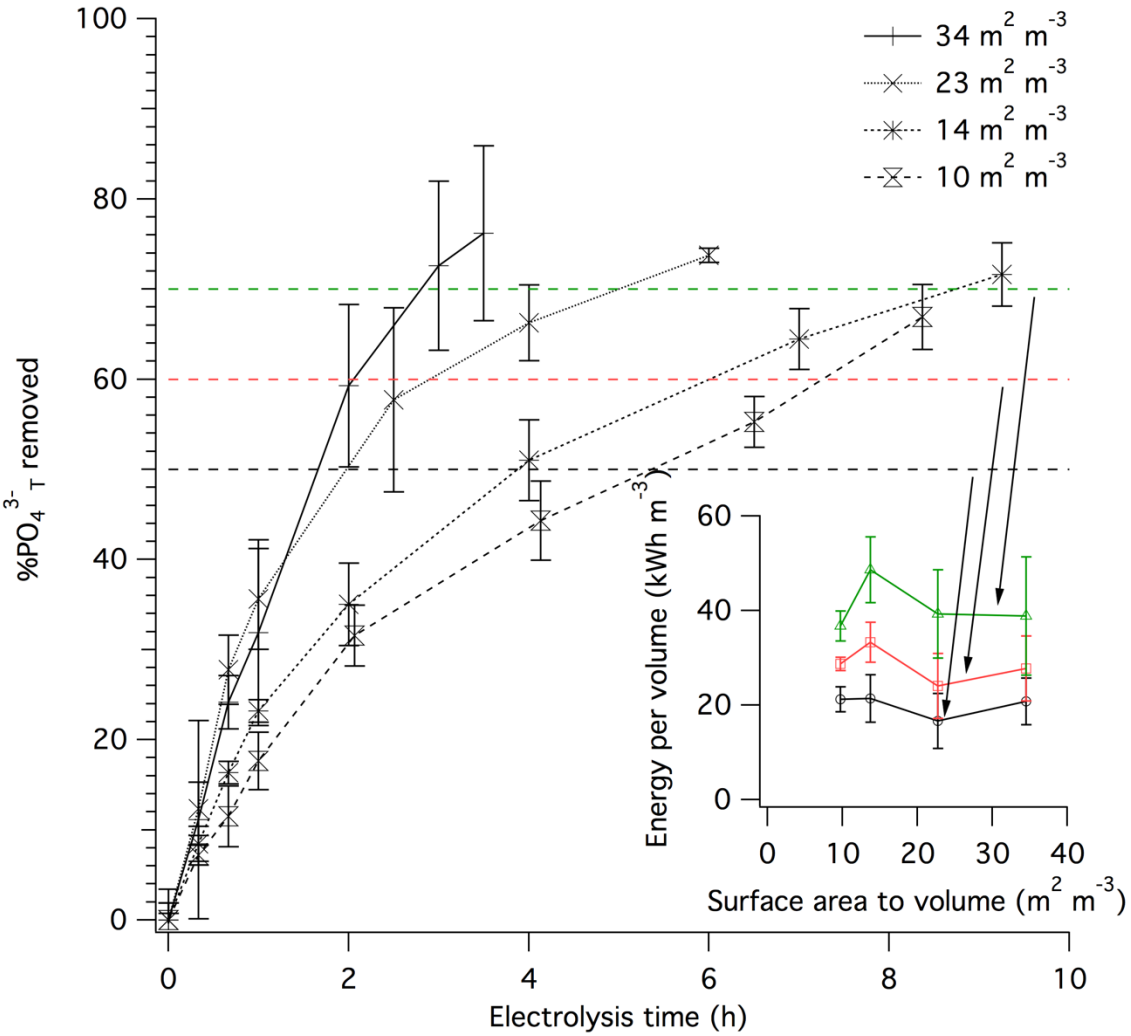

Figure S4.9: Percent phosphate removal during galvanostatic electrochemical treatment (10 mA cm^{-2}) of different electrode surface area to volume of synthetic wastewater ratios: 34 m^2 m^{-3}, 23 m^2 m^{-3}, 14 m^2 m^{-3}, and 10 m^2 m^{-3}. Inset: Energy per volume of wastewater required to achieve 50% (green triangles), 60% (red squares), and 70% (black circles) phosphate removal for the different volumes of synthetic wastewater. Error bars represent ± one standard deviation of 3 replicates.

Table S4.1: Experimental conditions for synthetic wastewater tests

Ref #	$[Ca^{2+}]_0$ mM	$[Mg^{2+}]_0$ mM	$[PO_4^{3-}]_{T,0}$ mM	TIC_0 [a] mM	j [b] mA cm^{-2}	pH_{fin} calculated [c]	$\%Ca^{2+}$ removed	$\%PO_4^{3-}{}_T$ removed
A	1.04	0.00	0.99	16	10	9.3	82 ± 6	55 ± 3
B	0.34	0.99	0.50	16	10	9.5	50	44
C	0.57	0.94	0.49	16	10	9.6	66	62
D	0.84	0.94	0.49	16	10	9.2	52	61
E	1.07	0.00	0.59	16	52	9.7	81 ± 5.6	82 ± 2.5
F	0.54	0.00	0.56	16	10	9.7	78 ± 0.5	55 ± 2
G	0.19	0.00	0.59	16	10	9.6	41 ± 4	24 ± 4
H	1.45	0.96	0.62	17	9	9.0	47 ± 3	75 ± 8
I	0.85	0.24	1.23	60	11	8.8	53 ± 3	25 ± 8
J	0.89	0.00	1.10	16	10	8.9	66 ± 8.5	33 ± 6
K	0.96	0.00	0.53	16	10	9.5	71 ± 3	76 ± 9.5
L	1.05	0.35	0.59	16	10	9.4	69 ± 3	77 ± 3
M	1.05	0.68	0.56	16	10	9.6	74 ± 3	84 ± 4
N	0.99	1.06	0.53	16	10	9.4	62 ± 6.6	78 ± 7
O	1.10	0.00	0.57	30	10	9.6	74 ± 5	71 ± 3
P	1.10	0.00	0.61	60	10	9.4	67 ± 4	57 ± 3
Q	0.15	0.05	1.30	16	10	9.4	40 ± 3	17 ± 0.6
R	0.15	0.15	0.60	16	10	9.6	38 ± 3	19 ± 6.7
S	0.92	0.00	0.53	16	3	9.0	55 ± 1.5	50 ± 3.7
T	0.95	0.00	0.52	16	5	9.6	78 ± 2.8	75 ± 1.6
U	0.99	0.00	0.45	16	4	9.3	67 ± 3.2	63 ± 1
V	0.99	0.00	0.45	16	6	9.3	74 ± 3.1	77 ± 3

[a] Total Inorganic Carbon $TIC_0 = [HCO_3^-]_0 + [CO_3^{2-}]_0$. [b] current density. [c] The cathodic pH was estimated assuming that the solution at the cathode surface was equilibrated (SI=1) with respect to electrochemically precipitated hydroxyapatite ($K_{sp} = 5\ 10^{-47}$) and that $[Ca^{2+}]$ and $[PO_4^{3-}]$ at the cathode were the same as measured in solution at the end of the experiment (when ion concentrations had stabilized).

4.7. References

American Public Health, A. (1995). *Standard Methods for the Examination of Water and Wastewater* (19th ed.). Washington, DC: American Public Health Association,, A. W. W. A., Water Environment Federation.

Amjad, Z., Koutsoukos, P. G., & Nancollas, G. H. (1984). The crystallization of hydroxyapatite and fluorapatite in the presence of magnesium ions. *Journal of Colloid and Interface Science, 101*(1), 250-256. doi:10.1016/0021-9797(84)90025-0

Cao, X., & Harris, W. (2007). Carbonate and magnesium interactive effect on calcium phosphate precipitation. *Environmental science & technology, 42*(2), 436-442.

Cao, X., Harris, W. G., Josan, M. S., & Nair, V. D. (2007). Inhibition of calcium phosphate precipitation under environmentally-relevant conditions. *Science of The Total Environment, 383*(1–3), 205-215. doi:10.1016/j.scitotenv.2007.05.012

Cho, K., & Hoffmann, M. R. (2014). Urea Degradation by Electrochemically Generated Reactive Chlorine Species: Products and Reaction Pathways. *Environmental science & technology, 48*(19), 11504-11511. doi:10.1021/es5025405

Cho, K., & Hoffmann, M. R. (2015). BixTi1–xOz Functionalized Heterojunction Anode with an Enhanced Reactive Chlorine Generation Efficiency in Dilute Aqueous Solutions. *Chemistry of Materials, 27*(6), 2224-2233. doi:10.1021/acs.chemmater.5b00376

Cho, K., Qu, Y., Kwon, D., Zhang, H., Cid, C. A., Aryanfar, A., & Hoffmann, M. R. (2014). Effects of Anodic Potential and Chloride Ion on Overall Reactivity in Electrochemical Reactors Designed for Solar-Powered Wastewater Treatment. *Environmental science & technology, 48*(4), 2377-2384. doi:10.1021/es404137u

Comninellis, C., & Chen, G. (2010). *Electrochemistry for the Environment* (Vol. 2015). New York, NY: Springer-Verlag.

Conley, D. J., Paerl, H. W., Howarth, R. W., Boesch, D. F., Seitzinger, S. P., Havens, K. E., . . . Likens, G. E. (2009). Controlling eutrophication: nitrogen and phosphorus. *Science, 323*(5917), 1014-1015. doi:10.1126/science.1167755

Cordell, D., Rosemarin, A., Schröder, J. J., & Smit, A. L. (2011). Towards global phosphorus security: A systems framework for phosphorus recovery and reuse options. *Chemosphere, 84*(6), 747-758. doi:10.1016/j.chemosphere.2011.02.032

Correll, D. L. (1998). The role of phosphorus in the eutrophication of receiving waters: a review. *Journal of environmental quality, 27*(2), 261-266.

Dahms, H., & Croll, I. M. (1965). The Anomalous Codeposition of Iron-Nickel Alloys. *Journal of The Electrochemical Society, 112*(8), 771-775. doi:10.1149/1.2423692

Dai, H., Lu, X., Peng, Y., Yang, Z., & Zhsssu, H. (2017). Effects of supersaturation control strategies on hydroxyapatite (HAP) crystallization for phosphorus recovery from wastewater. *Environmental Science and Pollution Research, 24*(6), 5791-5799. doi:10.1007/s11356-016-8236-2

de-Bashan, L. E., & Bashan, Y. (2004). Recent advances in removing phosphorus from wastewater and its future use as fertilizer (1997–2003). *Water Research, 38*(19), 4222-4246. doi:10.1016/j.watres.2004.07.014

Fuierer, T. A., LoRe, M., Puckett, S. A., & Nancollas, G. H. (1994). A Mineralization Adsorption and Mobility Study of Hydroxyapatite Surfaces in the Presence of Zinc and Magnesium Ions. *Langmuir, 10*(12), 4721-4725. doi:10.1021/la00024a054

Fumasoli, A., Etter, B., Sterkele, B., Morgenroth, E., & Udert, K. M. (2016). Operating a pilot-scale nitrification/distillation plant for complete nutrient recovery from urine. *Water Science and Technology, 73*(1), 215-222.

Gibson, I. R., Best, S. M., & Bonfield, W. (1999). Chemical characterization of silicon-substituted hydroxyapatite. *Journal of Biomedical Materials Research, 44*(4), 422-428. doi:10.1002/(SICI)1097-4636(19990315)44:4<422::AID-JBM8>3.0.CO;2-#

Golubev, S. V., Pokrovsky, O. S., & Savenko, V. S. (1999). Unseeded precipitation of calcium and magnesium phosphates from modified seawater solutions. *Journal of Crystal Growth, 205*(3), 354-360. doi:10.1016/S0022-0248(99)00219-5

Gorni-Pinkesfeld, O., Shemer, H., Hasson, D., & Semiat, R. (2013). Electrochemical Removal of Phosphate Ions from Treated Wastewater. *Industrial & Engineering Chemistry Research, 52*(38), 13795-13800. doi:10.1021/ie401930c

Gustafsson, J. P. (2014). Visual MINTEQ ver. 3.1 (released 2014). Retrieved from http://vminteq.lwr.kth.se/

Hoffmann, M. R., Aryanfar, A., Cho, K., Cid, C. A., Kwon, D., & Qu, Y. (2013).

Huang, X., Qu, Y., Cid, C. A., Finke, C., Hoffmann, M. R., Lim, K., & Jiang, S. C. (2016). Electrochemical disinfection of toilet wastewater using wastewater electrolysis cell. *Water Research, 92*, 164-172. doi:10.1016/j.watres.2016.01.040

Hug, A., & Udert, K. M. (2013). Struvite precipitation from urine with electrochemical magnesium dosage. *Water Research, 47*(1), 289-299.

Inskeep, W. P., & Silvertooth, J. C. (1988). Kinetics of hydroxyapatite precipitation at pH 7.4 to 8.4. *Geochimica et Cosmochimica Acta, 52*(7), 1883-1893. doi:10.1016/0016-7037(88)90012-9

Ito, A., Maekawa, K., Tsutsumi, S., Ikazaki, F., & Tateishi, T. (1997). Solubility product of OH-carbonated hydroxyapatite. *Journal of Biomedical Materials Research, 36*(4), 522-528. doi:10.1002/(SICI)1097-4636(19970915)36:4<522::AID-JBM10>3.0.CO;2-C

Jasper, J. T., Shafaat, O. S., & Hoffmann, M. R. (2016). Electrochemical Transformation of Trace Organic Contaminants in Latrine Wastewater. *Environ Sci Technol, 50*(18), 10198-10208. doi:10.1021/acs.est.6b02912

Jasper, J. T., Yang, Y., & Hoffmann, M. R. (2017). Toxic Byproduct Formation during Electrochemical Treatment of Latrine Wastewater. *Environmental science & technology, 51*(12), 7111-7119. doi:10.1021/acs.est.7b01002

Kapolos, J., & Koutsoukos, P. G. (1999). Formation of Calcium Phosphates in Aqueous Solutions in the Presence of Carbonate Ions. *Langmuir, 15*(19), 6557-6562. doi:10.1021/la981285k

Karunanithi, R., Szogi, A., Bolan, N. S., Naidu, R., Ok, Y. S., Krishnamurthy, S., & Seshadri, B. (2016). Chapter 27 - Phosphorus Recovery From Wastes# *Environmental Materials and Waste* (pp. 687-705): Academic Press.

Kruk, D. J., Elektorowicz, M., & Oleszkiewicz, J. A. (2014). Struvite precipitation and phosphorus removal using magnesium sacrificial anode. *Chemosphere, 101*, 28-33. doi:10.1016/j.chemosphere.2013.12.036

Lacasa, E., Cañizares, P., Sáez, C., Fernández, F. J., & Rodrigo, M. A. (2011). Electrochemical phosphates removal using iron and aluminium electrodes. *Chemical Engineering Journal, 172*(1), 137-143. doi:10.1016/j.cej.2011.05.080

Loeppert, R. H., & Suarez, D. L. (1996). Carbonate and gypsum. In D. L. Sparks (Ed.), *Methods of Soil Analysis, Part 3 Chemical Methods* (2 ed.). Madison, WI: American Society of Agronomy.

McDowell, H., Gregory, T. M., & Brown, W. E. (1977). Solubility of Ca5(P04)3OH in the System Ca(OH)2-H3P04-H20 at 5, 15, 25, and 37 °C. *Journal of Research of the National Bureau of Standards – A. Physics and Chemistry, 81A*(2-3), 273-281.

Mihelcic, J. R., Fry, L. M., & Shaw, R. (2011). Global potential of phosphorus recovery from human urine and feces. *Chemosphere, 84*(6), 832-839.

Moriyama, K., Kojima, T., Minawa, Y., Matsumoto, S., & Nakamachi, K. (2001). Development of Artificial Seed Crystal for Crystallization of Calcium Phosphate.

Environmental Technology, 22(11), 1245-1252. doi:10.1080/09593330.2001.9619163

Morse, G. K., Brett, S. W., Guy, J. A., & Lester, J. N. (1998). Review: Phosphorus removal and recovery technologies. *Science of The Total Environment, 212*(1), 69-81. doi:10.1016/S0048-9697(97)00332-X

Oehmen, A., Lemos, P. C., Carvalho, G., Yuan, Z., Keller, J., Blackall, L. L., & Reis, M. A. (2007). Advances in enhanced biological phosphorus removal: from micro to macro scale. *Water Res, 41*(11), 2271-2300. doi:10.1016/j.watres.2007.02.030

Okazaki, M., Takahashi, J., & Kimura, H. (1986). Unstable behavior of magnesium-containing hydroxyapatites. *Caries Research, 20*(4), 324-331.

Putnam, D. F. (1971). Composition and concentrative properties of human urine. *NASA Contractor Report CR-1802*.

Shirkhanzadeh, M. (1998). Direct formation of nanophase hydroxyapatite on cathodically polarized electrodes. *Journal of Materials Science: Materials in Medicine, 9*(2), 67-72. doi:10.1023/a:1008838813120

Simons, A., Solomon, D., Chibssa, W., Blalock, G., & Lehmann, J. (2014). Filling the phosphorus fertilizer gap in developing countries. *Nature Geoscience, 7*(1), 3-3. doi:10.1038/ngeo2049

Spanos, N., & Koutsoukos, P. G. (1998). Kinetics of precipitation of calcium carbonate in alkaline pH at constant supersaturation. Spontaneous and seeded growth. *The Journal of Physical Chemistry B, 102*(34), 6679-6684.

Sprio, S., Tampieri, A., Landi, E., Sandri, M., Martorana, S., Celotti, G., & Logroscino, G. (2008). Physico-chemical properties and solubility behaviour of multi-substituted hydroxyapatite powders containing silicon. *Materials Science & Engineering, C: Biomimetic and Supramolecular Systems, 28*(1), 179-187. doi:10.1016/j.msec.2006.11.009

TenHuisen, K. S., & Brown, P. W. (1997). Effects of magnesium on the formation of calcium-deficient hydroxyapatite from CaHPO4· 2H2O and Ca4 (PO4) 2O. *Journal of Biomedical Materials Research Part A, 36*(3), 306-314.

Tran, N., Drogui, P., Blais, J.-F., & Mercier, G. (2012). Phosphorus removal from spiked municipal wastewater using either electrochemical coagulation or chemical coagulation as tertiary treatment. *Separation and Purification Technology, 95*, 16-25. doi:10.1016/j.seppur.2012.04.014

Udert, K. M., Larsen, T. A., & Gujer, W. (2006). Fate of major compounds in source-separated urine. *Water Science and Technology, 54*(11-12), 413-420. doi:10.2166/wst.2006.921

Wang, C. C., Hao, X. D., Guo, G. S., & van Loosdrecht, M. C. M. (2010). Formation of pure struvite at neutral pH by electrochemical deposition. *Chemical Engineering Journal, 159*(1–3), 280-283. doi:10.1016/j.cej.2010.02.026

Weres, O. (2009). U.S. Patent 7,494,583.

Weres, O., & O'Donnell, H. E. (2003). U.S. Patent 6,589,405. U.S. Patent.

White, G. C. (2010). *White's handbook of chlorination and alternative disinfectants*. Hoboken, NJ: John Wiley & Sons.

World Bank. (2015). Global Economic Monitor Commodities, http://databank.worldbank.org/.

Yang, Y., Shin, J., Jasper, J. T., & Hoffmann, M. R. (2016). Multilayer Heterojunction Anodes for Saline Wastewater Treatment: Design Strategies and Reactive Species Generation Mechanisms. *Environmental science & technology, 50*(16), 8780-8787.

Chapter 5

PRACTICAL APPLICATIONS

5.1. In summary

This thesis is based on the pursuit of bringing an appealing, adequate, and sustainable sanitation solution for people lacking access to safe sanitation. In the following paragraphs, I recapitulate the main findings and potential future directions of the research described in Chapter 2, 3, and 4. I also describe the barriers to adoption of the Solar Toilet technology and how they are addressed. Finally, I give ideas on potential use of the electrochemical treatment technology in other systems than Solar Toilets.

The findings in **Chapter 2** gave us a better understanding of the treatment technology under testing conditions close to the potential usage of the technology. The prototypes of the electrochemical wastewater treatment system – or the Caltech Solar Toilets, tested in the US, China, and India – proved to be working reasonably well. The field testing confirmed the efficacy of disinfection as well as ammonia oxidation to chloramines by electrochemically generated reactive chlorine species as previously measured in laboratory conditions (Cho & Hoffmann, 2015; Huang et al., 2016). The electrolysis process also oxidized organic contaminants quantified by a removal of chemical oxygen demand. Nevertheless, the efficacy of electrochemical oxidation comes at a relatively high energy cost (30-40 Wh L^{-1} of toilet wastewater) compared to standalone biological treatment systems which can be an order of magnitude lower (Metcalf & Eddy, 2014).

One approach to decrease the energy cost associated with the electrochemical oxidation of organic species was discussed in **Chapter 3**. The use of microbial fuel cell systems fed by human urine from a water-free urinal proved to be a successful

pretreatment step. The microbial fuel cells enabled the removal of more than 50% of the chemical oxygen demand from urine before it entered the electrochemical reactor. Although the catholyte produced inside the microbial fuel cell ceramic tubes was less contaminated by bacteria from the seeding sludge than the anolyte (urine), the catholyte could not be guaranteed to be pathogen-free. Therefore, it cannot be reused for irrigation because of the risk of human contact. One possible reuse found by Gajda and coworkers (Gajda, Greenman, Melhuish, & Ieropoulos, 2016) would be to use the alkaline catholyte as a precipitation agent for removing heavy metals from contaminated waters. Its reuse as a caustic solution for destruction of helminth cysts can also be envisaged. Finally, with added electronics developed by Ieropoulos and coworkers (data not published), the microbial fuel cell system produces electricity that is harvested and stored in a battery in order to power a pump for approximately two minutes a day. This pumping is sufficient to make the microbial fuel cell pre-treatment step energy neutral or even energy positive when the energy needed for chemical oxygen removal by electrolysis is taken into accounted.

The potential for nutrient recovery and reuse caught my attention when I observed a white precipitate forming on the stainless-steel cathodes and inside the electrochemical reactor after multiple electrolysis cycles. Later, I identified the precipitate as Mg-containing hydroxyapatite. I investigated precipitation kinetics as well as the maximum percent PO_4^{3-} recovery as described in **Chapter 4**. The initial concentration of PO_4^{3-} and Ca^{2+} in toilet wastewater played a major role in the initial precipitation kinetics and the final amount of precipitated PO_4^{3-} that could be recovered.

5.2. Barriers to wide adoption of the technology

5.2.1. Is the lack of social status surrounding toilets a problem?

I believe that the Caltech Solar Toilet technology developed in this thesis has a great potential for bringing a high level of sanitation service while requiring little energy and no water. A high quality sustainable treatment system could make toilets be appealing objects that lead to a higher social status and a better life for people to adopt them (Barrington & Bartram, 2017). Cell phones are objects of social status recognition and they are seen by a lot of people living in poverty as a way to increase their standard of living (Aker & Mbiti, 2010; Sam, 2017).

This social phenomenon has been illustrated with the quasi-ubiquitous usage of cell phones in developing countries in recent years. For instance, India has seen an exponential growth in cell phones subscriptions from approximately 0 to more than 900 million between 1995 and 2014, while the number of people practicing open defecation merely decreased from 680 to 600 million (Figure 5.1). The rather slow decrease in open defecation in India despite multiple government programs to subsidize sanitation adoption (Hueso & Bell, 2013) might come for the fact that there has not been a technology that people would adopt as fast as they adopted cell phones. Therefore, the Caltech Solar Toilet as a standalone, low-energy requirement product that can enable the use a hygienic and non-odorous flush toilet without consuming water might be considered as aspirational as a cell phone can be.

5.2.2. A smart maintenance system for a truly sustainable solution

It is a challenge to manufacture a product with very little defects and it is an even greater challenge to provide a simple and effective repair solution when failure arises,

especially in the case of onsite toilet wastewater treatment. If the system fails, the repair has to be done quickly, otherwise its users will not be able to go! The understanding of the technical challenges encountered during prototyping and testing (**Chapter 2**) have led to a detailed Failure Mode Effects Analysis of the Caltech Solar Toilet. The information gathered by the Failure Mode Effects Analysis can be combined with a suite of sensors and data processing units to understand the failure of the toilet systems when deployed.

The many years of field testing taught me that a lack of skilled maintenance professionals makes repair of the Caltech Solar Toilet problematic. Most repairs are simple, requiring only a screwdriver, yet without interactive instructions, units could not be serviced easily. For this reason, a Smart Maintenance Solution called “Seva” (service in Hindi) is currently in development with the help of Cody Finke, Anastasia Hanan, Eitam Shafran, and Hugo Leandri. This initial idea won first prize in Vodafone's Wireless Innovation Project competition and is now in the prototyping phase.

The system uses an array of inexpensive sensors (water level, pressure sensor, ORP sensor, turbidity sensor, etc.) placed at different steps of the process (Figure 5.2). An inexpensive computer and controller module named the “Seva Module”, consisting of a Rasperry Pi 3 (Raspberry Pi Foundation, United Kingdom) coupled with an Arduino platform (Arduino, Italy), is reading signals from the sensors embedded in the treatment system. The Seva Module is then able to determine if the treatment system has failed, and how. It then automatically sends a text or audio cell phone message to a trained operator, letting the operator know that he/she should come

and repair the toilet. An application running on the operator's smartphone can provide the operator with step-by-step pictorial instructions on how to replace the broken part. Thus, the Seva Module technology has the potential to create jobs for low-skilled operators and ensure that the users have uninterrupted access to safe sanitation.

5.2.3. Standardization can boost the market for onsite sanitation systems

The development of new technologies for treating human waste under the "Reinvent the Toilet Challenge" set by the Bill & Melinda Gates Foundation is leading to new products entering the sanitation market. Although the total addressable market is huge with 4.5 billion potential customers, their willingness and their ability to pay a premium for effective sanitation is not trivial. This barrier could overcome by making sure products are safe and effective. This is best done by setting an international standard that guarantees the quality and effectiveness of products or services (ISO, 2011).

The International Organization for Standardization (ISO) is the most recognized international standardization body with 162 member countries. An ISO standard under project number PC 305 is currently being developed for the purpose of guaranteeing a quality of treatment wherever a qualified sanitation unit would be installed. This ISO standard focuses on the "requirements for the quality of the outputs from the sanitation system (that) are given for solid and liquid discharges as well as odor, air, and noise emissions." I am one of the experts who has developed the requirements for effective onsite sanitation systems that would be qualified under

this new standard. The Draft International Standard has been submitted to ISO and is currently being reviewed by all ISO member countries before voting.

5.3. Applicability of the electrochemical technology to other industries

As the electrochemical oxidation of chloride to reactive chlorine species is very effective for ammonia removal and disinfection of human wastewater but it consumes a high amount of electrical energy, especially if high amounts of COD removal are needed. We can envisage this technology to be used for other types of wastewater than toilet waste. The work I performed under EPA-SBIR grant EPD14026 demonstrated that nitrogen removal and disinfection of household septic systems can be obtained but are limited due to the low chloride concentration of domestic waste (less than 100 ppm [Cl^-]). One approach to solve this problem could be to divert a portion of the domestic wastewater that has a high [Cl^-] and [NH_3] to the electrochemical system while the rest would remain in the septic system. Other usages of the technology could focus on types of wastewater where disinfection is crucial, such as industrial laundry, food industry, or localized generation of an oxidizing solution for cleaning purposes.

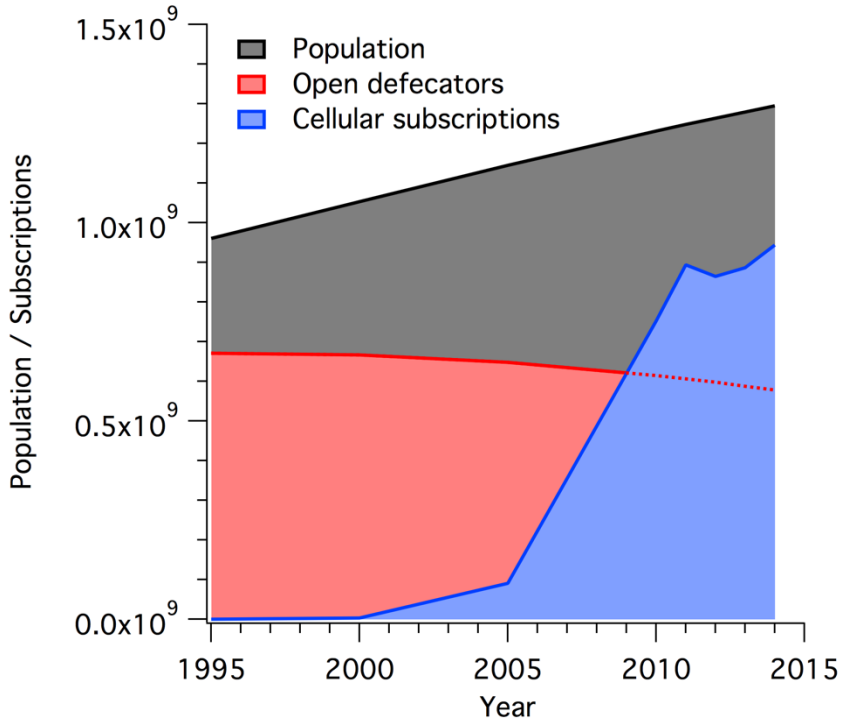

Figure 5.1: Indian population, number of open defecators, and cellular subscriptions in the country between 1995 and 2014. (World Bank, 2016)

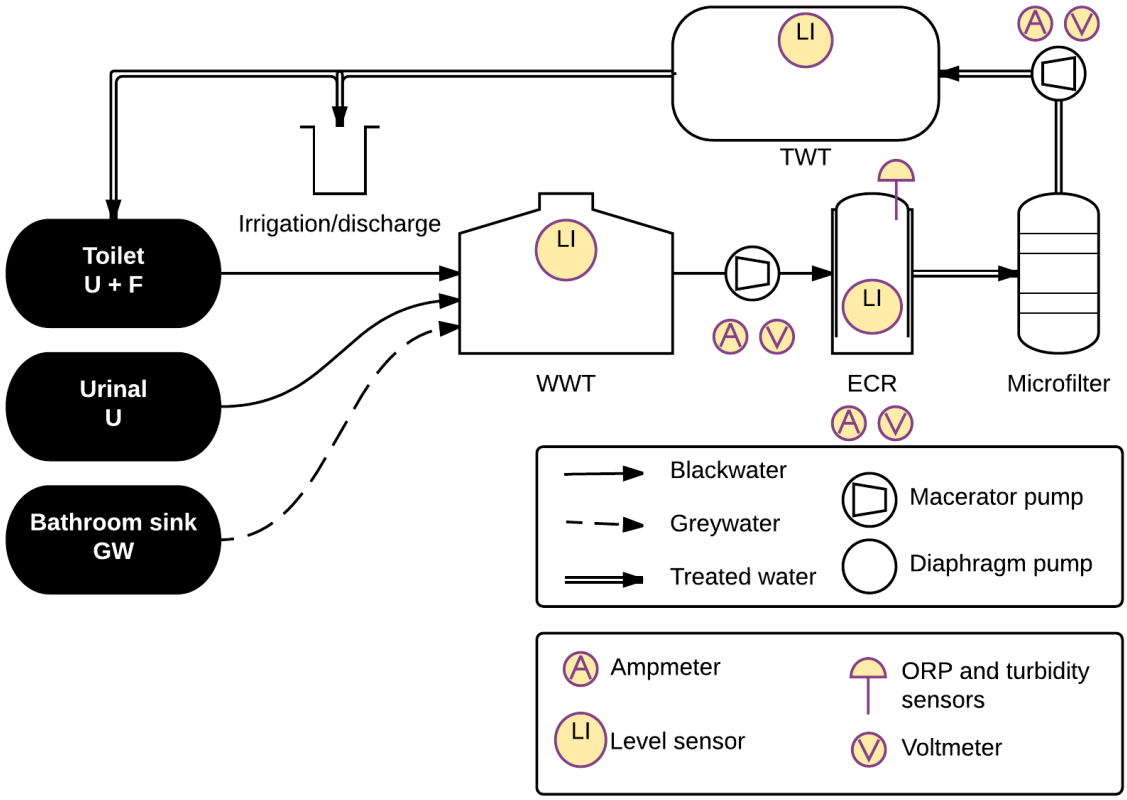

Figure 5.2: Simplified flow diagram of the Caltech Solar Toilet with sensors (purple and yellow) placed at different steps of the process

5.4. References

Aker, J. C., & Mbiti, I. M. (2010). Mobile Phones and Economic Development in Africa. *Journal of Economic Perspectives, 24*(3), 207-232. doi:10.1257/jep.24.3.207

Barrington, D. J., & Bartram, J. (2017). Toilet marketing campaigns in developing countries erode people's dignity – this is not acceptable. *The Conversation*. Retrieved from

Cho, K., & Hoffmann, M. R. (2015). BixTi1–xOz Functionalized Heterojunction Anode with an Enhanced Reactive Chlorine Generation Efficiency in Dilute Aqueous Solutions. *Chemistry of Materials, 27*(6), 2224-2233. doi:10.1021/acs.chemmater.5b00376

Gajda, I., Greenman, J., Melhuish, C., & Ieropoulos, I. A. (2016). Electricity and disinfectant production from wastewater: Microbial Fuel Cell as a self-powered electrolyser. *Sci Rep, 6*, 25571. doi:10.1038/srep25571

Huang, X., Qu, Y., Cid, C. A., Finke, C., Hoffmann, M. R., Lim, K., & Jiang, S. C. (2016). Electrochemical disinfection of toilet wastewater using wastewater electrolysis cell. *Water Research, 92*, 164-172. doi:10.1016/j.watres.2016.01.040

Hueso, A., & Bell, B. (2013). An untold story of policy failure: the Total Sanitation Campaign in India. *Water Policy, 15*(6), 1001-1017.

ISO. (2011). *Economic benefits of standards – International case studies*. Geneva, Switzerland.

Metcalf, & Eddy. (2014). *Wastewater Engineering: Treatment and Resource Recovery*: McGraw-Hill international ed.

Sam, S. (2017). Towards an empowerment framework for evaluating mobile phone use and impact in developing countries. *Telematics and Informatics, 34*(1), 359-369. doi:10.1016/j.tele.2016.06.003

World Bank. (2016). World Development Indicators, http://databank.worldbank.org/.